Detection and Measurement of Nuclear Radiation (1962)

Pages
147

Size
6 x 9

ISBN
0309300045

O'Kelley, G. D.; Subcommittee on Radiochemistry; Committee on Nuclear Science; National Research Council

COMMITTEE ON NUCLEAR SCIENCE

LIAISON MEMBERS

SUBCOMMITTEE ON RADIOCHEMISTRY

CONSULTANTS

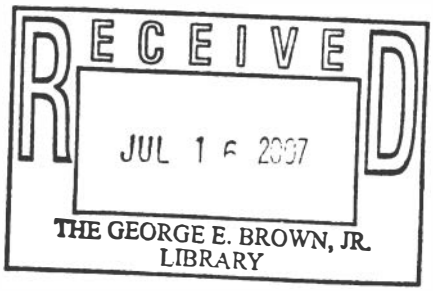

Detection and Measurement of Nuclear Radiation

G. D. O'KELLEY

Oak Ridge National Laboratory
Oak Ridge, Tennessee

Issuance Date: April 1962

Subcommittee on Radiochemistry
National Academy of Sciences—National Research Council

Printed in USA. Price $1.50. Available from the Office of Technical Services, Department of Commerce, Washington 25, D. C.

FOREWORD

The Subcommittee on Radiochemistry is one of a number of subcommittees working under the Committee on Nuclear Science within the National Academy of Sciences - National Research Council. Its members represent government, industrial, and university laboratories in the areas of nuclear chemistry and analytical chemistry.

The Subcommittee has concerned itself with those areas of nuclear science which involve the chemist, such as the collection and distribution of radiochemical procedures, the establishment of specifications for radiochemically pure reagents, availability of cyclotron time for service irradiations, the place of radiochemistry in the undergraduate college program, etc.

This series of monographs has grown out of the need for up-to-date compilations of radiochemical information, procedures, and techniques. The Subcommittee has endeavored to present a series which will be of maximum use to the working scientist and which contains the latest available information. Each monograph collects in one volume the pertinent information required for radiochemical work with an individual element or with a specialized technique.

An expert in the particular radiochemical technique has written the monograph. The Atomic Energy Commission has sponsored the printing of the series.

The Subcommittee is confident these publications will be useful not only to the radiochemist but also the the research worker in other fields such as physics, biochemistry or medicine who wishes to use radiochemical techniques to solve a specific problem.

W. Wayne Meinke, Chairman
Subcommittee on Radiochemistry

PREFACE

This volume on detection and measurement of nuclear radiation has been prepared as one of a series of monographs on radiochemical techniques which will parallel the series on radiochemistry of the elements. The material contained in this monograph represents a slight expansion of a contribution by the author to a chapter entitled "Nuclear Chemistry," for inclusion in Technique of Inorganic Chemistry, edited by H. B. Jonassen, and to be published by Interscience Publishers.

It is a pleasure for the author to express his sincere appreciation to N. R. Johnson and E. Eichler, who, in addition to their responsibilities as co-authors of the Nuclear Chemistry chapter, made numerous useful suggestions during the preparation of the material included here. The author also gratefully acknowledges other members of the Oak Ridge National Laboratory staff for helpful discussions and criticism of the manuscript, especially R. K. Abele, J. L. Blankenship, A. Chetham-Strode, V. A. McKay, J. R. Tarrant, and F. J. Walter.

Finally, the writer wishes to express his most sincere appreciation to Mrs. I. W. Hodge for typing not only the final manuscript, but several drafts as well, all with accuracy and perseverance.

G. D. O'Kelley
December, 1961

CONTENTS

Detection and Measurement of Nuclear Radiation

G. D. O'KELLEY
Oak Ridge National Laboratory *
Oak Ridge, Tennessee

I. GENERAL INTRODUCTION

During the past few years, the technique of radiation characterization has undergone a rapid transformation. New materials of construction have made possible a number of improvements in conventional detectors, while several new detector types have been made available to the experimenter.

Improvements in detectors have been accompanied by the development of more versatile and reliable electronic measuring equipment. Where once it was possible to record only the number of events in a certain detector, it is now quite common to record complicated spectral data. Many of the new techniques in nuclear data processing were inspired by progress in digital computer technology, which has resulted in a very desirable compatibility between modern nuclear equipment and digital computers. As a result, it now is possible to record and process information from a radiation detection system in a highly automated manner.

In writing this monograph, the author has tried to keep in mind the needs of those nuclear chemists who, because they are not trained in electronics, find themselves confused by the bewildering array of equipment available for radiation measurement. The newcomer to the nuclear field is especially likely

---

*Operated for the U. S. Atomic Energy Commission by Union Carbide Nuclear Company.

to need guidance in selecting a counting system appropriate to his needs. Therefore, it was felt that a review of the nuclear radiation detection problem was in order, with particular emphasis on new methods and their practical aspects. A description of the subject matter is given below.

It will be convenient to consider first the detector, in which the radiation interacts. Each type of detector will be discussed both in terms of its principle of operation and its applicability to various problems in counting and spectrometry. The most common detectors make use of one of the two main processes by which radiation transfers energy to a stopping material, i.e., excitation and ionization. In the detectors to be discussed, molecular dissociation is of small importance; however, this effect is the basis of the chemical dosimeters which find important applications in health physics.

One of the most useful and versatile detectors now in use is the scintillation counter, which uses the fluorescent light emitted when charged particles pass through certain stopping materials. The basic process here is excitation, although the interaction of the stopping medium with the incident particle may involve ionization and molecular dissociation as well.

Several types of radiation detectors make use of the ionization produced by the passage of charged particles. This class of detector includes ionization chambers, semiconductor radiation detectors, proportional counters, and Geiger counters. If the incident radiation consists of charged particles such as alpha particles or electrons, the ionization is produced directly (primary ionization); however, uncharged species such as gamma rays or neutrons must first interact with the detector to produce charged particles, and the ionization in this case is a secondary process.

Although it is not usually necessary for an experimenter to be familiar with the details of the electronic circuits used in his equipment, it is essential that he should understand the functions and limitations of each component of his system. It is from this point of view that the discussion of auxiliary electronic instrumentation was written. No schematic diagrams are used to describe the various electronic devices--such details are available elsewhere; instead, the function of each instrument is described in more general terms. Block diagrams and wave forms are used where necessary. Care has been taken

to define the more important technical terms used for describing the performance of nuclear counting equipment, in the hope that this will help the experimenter interpret published specifications of commercial equipment.

Other topics which were deemed appropriate to this discussion of radiation measurement are low-level counting, absolute counting, and the mounting of radioactive sources. The subject of counting statistics was omitted, as this will be covered in a later monograph of the series.

A truly complete treatment of a subject as complex as nuclear radiation detection and measurement is obviously not possible in a survey of this length; however, each section includes a reading list. The following general reviews are recommended for a more detailed description of the principles and applications of detection methods than is given here:

1. D. R. Corson and R. R. Wilson, Rev. Sci. Instr., 19, 207 (1948); R. R. Wilson, D. R. Corson, and C. P. Baker, Particle and Quantum Detectors, Preliminary Report No. 7, National Research Council, Washington, D. C., January, 1950.
2. S. Flügge and E. Creutz, eds., Handbuch der Physik - Encyclopedia of Physics, Vol. XLV, Springer, Berlin, 1958.
3. W. H. Jordan, Ann. Rev. Nuclear Sci., 1, 207 (1952).
4. S. A. Korff, Electron and Nuclear Counters, D. Van Nostrand Co., New York, 1955.
5. W. J. Price, Nuclear Radiation Detection, McGraw-Hill, New York, 1958.
6. B. Rossi and H. H. Staub, Ionization Chambers and Counters, McGraw-Hill, New York, 1949.
7. K. Siegbahn, ed., Beta- and Gamma-Ray Spectrometry, North Holland Publishing Co., Amsterdam, 1955.
8. A. H. Snell, ed., Nuclear Instrumentation and Methods, Wiley, New York, 1962.
9. H. H. Staub in E. Segre, ed., Experimental Nuclear Physics, Vol. I, Part I, Wiley, New York, 1953.
10. D. H. Wilkinson, Ionization Chambers and Counters, Cambridge University Press, Cambridge, 1950.
11. L. C. L. Yuan and C. S. Wu, eds., Methods of Experimental Physics, Vol. 5A, "Nuclear Physics," Academic Press, New York, 1961.

II. SCINTILLATION METHODS*

1. Introduction

One of the earliest methods for detection of charged particles involved counting the scintillations produced in a phosphor screen. Such a device was employed by Rutherford and his collaborators in their famous study of alpha-particle scattering by nuclei. The scintillation method eventually gave way to electrical counters, which were more reliable and capable of functioning at high rates.

Modern scintillation counters followed closely the development of high-gain photomultiplier tubes. Combining various scintillating materials with a photomultiplier to count the scintillations has resulted in the most versatile detector available for nuclear research.

Present-day scintillation counters possess a number of advantages over gas counters: They not only indicate the presence of a particle, but also may be used to record the rate of energy loss, or the energy if the scintillator is thick enough. With the proper combination of scintillator and photomultipler tube, the detector is ideally suited to high counting-rate applications. The high density of solid or liquid scintillators has made the scintillation counter the most efficient gamma-ray detector available.

A functional diagram of a scintillation detector is shown in Fig. 1. The energy of the incident radiation is converted to light in the scintillator. The reflector and optical coupling ensure that this light is transmitted efficiently to the photocathode, where the light energy is converted to a burst of photoelectrons. An electrostatic focusing electrode collects the photoelectrons and focuses them on the electron multiplier structure.

The electron multiplier increases the number of electrons by secondary electron emission from a cascade of elements called dynodes. The multiplication of a typical dynode is about 4; hence, the overall current gain for the standard, 10-stage multiplier is $(4)^{10}$, or about 10^6. A variety of

*For general references on scintillation detectors and applications, see Bell,[1] Crouthamel,[2] Mott and Sutton,[3] Murray,[4] and O'Kelley.[5]

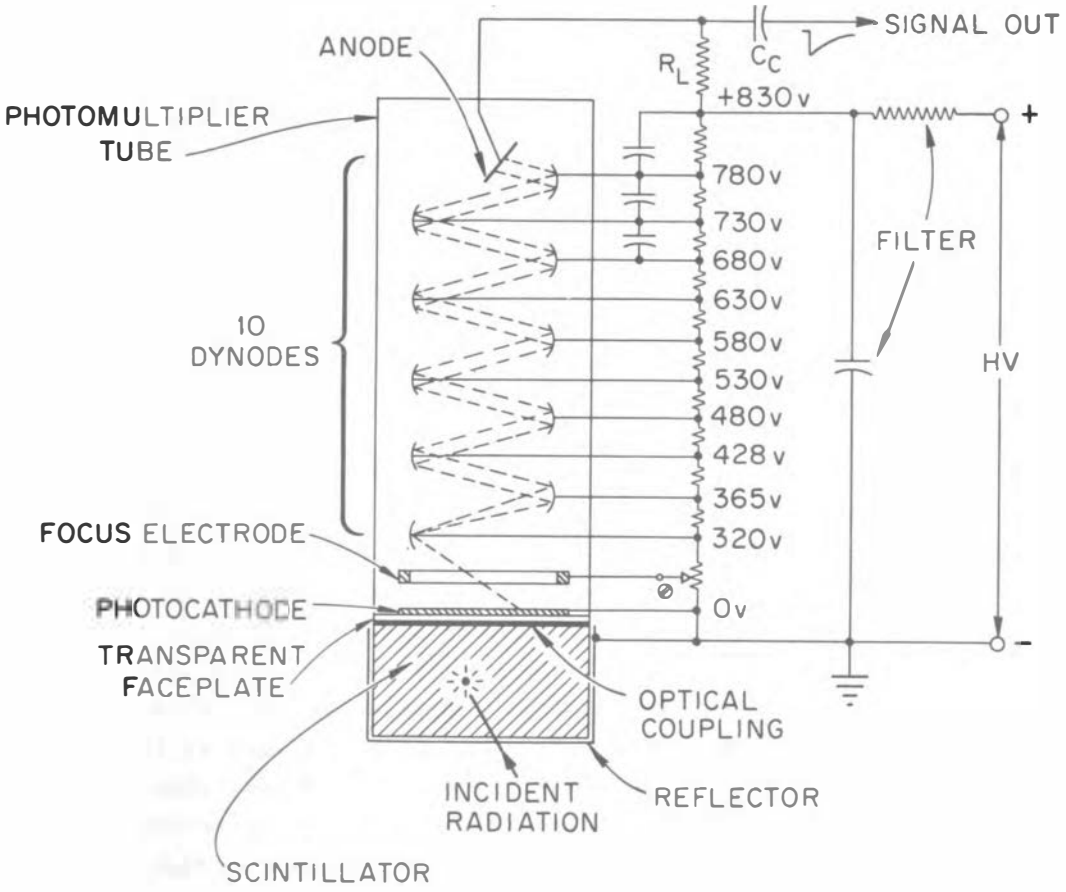

Fig. 1. Diagram of a scintillation counter, illustrating schematically the way in which light from the scintillator is coupled to a photomultiplier tube. A typical wiring diagram is shown for the 10-stage photomultiplier operated with a positive high-voltage supply.

10-stage photomultiplier tubes are available, with overall gains of (0.6 to 5.0) x 10^6.

When a burst of electrons arrive at the anode, the current which flows through R_L yields a voltage drop which is coupled to the measuring equipment through the blocking capacitor C_c. This negative output pulse will generally have an amplitude of a few millivolts to perhaps a few volts. The rise time of the pulse, that is, the time for the pulse to rise from 10% to 90% of its maximum height, is determined by the lifetime of the excited state in the scintillator which emits the light, and by the time spread introduced by the multiplier. The time for the signal pulse to return to zero is determined by the product of

the net anode load resistance (R_L in parallel with the input resistance of the amplifier) and the capacitance of the signal lead to ground.

2. Electron Detection and Spectrometry

The scintillation method is very well suited to the detection of electrons. This subject will be considered at the outset, not only because of its intrinsic interest, but also as a necessary preliminary to a discussion of gamma-ray detection, in which photons are detected by the secondary electrons produced.

A. Scintillators. Organic scintillators are best for spectrometry and counting of electrons and beta distributions, largely because of their low effective atomic number. A low atomic number reduces the probability of backscattering, in which an electron incident on a scintillator may scatter out, leaving only a fraction of its original energy in the scintillator. This effect is worst at low energies and for high-atomic-number scintillators. The organic scintillators have an additional advantage in that their gamma-ray sensitivity is low, so beta particles may be counted in the presence of moderate gamma-ray fields. To reduce gamma-ray interference, the minimum thickness of scintillator required for electron detection should be used. Further remarks on scattering and correction for gamma-ray background will be found below.

It is convenient to divide organic scintillators into two classes: single crystals and solutions. Anthracene is typical of the single crystals, and because of its early popularity in the formative years of scintillation spectroscopy, it has become the standard against which other scintillators are usually compared. Characteristics of anthracene and a number of other typical organic scintillators are shown in Table 1. It will be seen that although anthracene yields the largest light output of any organic scintillator, its fluorescence decay is the slowest listed; therefore, applications which demand very rapid pulse rise times may require a scintillator with faster response at a sacrifice in pulse height.

Although much useful work has been performed using scintillating crystals, the development of liquid and solid (plastic) solution scintillators has endowed scintillation

TABLE 1. ORGANIC CRYSTAL SCINTILLATORS
(From Mott and Sutton, reference 3)

Material	Density, g/cm³	Relative Pulse Height for β Excitation	τ_e, nsec[a]	Wavelength of Maximum Emission, Å
Anthracene	1.25	100	23 to 38	4450
trans-Stilbene	1.16	46	< 3 to 8.2	3850
p-Terphenyl	1.23	30	4.5	4000
p-Quaterphenyl	-	94	4.2	4350

[a] τ_e = time for decay to 1/e of initial light intensity; one nsec = 10^{-9} sec.

counting with new scope. The liquid scintillators have the advantage of easy fabrication in almost unlimited volumes. Plastic scintillators are mechanically rugged and can be readily machined. Both liquid and plastic solutions can be obtained with fluorescence lifetimes as short as the best crystalline scintillators. Some examples of solution scintillators will be found in Table 2.

TABLE 2. ORGANIC SOLUTION SCINTILLATORS
(From Hayes, Ott, and Kerr, reference 6)

Solvent	Primary Solute[a] (g/l)	Secondary Solute[a] (g/l)	Relative Pulse Height[b]	Wavelength of Maximum Emission, Å
Toluene	PPO(4)[c]	POPOP(0.1)	61	-
Toluene	TP(4)	POPOP(0.1)	61	4320
Polyvinyltoluene	TP(36)	POPOP(1)	51	4300
Polyvinyltoluene	TP(36)	DPS(0.9)	52	3800

[a] Solute abbreviations:
PPO = 2,5-diphenyloxazole;
TP = *p*-terphenyl;
POPOP = 1,4-di(2-(5-phenyloxazolyl))-benzene;
DPS = *p*-*p*'-diphenylstilbene.

[b] Pulse height for electron excitation, relative to anthracene pulse height as 100.

[c] PPO is preferred for low-temperature applications because of the poor solubility of TP in cold toluene.

Solution scintillators may be made from two, or more often three, components. The bulk material is the solvent, in which a scintillating substance termed the primary solute is dissolved; another scintillator, called the secondary solute or wavelength shifter, is also usually included. It is generally accepted that the incident particle first dissipates its energy by producing free electrons and ionized and excited molecules of the solvent. Then, most of the energy is transferred by nonradiative processes to the primary solute. The amount of energy so transferred depends on the overlap between the emission spectrum of the solvent and the absorption spectrum of the primary solute.

Many of the primary solutes which may be used with the common hydrocarbon solvents fluoresce at such a short wave length that a conventional photomultiplier tube cannot efficiently make use of the light; for this reason, the secondary solute is added to the solution. The absorption band of this latter solute should overlap the emission band of the primary solute. The final emission should be shifted to a longer wavelength which falls within the photomultiplier response and for which the absorption of light by the solution is small.

The solute concentration in solution scintillators is rather low. As will be seen in Table 2, the primary solute concentration ranges from a few per cent for plastics down to less than one per cent for liquids. The required concentration of secondary solute is only a few per cent of that of the primary.

It is a familiar and often distressing fact that the addition of certain impurities to liquid scintillators, even in small concentrations, decreases the light output enormously. Clearly, any additive which interferes with the energy transfer sequence will tend to quench the fluorescence. Such quenching will occur if the foreign substance has an absorption band at the emission wavelength for the solvent or one of the solutes and if the energy thus transmitted is dissipated by processes which do not give rise to useful light. The mechanism of quenching has been under study for some time in several laboratories and has been discussed in a number of review articles.[7,8,9]

The choice of a solvent for a solution scintillator depends upon the application. For liquid solutions xylene is

usually preferred, because it yields the greatest pulse height for a particular primary solute. On the other hand, toluene exhibits a much smaller absorption of the fluorescent light and is recommended where large volumes are required. Also, toluene does not react with some of the common light reflectors used in scintillation counters to the extent that xylene does. Other solvents are used in cases where it is necessary to introduce materials which are insoluble in toluene or xylene. For example, water is only slightly soluble in the usual scintillator solution, and it has a strong quenching effect. Aqueous solutions can be introduced by using *p*-dioxane as the solvent and then reducing the quenching effect with naphthalene. The details of liquid scintillator preparation, together with applications to various problems, will be found in several reviews.[6,10]

Except for the fact that they are solid solutions, the composition and fluorescence properties of plastic scintillators are similar to those of liquid scintillators. The only important base plastics (solvents) in use are polystyrene and polyvinyltoluene; some examples are given in Table 2. From the standpoint of convenience in machining and polishing, a plastic is to be preferred over anthracene; however, it should be borne in mind that the pulse height from a plastic is only about half that of anthracene, which leads to poorer resolution in electron spectroscopy. In counting applications and in spectroscopy at high electron energies, the plastics are highly recommended because of their convenience.

B. Detector Arrangements. Several ways in which organic scintillators may be used are sketched in Fig. 2. In (a) is shown the simplest arrangement, a cylindrical crystal optically coupled to a photomultiplier tube. While this detector may be used for counting beta particles or electrons, it is not suitable for measurement of low-energy spectra because of the backscattering effect already described. Above about 1.5 Mev the backscattering probability is reduced to a point such that beta-ray spectra can be determined accurately with this simple detector, provided that the shape of the low-energy part of the spectrum is of no concern.

The scattering problem can be circumvented in a number of ways. A helpful technique is to collimate the electron beam striking a flat scintillator surface to insure that the

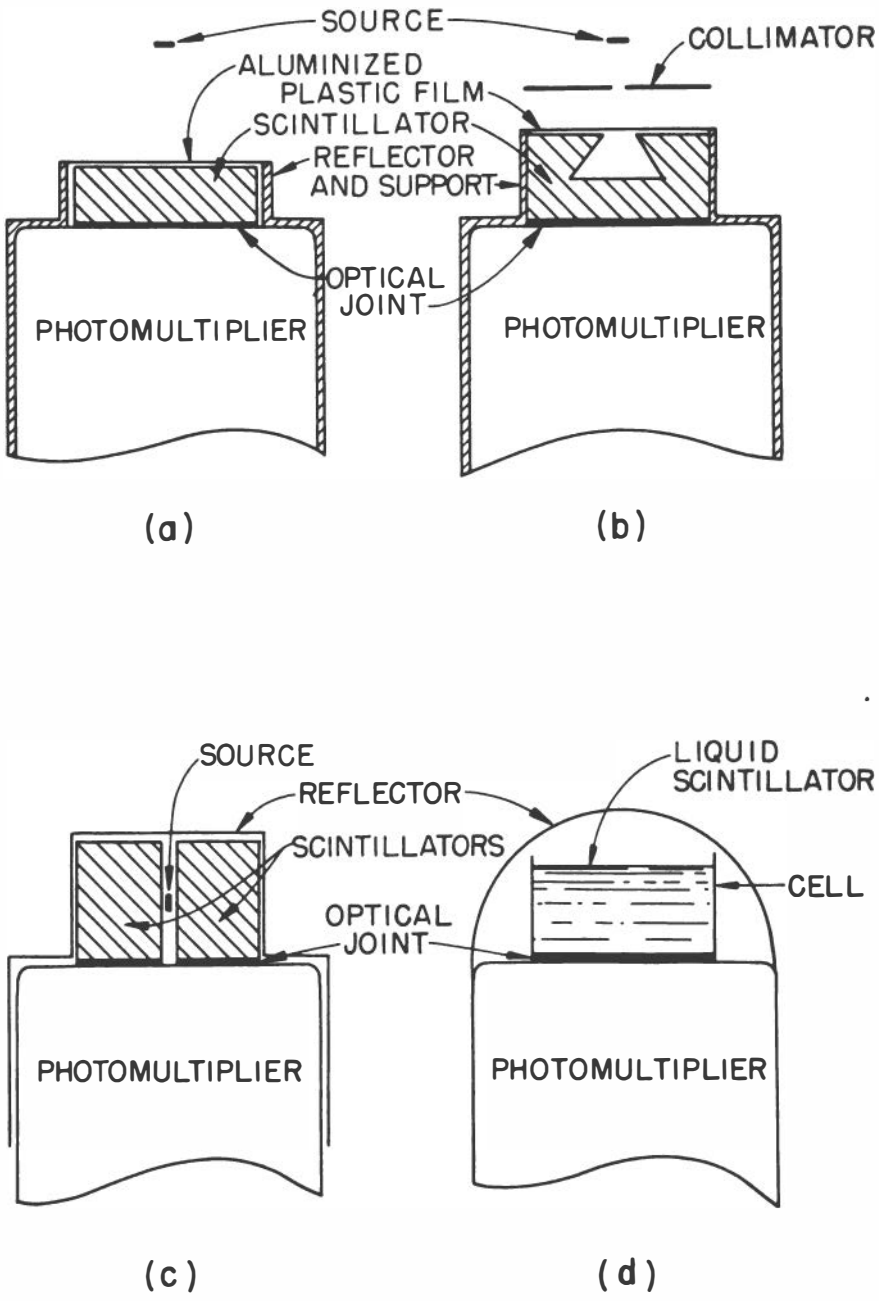

Fig. 2. Mounting arrangements for electron detectors using organic scintillators. (a) Flat scintillator. (b) "Hollow-crystal" spectrometer, with electrons collimated into a well. (c) "Split-crystal" spectrometer, in which the electron source is sandwiched between two scintillators. (d) A counter using a liquid scintillator, in which the beta emitter is dissolved.

particles will enter the surface near normal incidence and so will tend to penetrate deeply into the crystal before scattering. The "hollow-crystal" detector [see Fig. 2(b)] proposed by Bell[1] reduces the backscattering contribution by collimating the electrons into a conical hole in the scintillator, from which the probability of escape is low for the scattered electrons. Hollow-crystal spectrometers have for several years been used to measure beta spectra, and they have consistently given improved performance over a flat scintillator, both as regards energy resolution and backscattering.[11,12] A set of plastic scintillators machined and polished for use in hollow-crystal detectors is available commercially.*

Because all organic scintillators are somewhat gamma-sensitive, it is necessary to correct any beta spectrum data for the gamma-ray background, if the source is gamma radioactive. For the detectors sketched in Fig. 2(a), (b), this correction is obtained by interposing a beta absorber between source and detector and using the resultant gamma-induced spectrum for a "gamma background." Such a correction is only approximate, because the shape of the background spectrum obtained in this way is distorted by the contributions from bremsstrahlung and scattered photons produced in the absorber.

Another method for reducing the consequences of scattering is to surround the source with scintillator so that no scattered electrons are permitted to escape. This may be achieved in the "split-crystal" detector of Ketelle,[13] shown in Fig. 2(c). Here, the source is located between two scintillators arranged so that electrons scattered by one crystal are detected by the other. The nearly 4π geometry makes it difficult to measure the gamma-ray background with an absorber and leads to a high probability that gamma-induced counts may sum with pulses from coincident beta particles to yield a very confusing spectrum. Excellent spectra of "inner" beta groups have been measured with a split-crystal detector in coincidence with gamma rays[14] by use of beta-gamma coincidence techniques discussed in Section VI.7.

At low beta-particle energies (below about 200 kev), all of the methods described so far become rather difficult to

---

*Nuclear Enterprises, Ltd., 550 Berry Street, Winnipeg 21, Manitoba, Canada.

apply, because the response is somewhat sensitive to the treatment of the scintillator surfaces, and the source must be very thin to be free from scattering and absorption effects. These obstacles may be overcome by adding the radioactivity directly to an organic liquid scintillator, and thus making the source an integral part of the scintillator [Fig. 2(d)]. This is the basis of liquid scintillation counting, a method which has found widespread use in chemistry, particularly in tracer experiments using low-energy beta emitters such as C^{14}, S^{35}, Ca^{45}, and H^3. In some experiments it may be difficult to find a chemical form of the radioactive material which will not also quench the fluorescence. Liquid scintillation counting, including such special topics as the use of suspension and gels, is a rather specialized technique, and will not be treated further here; however, the interested reader will find useful information in some of the review articles[6,10,15] and in literature published by manufacturers of liquid scintillation counting equipment.

In addition to the general arrangements discussed above, there are a few other counting techniques which make use of the versatile plastic scintillators for special applications. One such technique for the assay of solutions is the use of scintillator beads proposed by Steinberg.[16] The detector is similar to that of Fig. 2(d), except the container is filled with small beads of plastic scintillator,* instead of a liquid scintillator. The solution whose radioactivity is to be determined is poured into the container; the liquid fills the interstices between the beads, and thus puts the liquid and solid phases in intimate contact. A suitable solution must be transparent to the light from the scintillator and must not attack the plastic beads; although these solution requirements somewhat restrict the use of the technique, the preparation of a sample can be extremely rapid, and the beads can be washed and used repeatedly.

Plastic scintillators may be conveniently fashioned into many other shapes. Plastic scintillator dishes for containing radioactive liquids may be mounted directly on a photomultiplier

*Suitable beads are: "B-Beads," manufactured by Pilot Chemical Co., 39 Pleasant Street, Watertown 72, Massachusetts; or NE 102 Spheres, obtainable from Nuclear Enterprises, Lts., 550 Berry Street, Winnipeg 21, Manitoba, Canada.

tube for counting. Capillary tubing made from plastic scintillator can be wound into a spiral and attached to a photomultiplier to make a very simple flow counter for beta-radioactive gases and liquids. Devices of this sort are available commercially.*

C. Electron and Beta Spectrometry. In addition to their use as counters, these organic scintillators are useful for determining electron and beta-ray energies. The consensus of the available experimental information indicates a linear pulse height-energy curve down to a low energy of ~100 kev; below this energy the response is also nearly linear, but with a slightly different slope.[17]

The response of an organic scintillator to monoenergetic electrons is mainly a gaussian peak whose width varies inversely with the square root of the energy. This energy dependence is predicted from the statistical variation in the number of photoelectrons at the photocathode and the electron multiplication processes within the photomultiplier tube; hence, the contibution to the peak width by the scintillator itself is small. For an anthracene hollow-crystal spectrometer a resolution (full width at half-maximum counting rate) of about 10% can be achieved at 624 kev, but if a plastic scintillator is used the resolution is only about 14%, because of the lower light output of the plastic.

Although the resolution of the electron scintillation spectrometer is poor compared with that of a magnetic spectrometer, the scintillation method has some appealing features. Used with a multichannel pulse-height analyzer (cf., Section VI.6.B., below) to display the distribution of pulse height ($\propto$ energy), it is possible to record the entire beta spectrum in a single counting interval. On the other hand, the magnetic spectrometer is a single-channel instrument, which can record only a single point on the spectrum at one time. The advantage of the scintillation spectrometer in studies of rapidly decaying sources is obvious. Further, the required scintillation detector is relatively inexpensive. Such simple spectrometers should find increased use in the analysis of mixtures of pure beta emitters and in distinguishing between tracers which possess similar gamma-ray spectra.

*Nuclear Enterprises, Ltd. 550 Berry Street, Winnipeg 21, Manitoba, Canada.

Before a careful analysis of the beta spectrum shape can be made, the pulse-height distribution must be corrected for finite instrumental resolution. This is especially important for beta-ray endpoints below about 1 Mev. Corrections for finite resolution can be made by using the method of Owen and Primakoff,[18] and assuming that the scintillator response is a gaussian whose width varies as $E^{-1/2}$. It was shown by Freedman, et al.,[19] that such a procedure corrected the spectrum near the maximum beta energy but did not account for the excess of events at low energies. This excess counting rate arises from scintillator backscattering, which is never completely eliminated in a low-geometry arrangement [for example, the detectors of Fig. 2(a) and (b)]. The typical response of a flat anthracene spectrometer to the electrons and beta rays from a Cs^{137} source is shown in Fig. 3, which includes a spectrum due to the internal conversion peak alone. It is seen that the backscattering "tail" is almost flat, and is about 6% of the peak height. Freedman, et al.,[19] developed an iterative method to correct the experimental data for both backscattering and resolution effects.

A comparison is made in Fig. 4 between two Fermi plots of the low-energy beta group of Cs^{137}. The upper curve shows the result obtained when the resolution distortion correction alone is applied, and the lower curve shows the improvement in the quality of the low-energy data when corrections are made for both resolution and backscattering.

The conventional correction procedures break down for beta groups below about 100 kev. This is because the resolution width becomes so large that most of the counts which appear to arise from events in the high-energy portion of the spectrum are actually due to low-energy electrons which fall within the detector resolution. Some idea of the resolution width at low energies can be gained by recalling that a good organic scintillation spectrometer with a resolution of 14% at 624 kev (Ba^{137m} conversion electrons) will exhibit a resolution of about 50% at 50 kev. These difficulties make it advisable to employ empirical corrections derived from data on low-energy beta emitters whose energies and spectral shapes are well known.

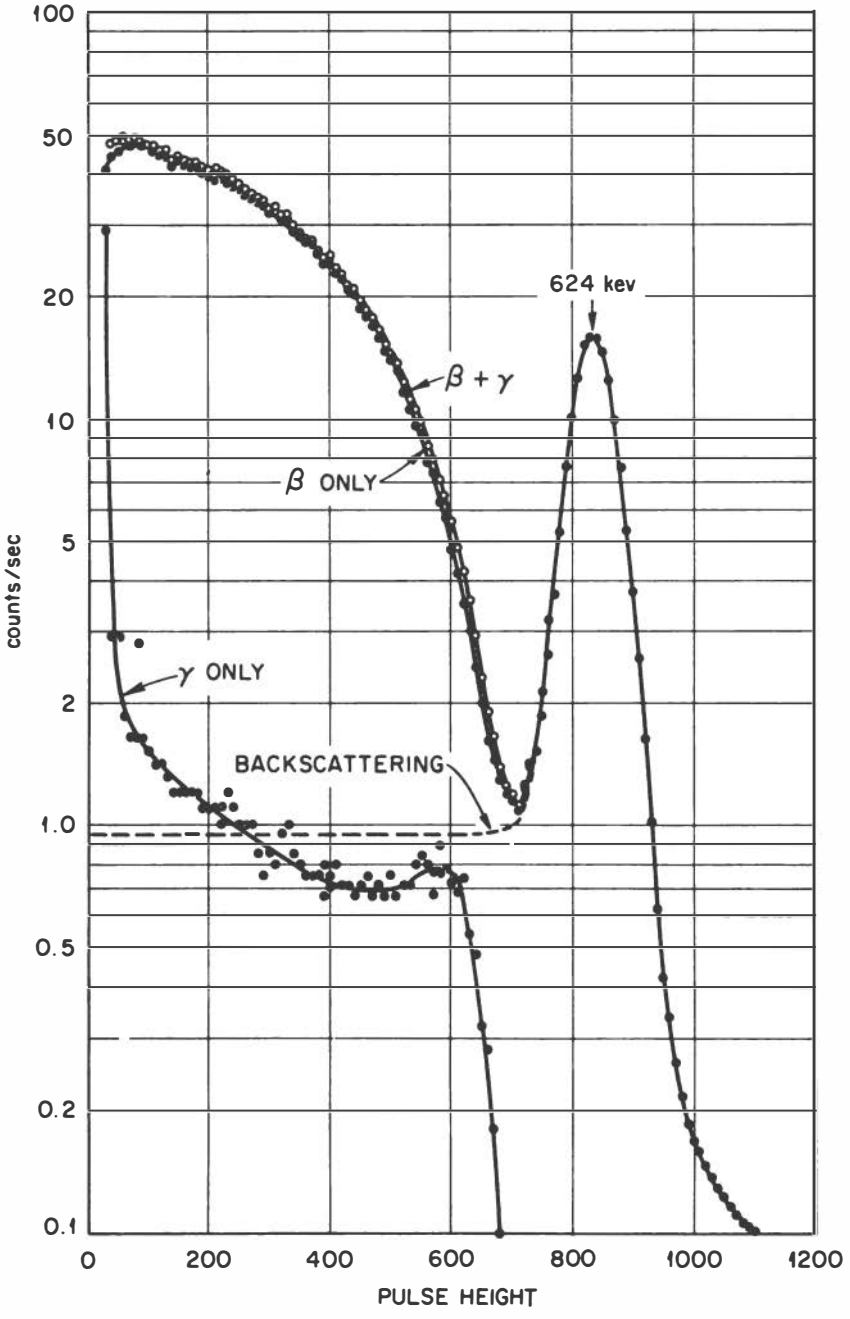

Fig. 3. Spectrum of a Cs^{137} source, measured on a flat anthracene crystal. The internal-conversion electron line at 624 kev and the continuum from the 523-kev beta group are shown. When the beta rays and electrons are stopped in an absorber, the background spectrum from the 662-kev gamma ray is obtained. A coincidence between 624-kev electrons and their associated X rays excludes the beta and gamma spectra, and leaves only the electron line and its scintillator backscattering spectrum.

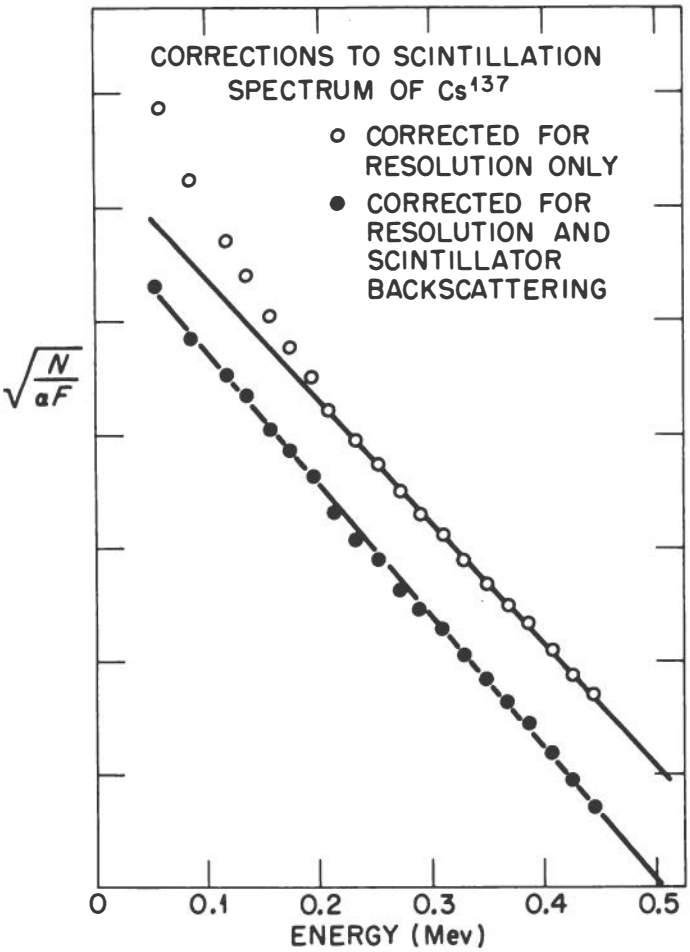

Fig. 4. Fermi plots of the low-energy beta-ray group of Cs^{137}. The upper curve was corrected for the unique spectrum shape and the scintillation spectrometer resolution. The lower curve shows the improvement obtained when the correction for scintillator backscattering is included (Gardner and Meinke[11]).

3. Gamma-Ray Counting and Spectrometry

A most important contribution of the modern scintillation technique has been made in the field of gamma-ray detection. The much higher density of solid gamma-ray scintillators gives them a stopping power (i.e., detection efficiency) for photons far greater than gas-filled counters. It is now quite feasible to prepare scintillating crystals large enough to stop completely a sizeable fraction of incident gamma rays; thus it is possible not only to count gamma events, but also to measure

energy spectra and gamma-ray intensities as well. The realization of these possibilities has put in the hands of the research chemist a versatile, precise tool.

A. Scintillator Considerations. To be effective for gamma-ray detection, a scintillator should be of high density and high atomic number; these requirements are best satisfied by the inorganic scintillators. Although there are many scintillating inorganic materials, only the activated alkali halides can be grown in single crystals of sufficient size and yet possess the required transparency to their emitted light.

Sodium iodide, activated with 0.1% TlI, is the only alkali halide scintillator in routine use. It has the high density of the alkali halides and has a moderately high effective atomic number. The light output in NaI(Tl) per Mev is the largest of any known scintillator and is about twice that of anthracene. Large single crystals of NaI(Tl) are readily obtainable and are highly transparent to their own fluorescent light, which is emitted in a band about 800 Å wide, centered at 4100 Å. This wavelength is quite compatible with the response of standard photomultipliers having an S-11 response. (See the discussion of photomultipliers in reference 3.) The fluorescence decay time is 0.25 μsec, comparatively short for an inorganic crystal.

Because of its higher effective atomic number, thallium-activated cesium iodide has been investigated as a gamma-ray scintillator. At present, crystals of CsI(Tl) are far more expensive to manufacture than crystals of NaI(Tl). Further, although moderate pulse-height resolution can be obtained, the usable light output is only about 40-45% that of NaI(Tl). This lower apparent output may arise because the fluorescent light is emitted at longer wavelengths, namely 4200-5700 Å, and consequently cannot be measured efficiently by an S-11 photomultiplier tube. Improved pulse height could probably be attained by using a photomultiplier tube with better response in the red, such as the low-noise, multialkali-cathode tubes. The decay time of the fluorescent light from CsI(Tl) is 1.2 μsec, which is rather long for many applications.

B. Mounting Sodium Iodide Crystals. The method chosen for mounting a NaI(Tl) crystal on its photomultiplier tube involves a consideration of the deliquescence of the crystal, its optical properties, and the necessity for avoiding gamma-ray scattering. For some uses the two latter considerations may be

relatively unimportant, but in all cases it is necessary to take great care that the crystal surfaces are not exposed to moisture. The usual procedure is to prepare a crystal for mounting in a dry-atmosphere box; once mounted, the crystal enclosure should contain a dry atmosphere or else be evacuated.

Whenever the largest possible light output is required, as in gamma-ray spectrometry, it becomes very important to gather the light and transmit it to the photomultiplier tube with the least possible attenuation. This is especially difficult when NaI(Tl) crystals of refractive index 1.77 must be optically coupled to glass faceplates with a refractive index of 1.5, because, if the surfaces are polished, much of the light tends to be critically reflected back into the crystal. The use of diffuse reflection at the crystal surfaces has been found to give higher and more uniform light output than specular reflection, since the probability is increased for light to be reflected onto the exit face of the crystal within the critical angle. The diffuse reflector surface is formed on the crystal by grinding all crystal surfaces, including the exit face. Any light escaping from the other crystal surfaces should also be returned by a diffuse reflector such as magnesium oxide or α-alumina.

If the NaI(Tl) detector is to be used as a spectrometer, it is important that any material surrounding the crystal be very thin. Otherwise, the gamma-ray spectrum will be distorted by Compton electrons and degraded gamma rays.

A crystal mount which used an enclosure made of 5-mil aluminum, coated on the inside with a thin optical reflector of α-alumina, was devised by Bell and co-workers[1] for use where crystal and photomultiplier were of approximately the same diameter. Detailed procedures for fabricating the metal can and applying the reflector have been published.[5] Figure 5 shows a crystal mount which is more easily mass-produced, and uses magnesium oxide powder as the diffuse optical reflector. Similar crystal-photomultiplier assemblies with good resolution are also available commercially.*

The light transmission from the crystal to the photomultiplier should be as efficient as possible; for this reason

*Harshaw Chemical Company, 1945 East 97th Street, Cleveland 6, Ohio.

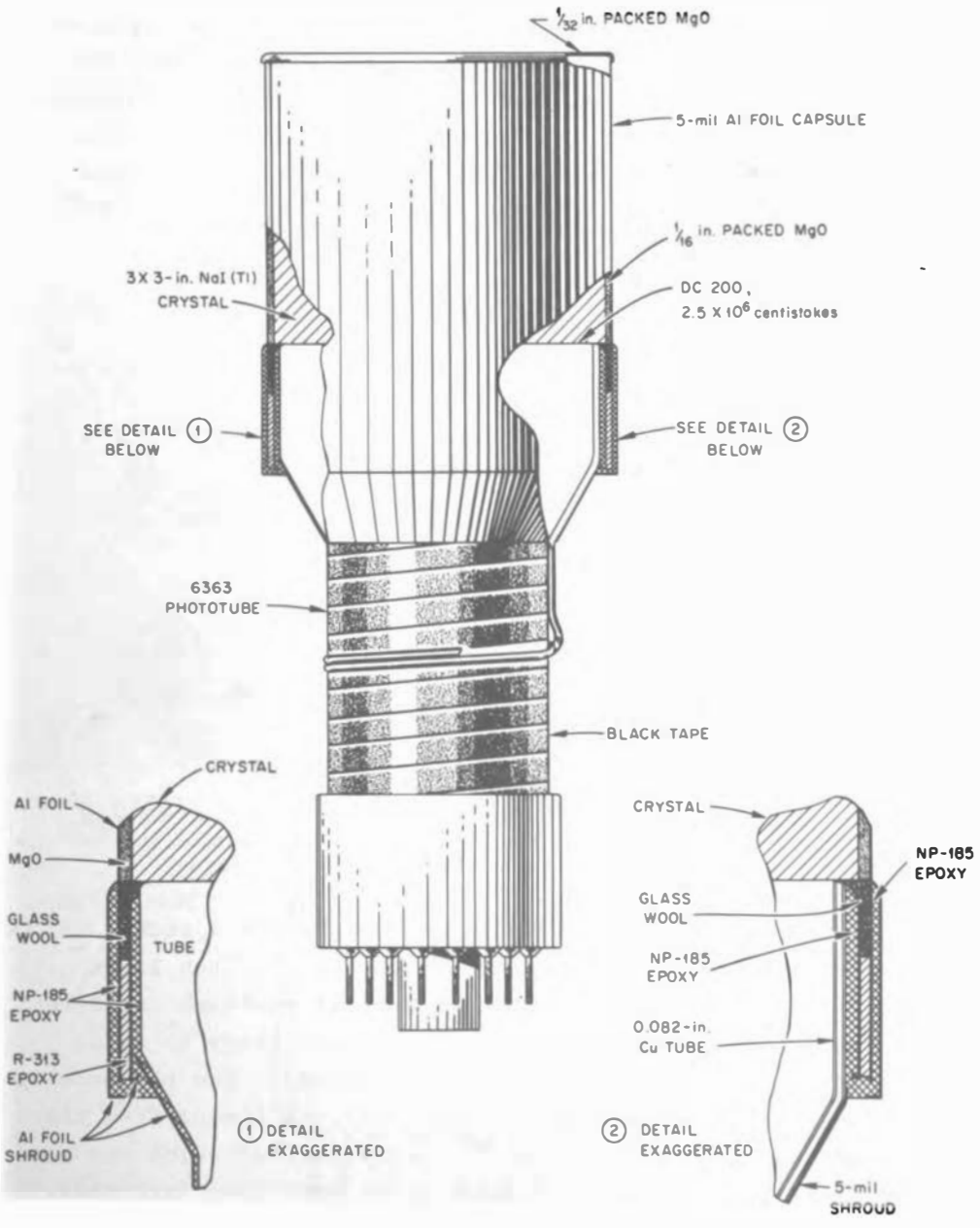

Fig. 5. Integral crystal mounting arrangement for a 3 x 3-inch NaI(Tl) crystal and 3-inch photomultiplier tube (V. A. McKay, Oak Ridge National Laboratory).

the crystal generally should be attached to the phototube by a single optical joint. In noncritical applications, such as simple counting, the loss of light from an additional optical seal and window may not be important. Here, an assembly is often used consisting of a crystal enclosed with its reflector in a thin can and optically coupled to a transparent window. Various crystal assemblies may then be attached to the same photomultiplier tube as required. Examples typical of such crystal mounts are shown in Fig. 6.

Fig. 6. Sealed NaI(Tl) crystal assemblies for a variety of applications. Transparent windows are provided for optical coupling to photo-multiplier tubes (Harshaw Chemical Company).

Mounting NaI(Tl) crystals larger than about 3 inches in diameter calls for a more elaborate technique. Such large crystals are very heavy, and the mechanical problems involved in constructing a large detector make it necessary to relax somewhat the requirements of a thin container. The response of a large crystal is not as sensitive to scattering from the container walls as are the smaller crystals, for which the mass ratio of NaI(Tl) to cladding material is much less favorable.

C. Special Counting Problems. Whenever gamma-emitting nuclides are used in radiochemistry some variation of the versatile NaI(Tl) scintillation counter is nearly always used. It will be the purpose of this section to set down a few of the uses to which these counters have been put.

Perhaps the most generally useful configuration is the well counter (see Fig. 7). Various sizes are available; an

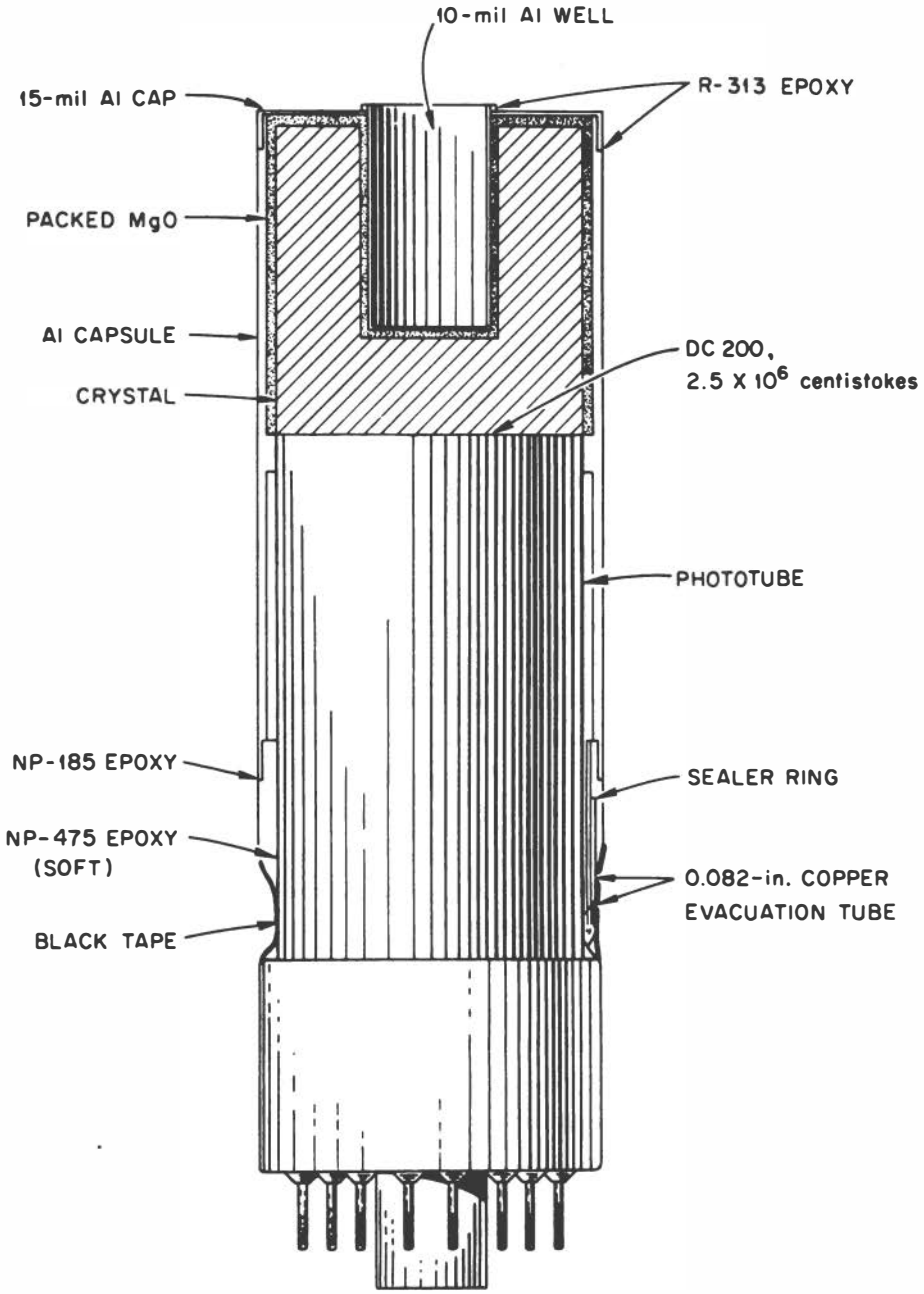

Fig. 7. An integral mounting arrangement for a 2 x 2-inch NaI(Tl) "well-type" crystal on a 2-inch photomultiplier tube (V. A. McKay, Oak Ridge National Laboratory).

inexpensive, yet efficient, detector is a NaI(Tl) crystal, at least 2 x 2 inches, with a 3/4-inch diameter well about 1-1/4 inches deep. Once the crystal has been mounted in a thin aluminum enclosure and a protective liner has been inserted to avoid the chance of permanent contamination of the crystal can, about 1/2 inch of the original diameter will be left for insertion of samples. The well counter is the most sensitive gamma-ray detector available and certainly one of the most convenient. To prepare a sample may involve only the transfer of a few ml of solution to a small test tube. Because of the penetrating nature of gamma rays, self-absorption in such sources is small, and further treatement of the sample to reduce the mass is usually not necessary. Commerical well-crystal counters are available which provide automatic sample changing and count recording for many samples.

In certain cases it may be desirable to assay large volumes of solution directly. A variation of the once-popular immersion counter is sketched in Fig. 8; if a 3 x 3-inch crystal is surrounded by solution as shown, samples of several liters can be accommodated. A more compact assembly uses a 3/4-inch diameter NaI(Tl) crystal, 3 inches long. The manufacturer* states that the efficiency of this detector is one-fifth that of a typical well-crystal with 5-ml capacity, but has a sample volume 30 times greater.

The increasing need to make measurements of flow systems has led to several modifications of the scintillation counter for use with both liquids and gases. An excellent flow counter can be made from a length of plastic tubing either laid across the face of a NaI(Tl) detector, wrapped around it, or the tubing may be doubled into a U and inserted into a well crystal. Crystal packages are also available with a hole drilled through along a diameter, so that a tube passing through the crystal is surrounded by NaI(Tl); an example is included in Fig. 6.

Other special methods which involve spectrometry rather than integral counting will be discussed in the following section.

D. Gamma-Ray Spectrometry. One of the most important applications of the NaI(Tl) scintillation detector is in the

*Atomic Accessories, Inc., 813 West Merrick Road, Valley Stream, New York.

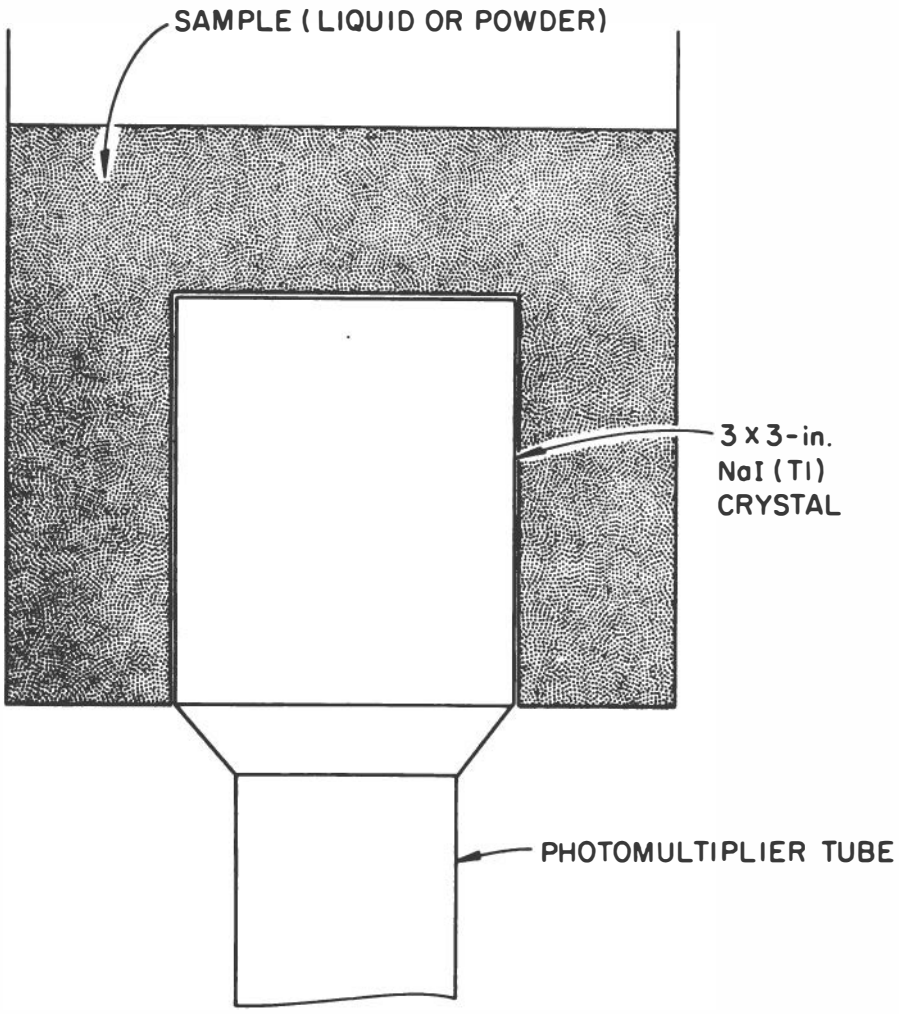

Fig. 8. Illustration of a way to obtain high counting efficiency for a scintillation counter used with large counting volumes.

field of gamma-ray spectrometry. Now that large, clear crystals of NaI(Tl) and photomultiplier tubes with uniform high-efficiency photocathodes are available, it is possible to make a spectrometer which will not only measure energies of gamma rays to high precision but also yield their intensities. Much of the popularity of the NaI(Tl) scintillation spectrometer in radiochemistry lies in its ability to differentiate between various gamma-ray components; hence, the presence of a particular nuclide in the spectrum of a mixture can be established by the characteristic energies observed, and the

amount of the nuclide can be determined quantitatively from the appropriate gamma-ray intensities.

Interaction of Gamma Rays in NaI(Tl). It should be recalled that gamma rays as such are not detected, but rather it is the secondary electrons produced by the interaction between the gamma rays and the crystal which give rise to the fluorescent light. Thus it is appropriate to discuss briefly the three processes (photoelectric effect, Compton effect, and pair production) by which gamma rays interact, in terms of their effects on the response of the scintillation spectrometer.

Partial absorption coefficients in NaI for these processes are shown in Fig. 9. Below about 100 kev, the photoelectric

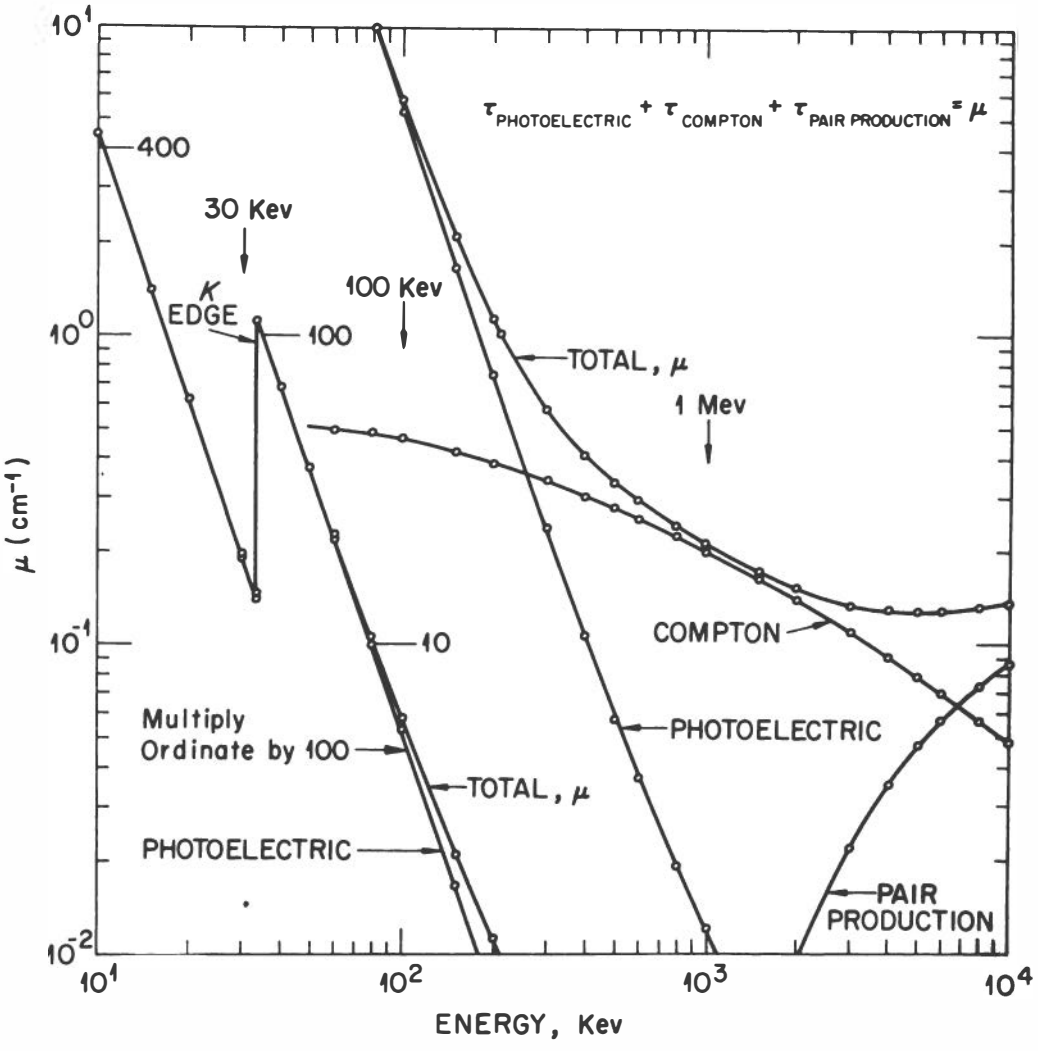

Fig. 9. Gamma-ray absorption coefficients in NaI(Tl) for various gamma-ray energies (Bell[1]).

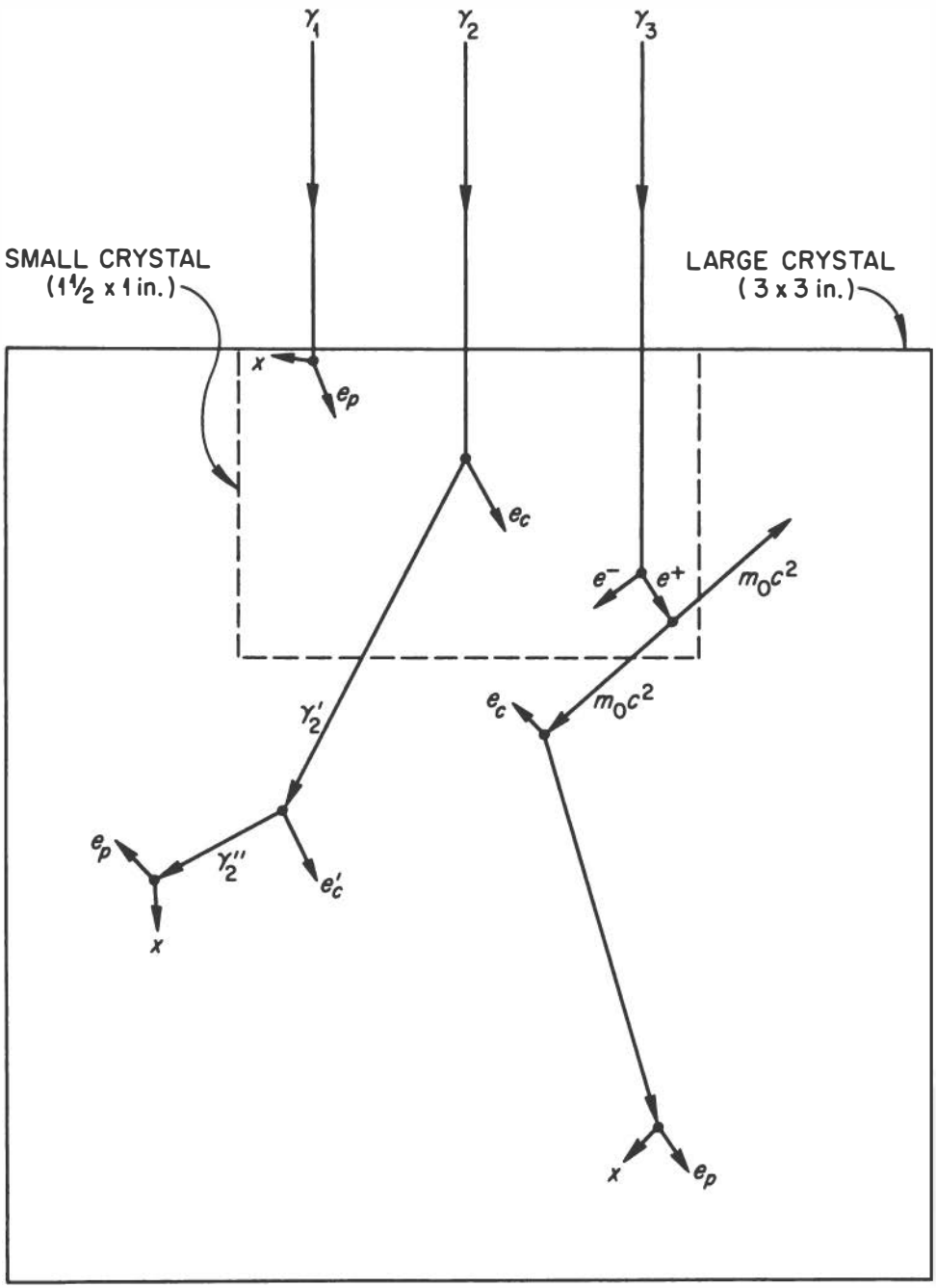

Fig. 10. Schematic representation of gamma-ray inter-interactions within NaI(Tl) crystals of two sizes.

effect is by far the most probable; however, the photoelectric effect shows such a rapid decrease in absorption coefficient with increasing energy, that the Compton effect is left as the dominant process in the intermediate-energy region. Pair production, which sets in at 1.02 Mev and increases rapidly in probability thereafter, becomes the most important of the processes at very high energies. In all of these processes, it is predominantly the iodine of NaI which, because of its high Z, interacts with the gamma rays.

An attempt to demonstrate qualitatively the practical importance of the effects listed above is shown in Fig. 10. The low-energy gamma ray γ_1 undergoes a photoelectric encounter within the first 1/8-inch of material through which it passes. The photoelectron, which has a very short range, is stopped in the NaI(Tl) and gives up its energy to the crystal. The iodine atom which released the electron is left with a vacancy, most probably in its K shell; the act of filling this vacancy yields a K X-ray. Usually the iodine X-ray is captured by the crystal, for its energy is only about 28 kev; however, since low-energy gamma rays are always stopped near the crystal surface, there exists a small but significant chance that the X-ray may escape the crystal surface entirely, and give a peak whose energy corresponds to the gamma energy minus the 28 kev of the X-ray.

Above a few hundred kev, multiple processes play an important role, and so it becomes necessary to take into account the crystal size in addition to the various absorption coefficients. In Fig. 10, γ_2 illustrates a Compton scatter by an intermediate-energy gamma ray. The Compton electron e_c is stopped and yields a light pulse proportional to the electron's kinetic energy; on the other hand, if the crystal is small the scattered photon γ_2' may not be stopped, and its energy will then be lost. The figure shows that in a larger crystal, further Comptron processes may occur until the energy of the scattered photon is reduced to an energy so low that a photoelectric event finally transfers the remaining gamma energy to the crystal. It is important to bear in mind that the stepwise process just described occurs very rapidly, compared with the speed of present-day electronic instruments; therefore, the interactions of γ_2 in the 3 x 3-inch crystal of Fig. 10 would give rise to a single electrical pulse whose height would correspond to the total energy of γ_2.

Pair production introduces a very complicated response, as illustrated by the case of γ_3 in Fig. 10. A high-energy gamma ray forms a positive and negative electron pair which carry off as kinetic energy the original gamma-ray energy, minus the 1.02 Mev (two electron rest masses) required to create them. The two short-range electrons stop, and their kinetic energy is acquired by the crystal. The positron annihilates, forming two photons, each with an energy of 0.51 Mev (m_0c^2) and correlated at 180^o. Once pair production occurs, the response depends on the probability that the annihilation photons will be captured. The example in Fig. 10 shows that in a small crystal, the probability is greatest for the escape of both photons; in a larger crystal, it is more likely that at least one of the photons will be stopped. To summarize, then, the pair-production response leads to three peaks in the pulse-height distribution: the full-energy peak, which corresponds to the capture of all the incident gamma-ray energy by the multiple processes; the "single-escape" peak, which signals the loss of one annihilation photon; and the "double-escape" peak, which indicates the loss of both annihilation photons.

Typical Gamma-Ray Spectra. The effects just described are illustrated by some representative gamma-ray spectra in Figs. 11-13. More detailed explanations will be found in references 1, 2, 5, and 20. Because the light output from NaI(Tl) is very nearly linear with respect to the energy deposited, the distribution in the height of the pulses from various NaI(Tl) scintillation spectrometers will be treated as energy spectra. All of the gamma-ray spectra described below will have semilogarithmic intensity scales and linear pulse-height (or energy) scales. This has the decided advantage that the wide range of counting rates encountered in gamma spectrometry can be easily accommodated; further, spectral shapes can be compared by superimposing two spectra plotted on the same log paper with identical energy scales, even though the absolute heights of the peaks may be very different.

A typical spectrum from a low-energy gamma ray is shown in Fig. 11. Although a large peak is present, arising from 22-kev X rays in the sample, let us direct our attention to the gamma-ray peak at 88.5 kev. Nearly all of the events in this peak are from the photoelectric effect near the crystal surface (cf., γ_1 of Fig. 10); a peak about 28-kev lower is due to

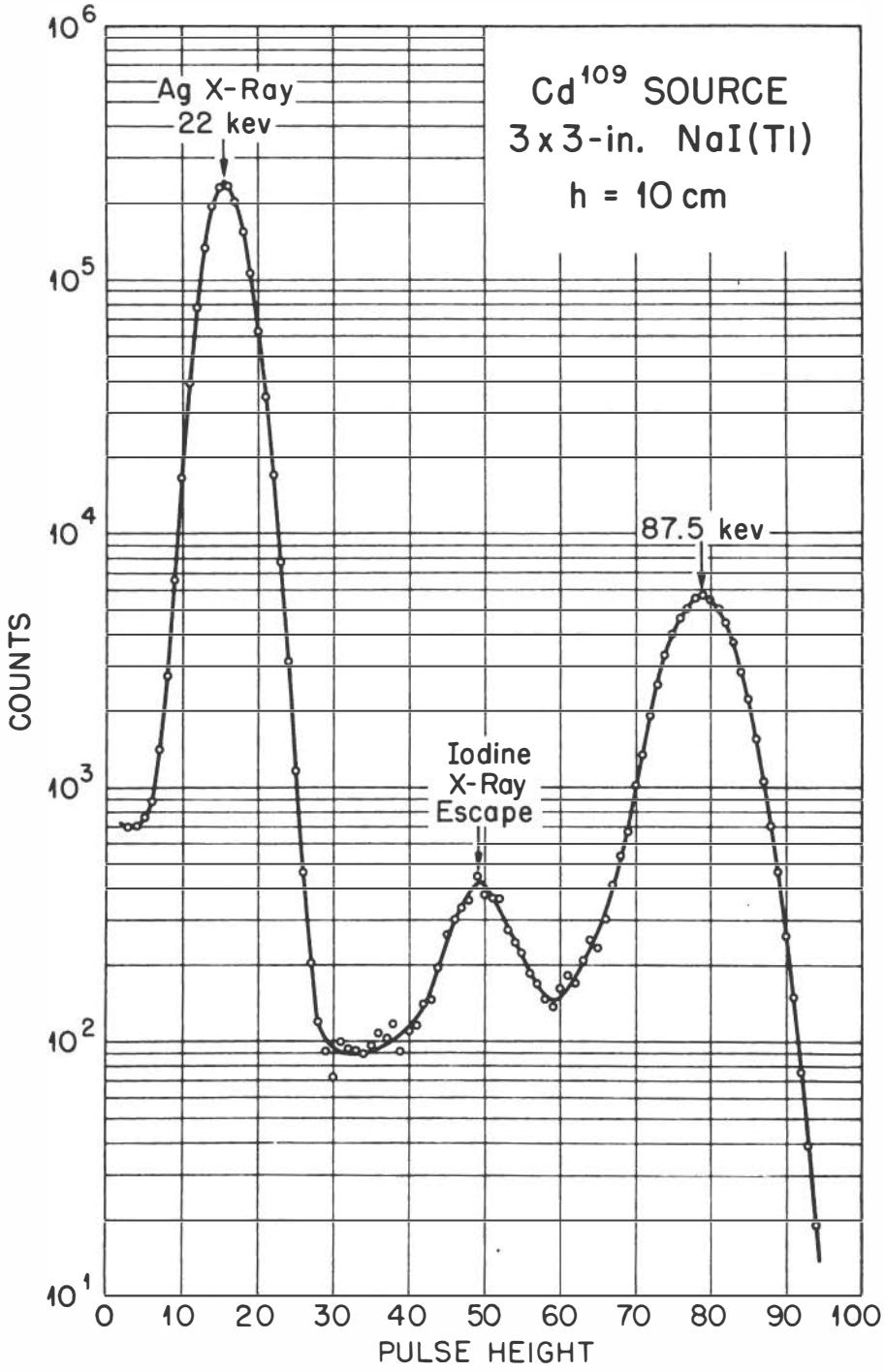

Fig. 11. Spectrum of 87.5-kev gamma rays and 22-kev X rays from a Cd^{109} source, illustrating the phenomenon of X-ray escape following detection of 87.5-kev gamma rays.

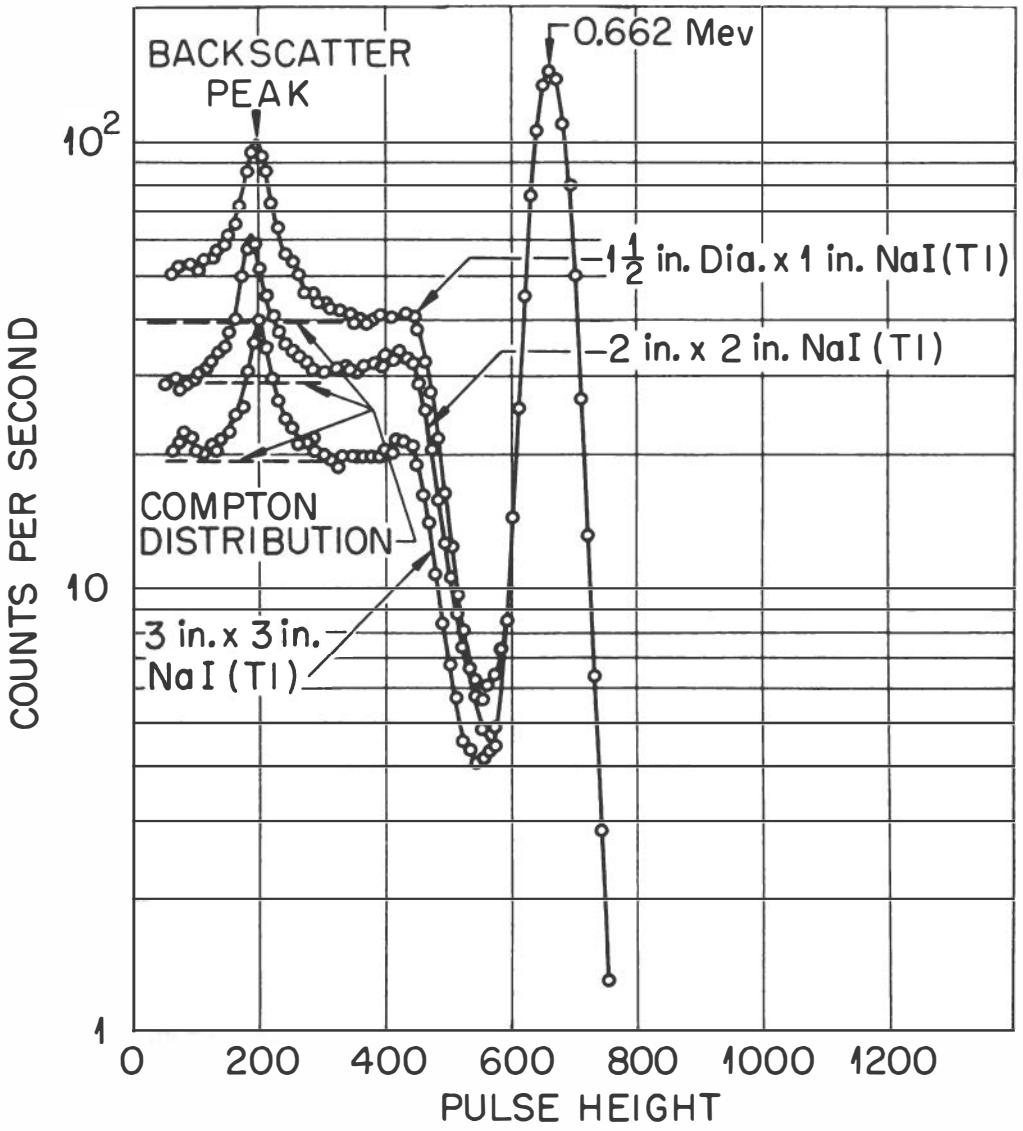

Fig. 12. Spectra obtained by measuring a Cs^{137} source with NaI(Tl) spectrometers of three crystal sizes (Heath[20]).

escape of the iodine K X-rays. As the gamma-ray energy increases, the photons penetrate more deeply into the crystal before they undergo photoelectric absorption, and so the probability for X-ray escape diminishes. In addition, because the energy separation between the full-energy peak and the X-ray escape peak is a very small fraction of the gamma energy, the X-ray escape phenomenon is not observed above about 170 kev.

A comparison is sketched in Fig. 12, which shows the spectra obtained at 0.662 Mev with NaI(Tl) crystals of different sizes. All of the spectra are normalized at the maximum of the full-energy peak. The smallest crystal yields a characteristic distribution below the main peak which results from an event in which a Compton-scattered photon is lost and the Compton electron is captured (cf., Fig. 10). It will be noted that as the crystal size increases, the probability for multiple processes also increases; this is manifested in an increase in the fraction of events falling within the main peak. Figure 12 shows that the ratio of the height of the full-energy peak to that of the Compton distribution is nearly twice as great for a 3 x 3-inch as for a 1-1/2 x 1-inch crystal. Of course the more nearly the response approximates a single peak for a single gamma-ray energy, the more useful the spectrometer becomes.

The complexity of the spectrum when pair production is involved may be seen in the spectrum of Na^{24} shown in Fig. 13. Two gamma rays are present in this source at 1.38 and 2.76 Mev. The full-energy peak and the two pair peaks stand out clearly in the high-energy portion of the spectrum. Note that in the smaller crystal there are relatively few multiple events leading to counts in the full-energy peak; in fact, the double-escape peak is the most intense of the three. This response may be contrasted with that of the 3 x 3-inch crystal, in which the contribution from multiple events has made the full-energy peak the most intense. Further, the probability of double escape is quite low. It may be of interest to note that the spectrum of the 1.38-Mev gamma ray shows no evidence of pair peaks; in practice, the effect of pair production is not detectable below about 1.5 Mev, even though the threshold falls at 1.02 Mev.

Environmental Effects. The gamma-ray spectra measured in a given situation will be complicated, in addition to the elementary interactions just described, by several important environmental effects. While space does not permit a complete treatment of such spurious responses here, a report by Heath[20] includes a valuable analysis of various experimental factors; some of Heath's findings as well as other related data will also be found in reference 5.

In the discussion which follows it will be convenient to

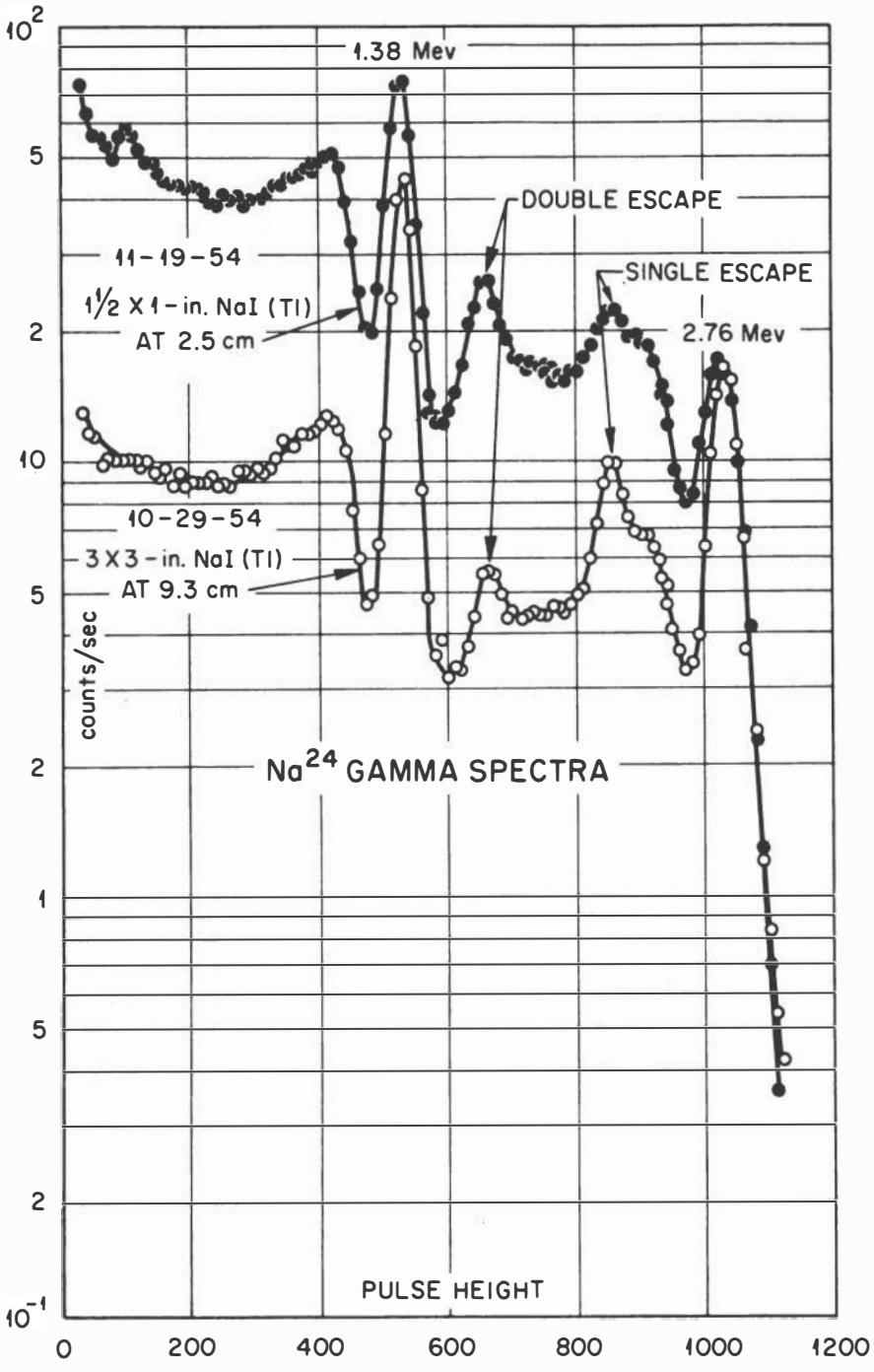

Fig. 13. Gamma-ray spectra of Na^{24}, using 1-1/2 x 1-inch and 3 x 3-inch NaI(Tl) spectrometers.

refer to Fig. 14, which shows a typical arrangement for a 3 x 3-inch NaI(Tl) detector situated in a Pb shield.

One of the most persistent experimental difficulties is scattering, whose consequences may take various forms. It is easy to show that, for Compton scattering at large angles, the energy of the scattered photon is nearly independent of the incident gamma-ray energy, and attains an almost constant value around 200 kev. Thus, large-angle scattering from shield walls, source holder, or other matter in the vicinity of the source (cf., Fig. 14) will be manifested as a peak at about 200 kev. This peak is generally called the backscatter peak. It may be reduced by making the inside dimensions of the shield very large, thus decreasing the geometry between the detector and shield walls. Heath[20] demonstrated that a shield made from lead yielded a much smaller backscatter peak than one made from iron.

Another form of scattering arises from the beta-ray absorber which is usually placed between the source and the detector to stop beta particles or electrons from the gamma-ray source. Because of the geometry involved, the scattering is restricted to small angles, and so the scattered photons detected in the NaI(Tl) crystal are only slightly reduced in energy. This has the effect on the gamma spectrum of filling in the "valley" between the Compton-electron distribution and the full-energy peak.

Secondary radiation from the shield walls may cause serious complications. If bare lead walls are used in a spectrometer shield and a source of low-energy gamma rays is inserted, then fluorescent lead X-rays are emitted from the walls and are detected by the NaI(Tl) crystal, causing a spurious 72-kev peak in the gamma spectrum. The mechanism for X-ray production is similar to that discussed above for X-ray escape from NaI(Tl) crystals. The best way to remedy this situation is to cover the lead surfaces with a sufficient thickness of a medium atomic number material, usually Cd, to attenuate the Pb X-rays to a negligible level; the Cd is covered in turn by a thin veneer of Cu to absorb any fluorescent radiation from the Cd.

When very intense high-energy gamma rays are present in the source, it is common to observe a peak at 0.511 Mev in the gamma-ray spectrum. This peak is due to pair production in

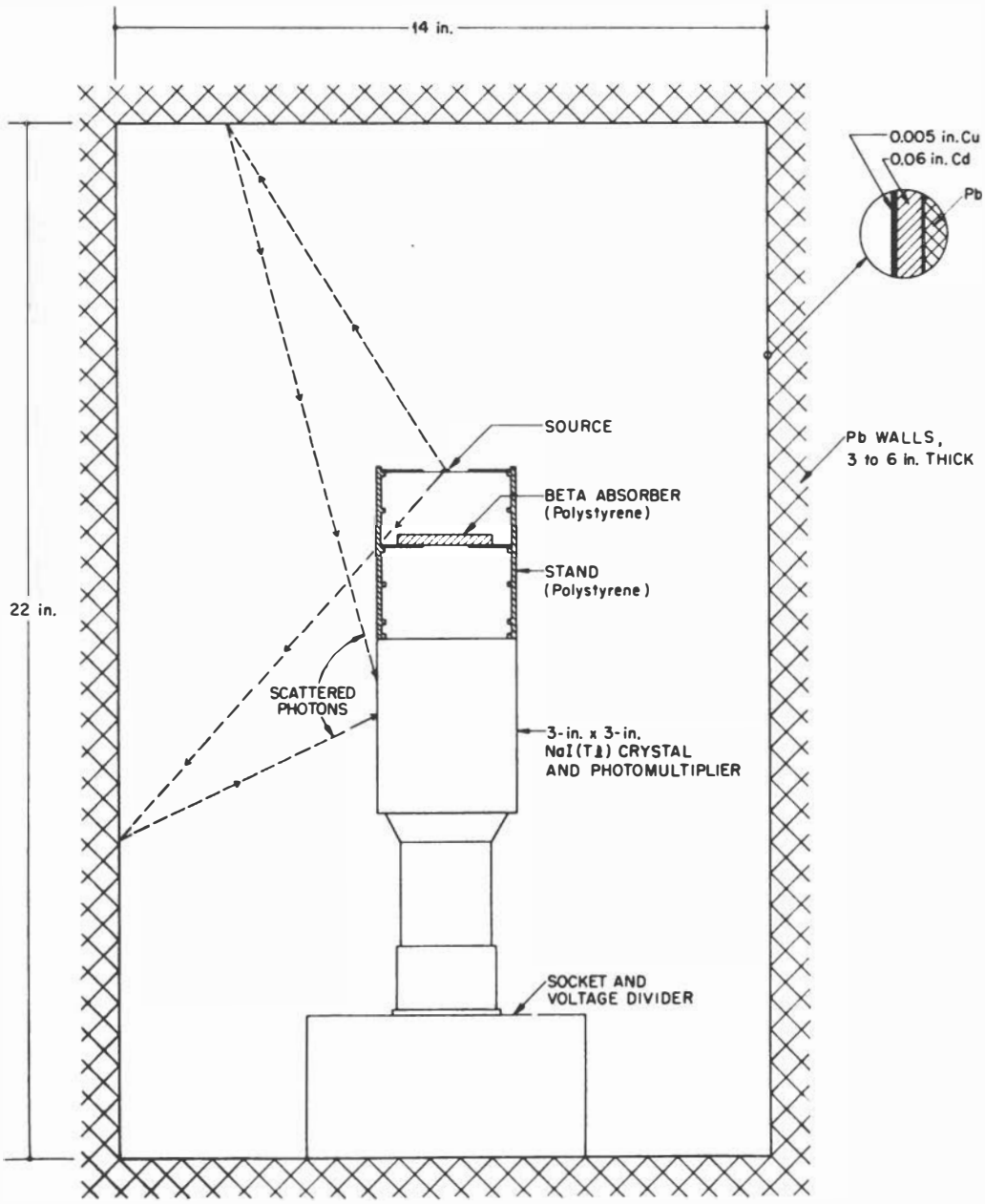

Fig. 14. Cross-section of a typical scintillation spectrometer installation, showing the 3 x 3-inch NaI(Tl) detector assembly, the lead shielding with "graded" liner, and the use of a low-mass support for the source and beta absorber. The origin of scattered photons is illustrated.

the Pb shield walls, with escape of annihilation radiation. Just as in the case of environmental scattering, the secondary radiation from the photoelectric effect and from pair production may be markedly reduced by increasing the separation between the shield walls and the source-detector combination.

Internal bremsstrahlung produced in the source and external bremsstrahlung emitted when beta rays are stopped in the absorber will be detected just as any other electromagnetic radiation. Therefore, when the number of gamma rays per beta disintegration is low, a prominent contribution from bremsstrahlung will be noted. Such an effect is shown as an upturn at low energies, with much the same shape as a decreasing exponential function added to the gamma-ray response (see Fig. 15).

Analysis of Gamma-Ray Spectra. The gamma-ray scintillation spectrometer has proved to be an important tool for the quantitative determination of gamma intensities. Since the true shape of the Compton electron distribution for a single gamma-ray energy is so obscured by the spurious effects which have just been described, the area of the full-energy peak is generally chosen as the basis for intensity measurements. The spectrum exhibited by a source which emits gamma rays of several energies will be a summation of the responses to the individual gamma rays. The process by which accurate intensities may be obtained involves first breaking down the gross spectrum into its components ("spectral decomposition"), from which the areas of the full-energy peaks may then be extracted.

The above discussion demonstrates that the pulse-height distribution of a NaI(Tl) spectrometer arising from the interaction of a single incident gamma-ray energy contains not just a full-energy peak, but in addition a complicated spectrum down to zero energy. In the course of performing a spectral decomposition, it is essential that the complete spectrum shape be used, and not just the full-energy peak. The detailed shape of the spectrum from a single gamma ray, or from a particular sample, is often called the response function.

The decomposition is relatively straightforward if the gamma-ray spectrum in question happens to be made up of gamma-ray components whose spectra can be determined individually. In such cases, the procedure to be followed simply involves normalizing the response function for the most energetic gamma

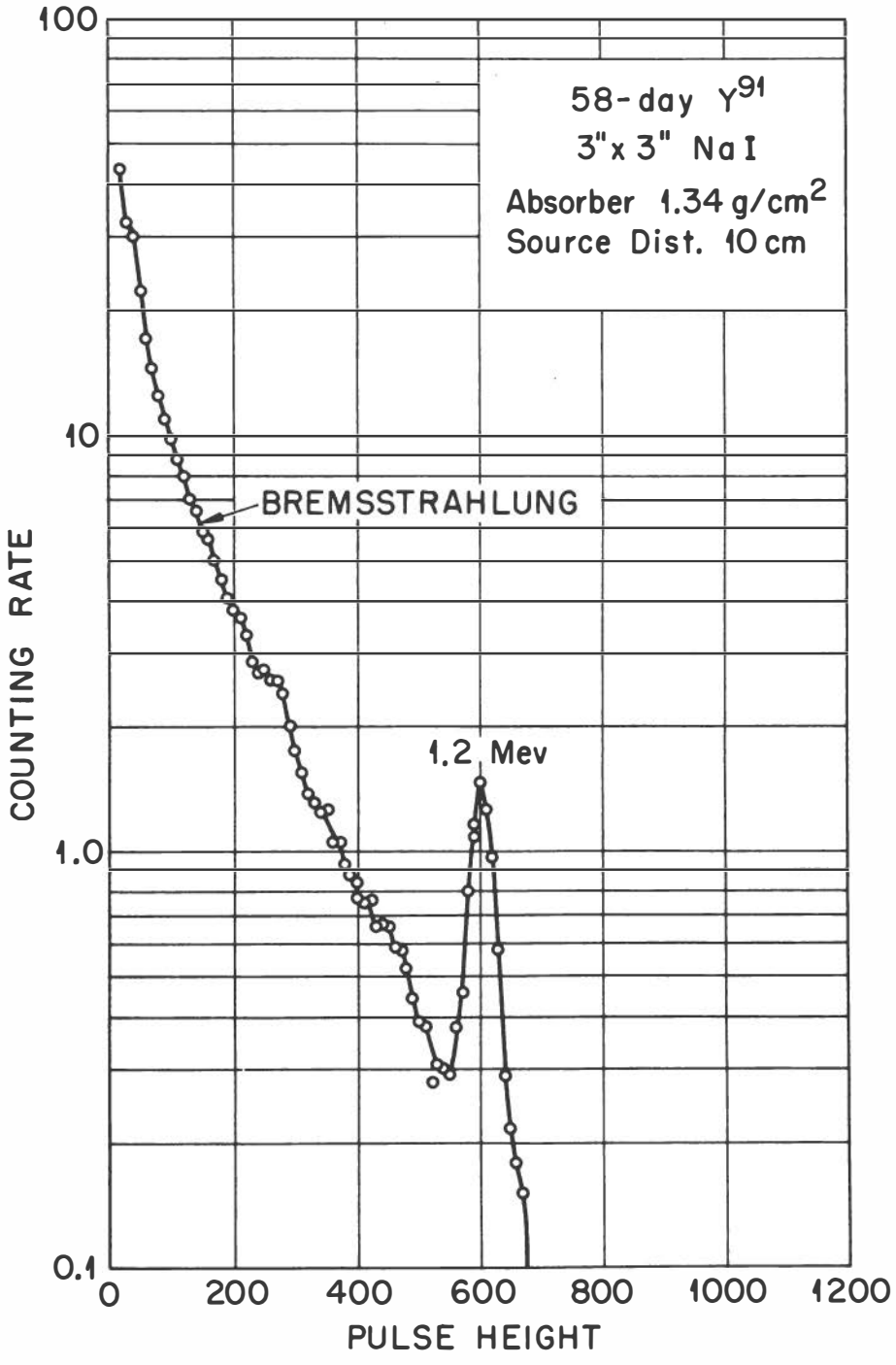

Fig. 15. Gamma-ray spectrum of 58-day Y^{91}, showing the bremsstrahlung spectrum characteristic of a source for which the beta-to-gamma intensity ratio is very large. (From Heath[20].)

ray to the experimental points at the full-energy peak; the response function is then drawn in and subtracted from the experimental data. The most energetic peak in the residue is fitted to the response function for that energy, and the subtraction process is repeated until all components have been "peeled off." An example of this process is shown in Fig. 16.

It should be emphasized that the response functions must be determined under conditions identical with those under which the unknown was measured, so the response function used in the analysis will include the same spectral distortions, such as backscatter peaks, which affected the unknown. A frequently overlooked effect is the variation in gain with counting rate, which may occur in certain photomultiplier tubes and multichannel analyzers; for this reason it may be necessary to adjust the energy as well as intensity scales before attempting a point-by-point subtraction. There are commercial devices which permit an adjustable fraction of a standard spectrum to be subtracted from a pulse-height distribution stored in a multichannel analyzer memory. When using a system such as this, it is particularly important that no serious gain shifts occur with changes in counting rate.

It may not be possible to measure directly the response functions for the component gamma rays of an unknown spectrum; in this case, it is necessary to synthesize the required function from a measurement of gamma-ray standards over the energy range of interest. The full-energy peak is nearly gaussian, except on its low-energy side where the Compton spectrum contributes a slight distortion. By the use of standard spectra, the width parameter for the full-energy peak can be plotted as a function of energy, and values for the unknown can be evaluated. Other features of the spectrum can be constructed by interpolating on plots which correlate the coordinates (pulse height and counting rate relative to that for the full-energy peak) of various "key" points of the spectrum with the gamma-ray energy. Some of the key points which may be used are: the backscatter peak; the level, peak, and inflection of the Compton distribution; and the valley below the full-energy peak. If pair peaks are involved, their vital statistics must, of course, be included.

Once a particular full-energy peak has been resolved from the spectrum, the area under the peak $P(\gamma)$ may be obtained by summing the counting rates of the channels which contain the

peak, or by means of the equation

$$P(\gamma) = \frac{a_\gamma h}{0.564\ (\Delta E)}\ , \qquad (1)$$

where a_γ is the half-width of the gaussian peak at h/e; h is the peak height in the same units as $P(\gamma)$; and ΔE is the channel width. Both a_γ and ΔE must have the same units and typically may be expressed in pulse-height divisions, channels, or kev.

Use of Computers in Gamma-Ray Analysis. The decomposition of a very complex gamma-ray spectrum by the process just described is extremely tedious if all subtractions are performed manually, point by point. Although much useful work can be done in this way, hand calculations are limited to a rather small volume of data, and so digital computers promise to be very useful in the decomposition of complex spectra.

A situation in which the computer can, in principle, be most readily applied to the spectral decomposition problem is that for which the experimentally measured spectrum is made up of components whose spectra may be determined individually. This condition is often met in radioactivation analysis, and Kuykendall and Wainerdi[21,22] have investigated the use of a digital computer in an automatic activation analysis system. Their programs require a library of standard spectra and will not identify any gamma-ray peak whose response function does not appear in the library. Two computer programs have been written: (1) The half-life and gamma-ray energy are used[21] to identify each statistically significant peak in the spectrum. Starting at the high-energy end of the spectrum, the ordinate scale of each appropriate standard response function is normalized at the full-energy peak and subtracted from the total spectrum in sequence. (2) Another program[22] compares the unknown spectrum with the automatically selected library spectra in a simultaneous matrix solution.

Although programs using a spectrum library appear straightforward, they suffer from two defects. First, they cannot correct for calibration shifts, as has already been mentioned. Also, certain nuclides (e.g., many fission products) always occur in mixtures, and so the needed individual spectra cannot be determined. Therefore, a versatile gamma-ray unscrambling program must be capable of generating the required response

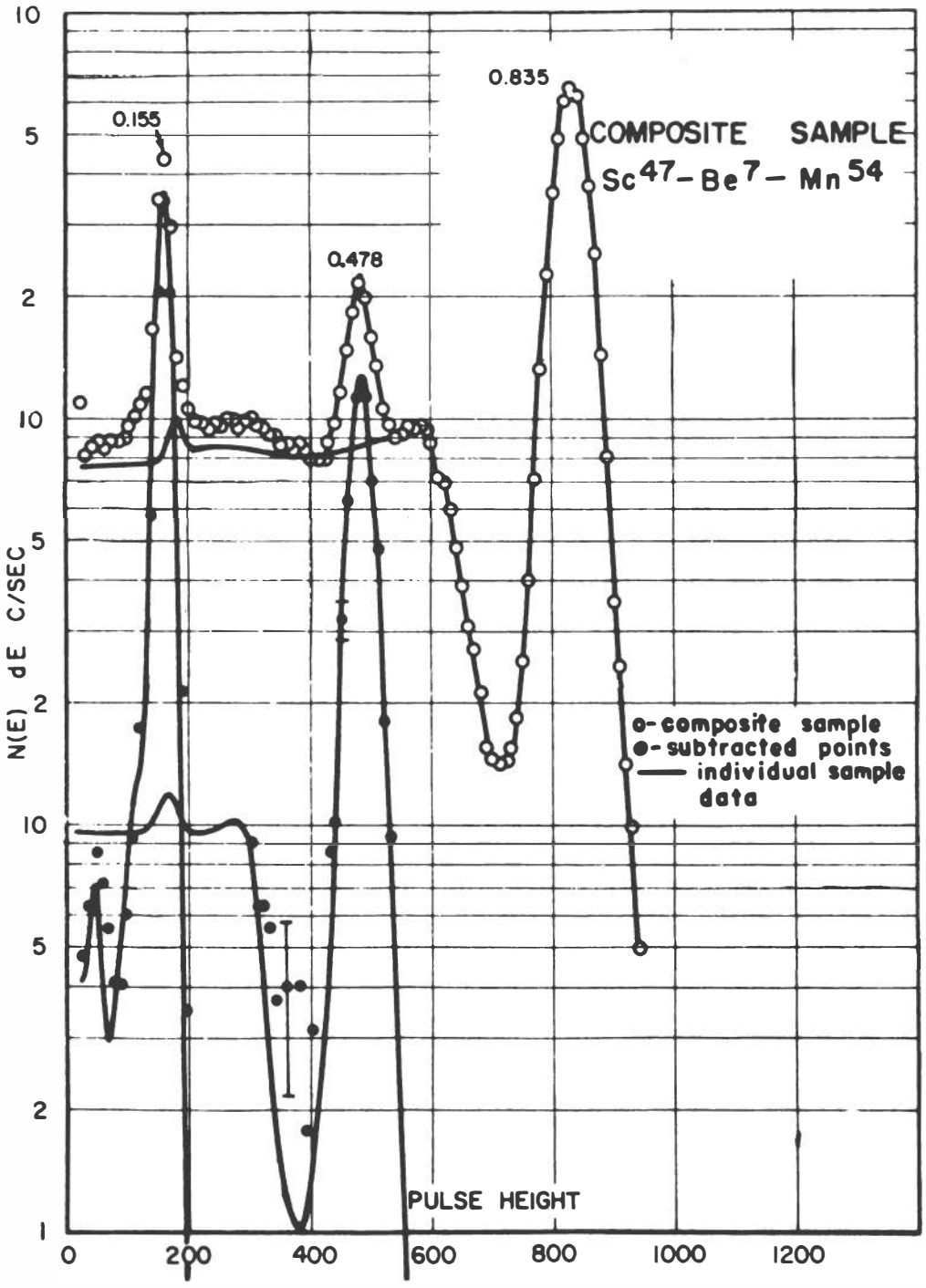

Fig. 16. Decomposition of a composite gamma-ray spectrum into its components by successive subtraction of standard spectral shapes (Heath[20]).

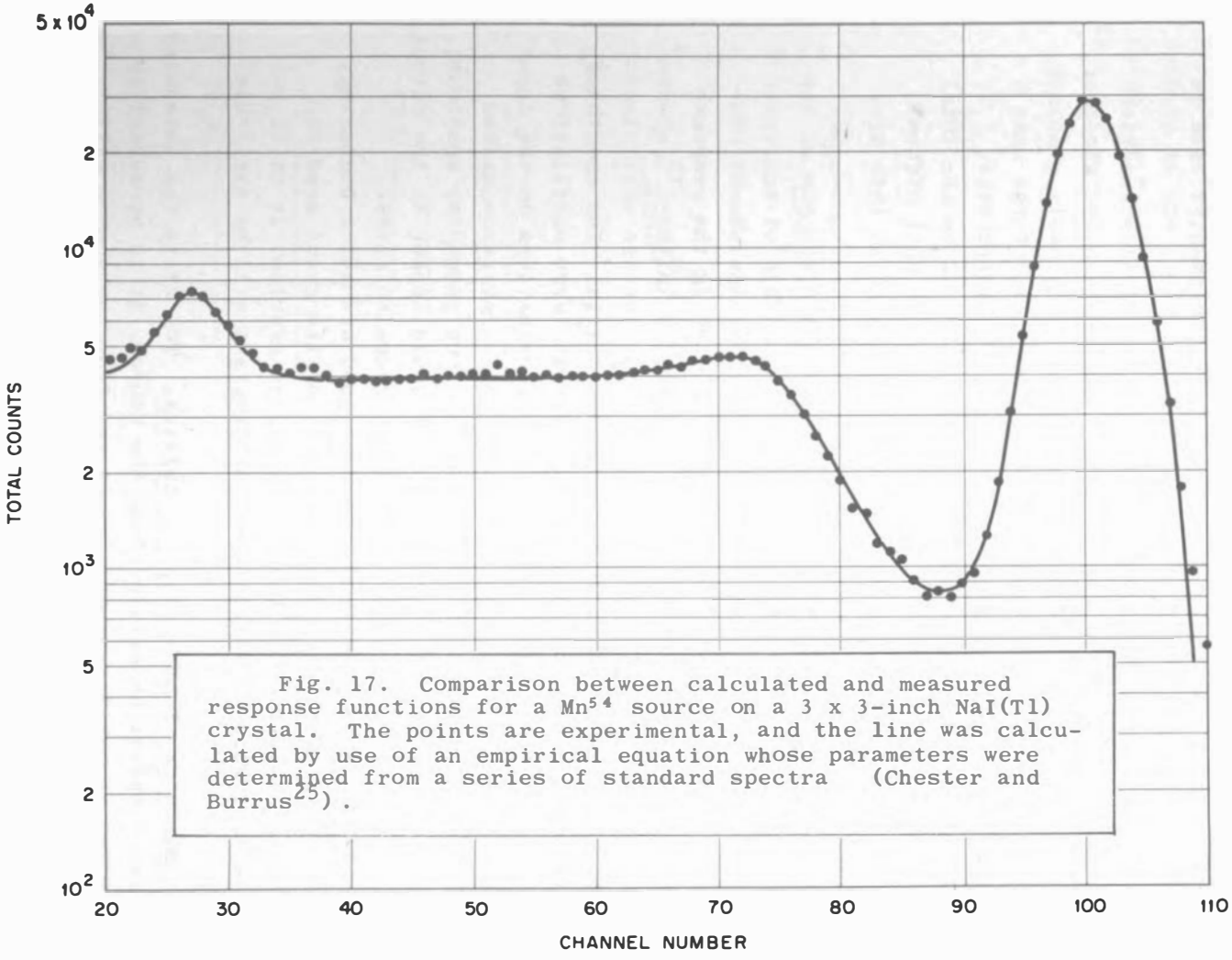

Fig. 17. Comparison between calculated and measured response functions for a Mn^{54} source on a 3 x 3-inch NaI(Tl) crystal. The points are experimental, and the line was calculated by use of an empirical equation whose parameters were determined from a series of standard spectra (Chester and Burrus[25]).

functions by using analytical expressions derived from standard spectra. Mathematical techniques for generating gamma-ray response functions have been described by West and Johnson,[23] Chester,[24,25] and Heath.[26] An example of a computed response function which accurately reproduces the experimental data is shown in Fig. 17.

The analytical methods for generating response functions have been used by West and Johnson,[23] Strickfaden and Kloepper,[27] and Heath[26] in their computer programs, which closely simulate the manual "peel-off" technique. These programs first make a gaussian fit to the highest-energy peak; the appropriate response function is calculated and subtracted from the total spectrum, and the process is repeated with the next highest energy peak. Continuous spectra are not suited to this type of analysis.

Some workers[24,25,28,29] have investigated the use of the so-called incremental methods, which are capable of analyzing both line spectra and continua. The method consists of constructing a response matrix whose k^{th} column is the response function if the full-energy peak is centered in the k^{th} channel. The input data from the gamma-ray spectrometer are multiplied by the smoothed inverse of the response matrix. The smoothing of the inverse matrix is needed to prevent large oscillations in the output data arising from small fluctuations in the input data.[28] When properly applied, the matrix inversion method should yield a smoothed version of the true gamma-ray spectrum; that is, a single gamma-ray component would appear in the output, not as a line, but rather as a single gaussian curve.

Although the programs just described are but a beginning, the results are encouraging. In view of the great need for practical solutions to the data analysis problem, it is to be hoped that more versatile computer programs will be available soon.

Determination of Gamma-Ray Intensities. To obtain the intensity of gamma radiation emitted from the source, it is necessary to know the probability that a gamma ray from the source will strike the crystal, and the probability that an incident gamma ray will cause an event in the full-energy peak. The former probability is just the solid angle Ω for the particular geometry, and the latter is often called the "intrinsic peak efficiency" $\epsilon_p(\gamma)$. Although it is very difficult to compute

$\epsilon_p(\gamma)$ exactly because of the multiple processes occurring within a large crystal, it is easy to compute the total intrinsic efficiency $\epsilon_T(\gamma)$, which is simply the probability that a gamma ray denoted by γ will produce a count once it strikes the crystal. The fraction of all counts in the spectrum which contribute to the full-energy peak is called the "peak-to-total" ratio, or "photofraction," and may be denoted by f (see Fig. 18).

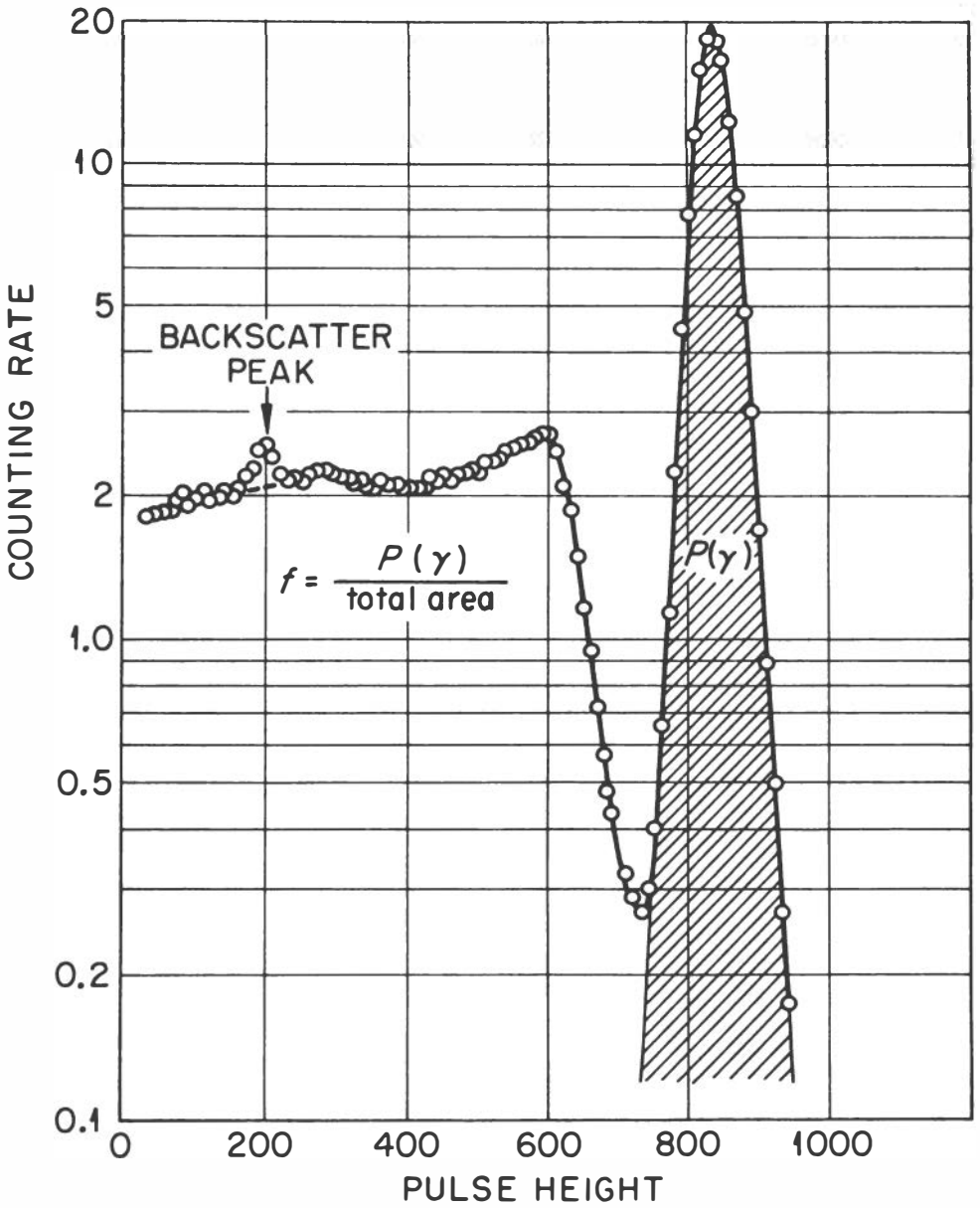

Fig. 18. Illustration of a measurement of the "peak-to-total" ratio f. Note that the backscatter peak is excluded from the total area.

Then, $\epsilon_p(\gamma) = f\ \epsilon_T(\gamma)$. It is very important that in the experimental determination of f, spectra be measured under conditions which reduce the effects of scattering as much as possible; otherwise, environmental scattering will add to the Compton electron spectrum and yield a high value for the area of the total spectrum.

Earlier it was mentioned that the full-energy peak was chosen for use in obtaining intensities because its area was free of spurious responses arising from the environment. Thus, once $\epsilon_p(\gamma)$ has been determined by the process just described, it may be applied to experiments having considerable differences in energy resolution and scattering conditions, just so the crystal dimensions and source-to-crystal distance remain the same.

Figure 19 presents values of $\epsilon_p(\gamma)$ for NaI(Tl) from the work of Lazar, et al.,[30] for 1-1/2 x 1-in. and 3 x 3-in. cylinders and a 3 x 3-in. cylinder with the top beveled at 45°, 1/2 in. from the edge. Values of $\epsilon_T(\gamma)$ computed at Oak Ridge and the values of $\Omega\ \epsilon_T(\gamma)$ computed by Wolicki, Jastrow, and Brooks[31] are compiled in a review by Mott and Sutton.[3] Heath[20] and Vegors, et al.,[32] extended these calculations of $\Omega\ \epsilon_T(\gamma)$ to include point, line, and disk sources located on the axis of several sizes of NaI(Tl) cylinders; they also included measurements of f for use in the calculation of ϵ_p.

The number of gamma rays of a given energy emitted from the source $N(\gamma)$ may be obtained from

$$N(\gamma) = \frac{P(\gamma)}{\Omega \epsilon_p(\gamma)} A \qquad (2)$$

where $P(\gamma)$, $\epsilon_p(\gamma)$, and Ω have the same meaning as above; the factor A corrects for gamma absorption in any material between source and detector, and in the absence of experimental corrections it may be approximated by $A = e^{\mu d}$.

It often happens that the gamma ray of interest is coincident with another gamma ray; in this instance the full-energy peak area will be decreased by coincident summing. This situation has been treated by Lazar and Klema,[33] who derived the following equation for the emission rate:

$$N(\gamma_1) = \frac{P(\gamma_1)}{\Omega\, \epsilon_p(\gamma_1)\ [1 - \Omega\, \epsilon_T(\gamma_2) \overline{W}(0^\circ) q_{2,1}]} \qquad (3)$$

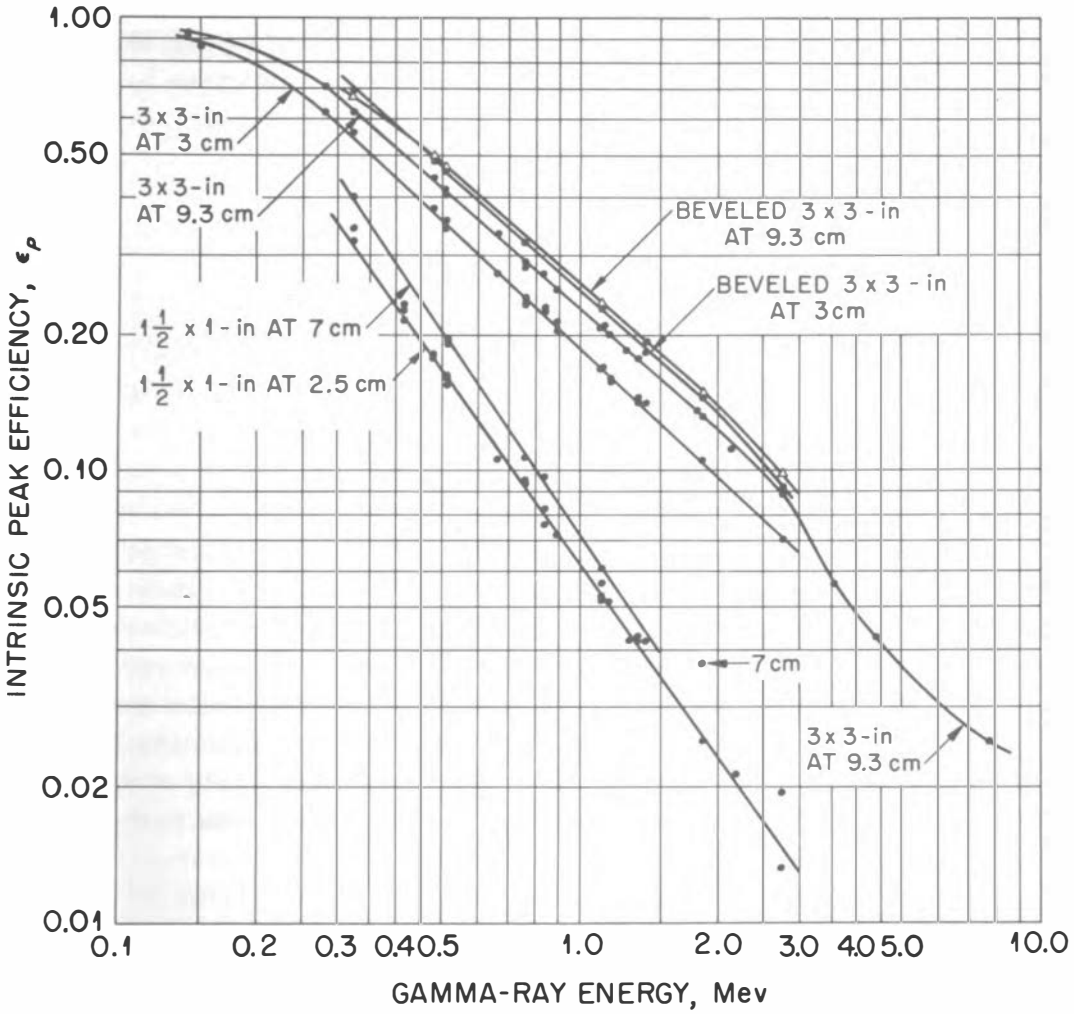

Fig. 19. Intrinsic peak efficiency ϵ_p 1-1/2 x 1-inch and 3 x 3-inch NaI(Tl) crystals (Lazar, et al.[30]).

Here, γ_1 denotes the gamma ray of interest; $q_{2,1}$ is the number of γ_2 in coincidence with γ_1; $\overline{W}(0^\circ)$ is the angular distribution function of the two gamma rays integrated over the surface of the crystal.[34] Since the correction $\Omega\epsilon_T(\gamma_2)\overline{W}(0^\circ)q_{2,1}$ is small under most conditions, only a small error results from setting $\overline{W}(0^\circ) = 1$, if the spin changes of the gamma transitions needed for the exact calculation of $\overline{W}(0^\circ)$ are not known.

Coincident summing of gamma rays leads to another important experimental implication. The gamma rays which are lost to their respective full-energy peaks appear in a "sum peak," whose apparent energy is the total energy of both gamma

rays. Since the crossover transition for a simple gamma cascade will also be detected at this energy, such a peak must be corrected for the area of the sum peak, which is given by:[33]

$$N_{CS} = \frac{P(\gamma_1)\ \Omega\epsilon_p(\gamma_2)\overline{W}(0^o)q_{2,1}}{1 - \Omega\ \epsilon_T(\gamma_2)\overline{W}(0^o)q_{2,1}} + N_r \ . \qquad (4)$$

The notation is the same as above, and the term N_r represents the contribution from random summing within the resolving time of the electronic system:

$$N_r \simeq 2\tau P(\gamma_1)P(\gamma_2) \ , \qquad (5)$$

where $P(\gamma_1)$ and $P(\gamma_2)$ are the areas of the full-energy peaks due to γ_1 and γ_2. The resolving time 2τ is usually about 1 μsec, and with the complexity of modern multichannel analyzer systems this quantity is very difficult to compute. It may be determined quite easily by measuring the random coincidence peak from a source which contains no true coincidences. An example of such a source is Mn^{54}, which emits only a single gamma ray at 0.838 Mev; consequently, the random sum peak will be found at about 1.7 Mev. From Eq. 5,

$$2\tau \simeq \frac{N_r}{[P(0.838)]^2} \ . \qquad (6)$$

Once 2τ has been determined by this method it can be used for any experiments with the same electronic system. Note also that 2τ, N_r, and $P(\gamma)$ must have the same time units.

4. Detection of Heavy Charged Particles

As has been mentioned, the earliest application of the scintillation method was to the detection of alpha particles. In its modern form the scintillation counter has found extensive use in counting and spectrometry of other heavy charged particles as well.

Because of the short range of alpha particles, the scintillator may be made very thin. This also insures that the response to more penetrating radiations such as electrons and

gamma rays will be small. The usual scintillator for counting is ZnS, activated by Ag. Although the light output is high, ZnS(Ag) is only available as a multicrystalline powder whose light transmission is poor; therefore, it is not used for measuring energy spectra.

The scintillator is usually deposited[35,36] by allowing ZnS(Ag) particles, ~ 20 μ in size, to settle from a water or alcohol suspension onto a glass or plastic disk which will serve as a light guide. Typical scintillators made by this technique have a surface density of 5-25 mg/cm². When the deposit is dry, it is usually sprayed with clear plastic or covered with a thin plastic film. Aluminizing the covering film inproves the light collection efficiency and may be used to protect the phototube from ambient light. The total thickness of material covering the scintillator proper should be < 1 mg/cm². Scintillator assemblies very similar to the above may be obtained from several manufacturers. The scintillator assembly is mounted by using silicon oil or grease as an optical coupling between the photomultiplier faceplate and the uncoated side of the glass or plastic light guide.

When it is desirable to use a scintillation device for determination of charged-particle energies, some inorganic scintillator other than ZnS(Ag) must be used. Thin clear disks of NaI(Tl) or CsI(Tl) are often employed. The resolution of these devices cannot compare with the resolution obtained with a gas-ionization or semiconductor detector, and so are not often used except in special situations. Further information on this subject may be found in recent reviews.[4,5]

III. IONIZATION CHAMBERS*

1. Ionization in Gases

Most of the experimental information about the stopping of charged particles in matter has been obtained from a study of the ionization produced. A very useful class of counters makes use of the ionization produced in a gas by collecting either the electron which is formed, or the ion pair, i.e., the electron and positive ion.

*See references (37), (38), (39), (40), and (41).

It will be recalled that the specific ionization of a charged particle in ion pairs per cm of path, dJ/dx, increases slowly to a maximum value a few mm from the end of the particle range, and then drops sharply. Specific ionization is related to the stopping power $-dE/dx$ by

$$dJ/dx = - (1/w)\ dE/dx \qquad (7)$$

where w is the average energy to produce one ion pair ("total ionization"). The total ionization is of considerable practical importance, because the appropriate value of w can be used to predict whether a particular energy loss will render detection possible.

The value of w varies for different stopping materials, but is remarkably constant for gases. Some typical values of w in gases are listed in Table 3 for electrons as primaries. It will be noted that w is always greater than the first ioni-

TABLE 3. SINGLE IONIZATION POTENTIALS J_0 COMPARED WITH AVERAGE VALUES OF w FOR ELECTRONS IRRADIATING VARIOUS GASES

Gas	J_0, ev[a]	w, ev[b]
H_2	15.6	36.9
N_2	15.7	34.9
O_2	12.5	31.3
He	24.6	41.3
Ne	21.6	35.9
Ar	15.8	26.3
Kr	14.0	24.4
Xe	12.1	22.1
CO_2	13.7	32.7
Air	----	34.2
CH_4	13.1	28.1

[a] Single ionization potentials of monatomic gases, from Dieke;[42] data on other gases from Craggs and Massey.[43]

[b] Average of values from recent literature, summarized in a review by Fulbright.[38]

zation potential. This probably happens because the electrons produced in primary ionization frequently have sufficient energy to cause further, or secondary ionization; also energy may be absorbed which is lost by excitation and dissociation.

The energy loss per ion pair is very nearly independent of particle energy and particle type. This immediately suggests that the integrated ionization J produced when an energy E is transferred, is given by $J = E/w$. Although in most cases this proportionality can be assumed, there is some evidence that a nonlinear relationship between J and E exists for alpha particles having energies less than about 0.1 Mev.[38]

Once free electrons and positive ions are formed, their behavior depends upon the nature of the gas and the electric field present. An electron makes many collisions with gas molecules, and although its direction of motion is randomized by such collisions, there is a net drift in an electric field along a direction parallel to the field lines. The drift velocity depends on the type of gas, its pressure, and the electric field strength.

Positive and negative ions move much more slowly through gases than do electrons. Further, ionic mobilities are relatively insensitive to changes in the applied electric field strength and the gas pressure. Therefore, in the interest of fast response, pulse ionization chambers are almost invariably arranged for electron collection.

Electrons may form negative ions by attaching themselves to neutral atoms or molecules--this effect is especially harmful in pulse ionization chambers using fast electron collection. Of the common gases, the halogens, oxygen, and water vapor are the most serious offenders. The rare gases, hydrogen, nitrogen, carbon dioxide, and methane have attachment coefficients 10^3 times smaller than the halogens, and are considered acceptable filling gases for ionization detectors.

2. Current Chambers

The essential parts of a gas ionization chamber are two electrodes insulated from each other, defining a gas-filled space between them. A parallel-plate ionization chamber operated as a current chamber is sketched in Fig. 20. The figure shows idealized current-voltage curves for a low- and a high-

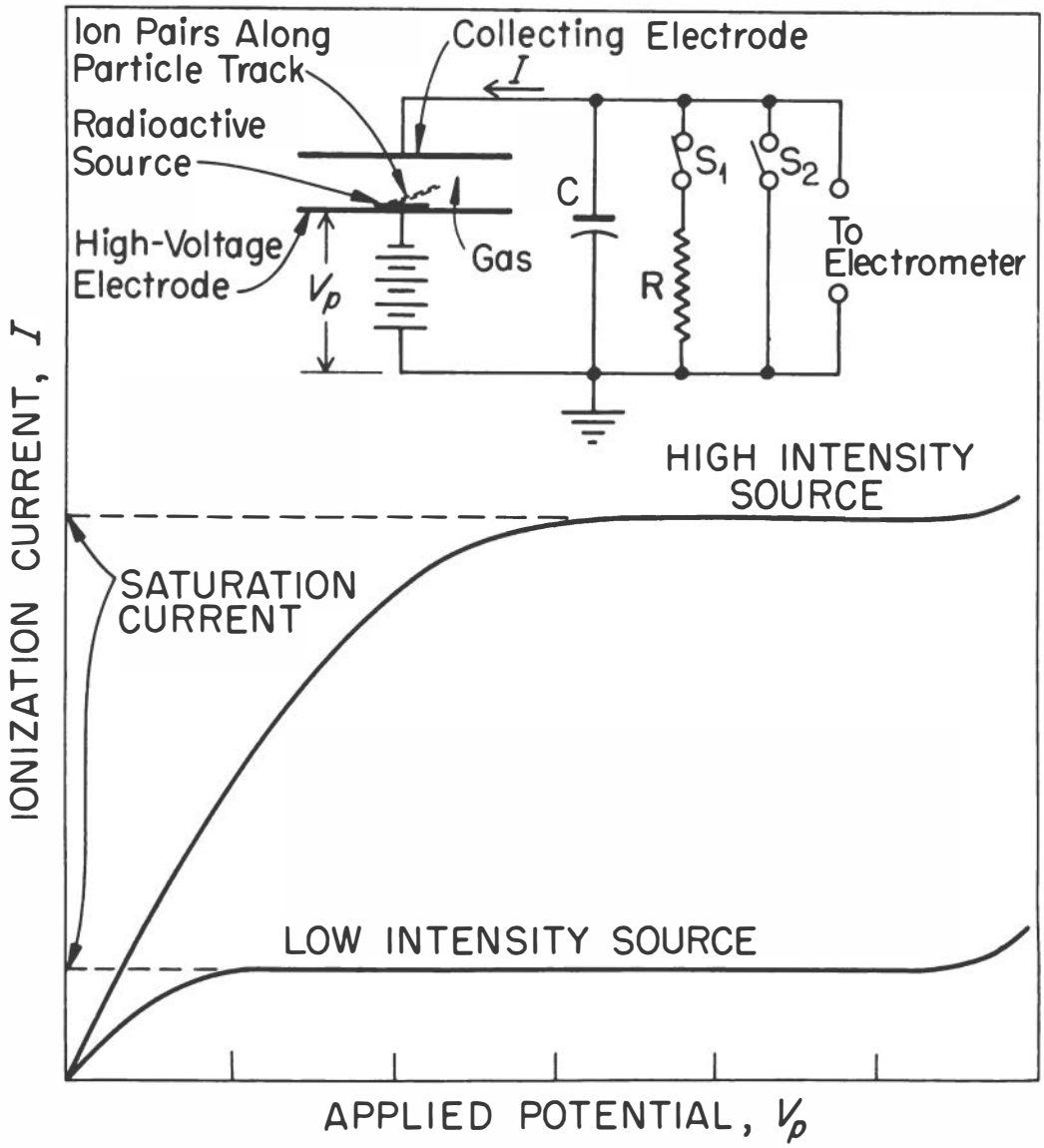

Fig. 20. Illustration of ionization chamber operation. Typical current-voltage curves are shown for different source intensities. The insert shows how a parallel-plate chamber is arranged for current measurement by the "IR-drop" method; for measurements by the "rate-of-drift" technique, both switches S_1 and S_2 must be opened (see text).

intensity source. At low applied voltage, there is a loss of charge through recombination of electrons and positive ions. As the potential is increased, the current flowing through resistance R from the collection of charge rises until it reaches a limiting value, the saturation current. At very high potential the current begins to rise again, due to the onset of gas multiplication (see Section V.1.).

The number of ion pairs formed per second n may be calculated from N, the rate at which particles are absorbed in the chamber, the average energy per particle $\bar{E}$, and w:

$$n = \frac{N \bar{E}}{w} . \qquad (8)$$

The steady-state saturation current I is obtained by multiplying by the electronic charge e (1.60×10^{-19} coulomb): $I = en$.

Thus, if sources having identical energy spectra (i.e., the same $\bar{E}$) are compared, the saturation current is proportional to the source strength N. This is the basis of the many ionization chamber instruments used for monitoring and assay purposes.

As shown in Fig. 20, the current is always measured in terms of a voltage, using an electrometer. For this reason, the method just described is called the "IR-drop" method, because the voltage across R is given by the product IR.

The currents of interest lie in a range of about 10^{-8} to 10^{-14} amp. The IR-drop method requires very high resistances for high sensitivity; however, in most cases it is not advisable to use resistors larger than 10^{12} ohms if special techniques are to be avoided. When the rate N is very low, the statistical variations in the measured voltage require careful analysis if high accuracy is required. For these reasons the rate-of-drift method is used for small currents ($< 10^{-12}$ amp.).

In the rate-of-drift method, the load resistance R is removed by opening S_1 (see Fig. 20). The collecting electrode is grounded by closing S_2; thus the voltage across C is zero. At the start of the measurement S_2 is opened, and the voltage after a time t is given by

$$V = 1/C \int_0^t Idt = It/C . \qquad (9)$$

The value used for C must include the combined capacitance of the chamber, leads, and electrometer input, and it typically lies in the range of 10-30 picofarads; therefore, the sensitivity is very high. Further, because the rate-of-drift makes available to the electrometer all the charge produced in the time t, this method is fundamentally more sensitive than the IR-drop method, in which charge is continuously consumed by the load.

The theory and design of electrometers and the properties of insulators suitable for ionization chambers have been reviewed by Fairstein.[37] Helpful suggestions on these techniques as applied to the determination of radioactive gases are given by Tolbert and Siri.[15]

3. Pulse-Type Chambers

When the rate of arrival of ionizing pulses is too low for convenient dc measurements, or when it is necessary to determine the energy distribution of particles stopped in the gas, the ionization chamber is operated as a pulse instrument. Here, the details of the collection process and the transient response of the ancillary equipment are both very important, since the complicated signal from the chamber is always observed distorted by the measuring system.

Consider a parallel-plate ionization chamber in which a single ion pair has just been formed (cf., Fig. 21). If the product RC is very large, the current through R can be neglected during the ion collection, and $V(t) = q(t)/C$, where $q(t)$ is the net charge collected and C is the total circuit capacitance. The ion pair influences the net charge not only by being collected, but also by electrostatic induction. At time t after the pair is formed, a charge $-q_+(t)$ and $-q_-(t)$ is induced on the collecting electrode by the positive ion and the electron, respectively. The potential is

$$V(t) = \frac{q_+(t) + q_-(t)}{C} \qquad (10)$$

At the time of formation, the ion and electron are both at x_0, and induce equal charges of opposite sign; therefore, $V(0) = 0$. The electron moves rapidly toward the collecting electrode,

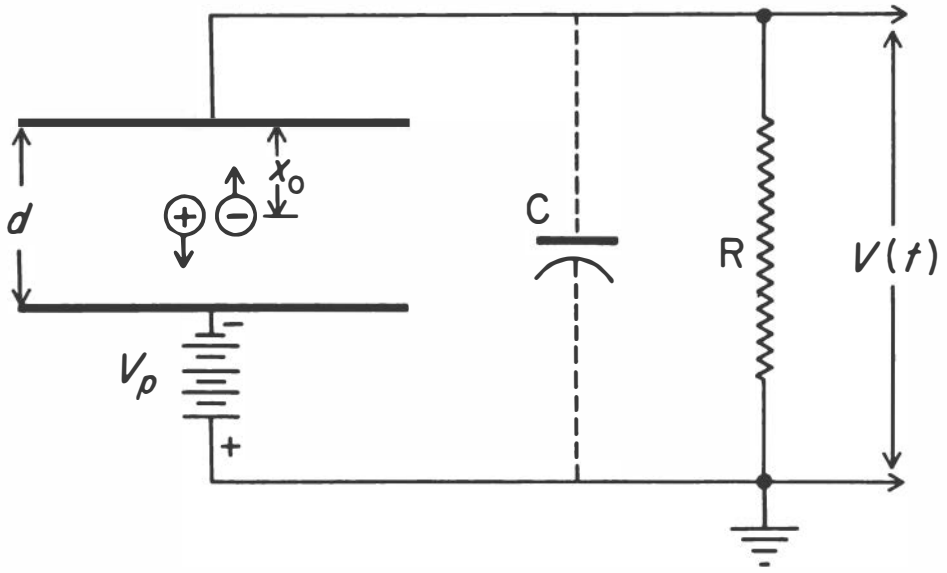

Fig. 21. Schematic representation of a parallel-plate ionization chamber in which one ion pair has just been formed.

causing a linear increase in $q_-(t)$ until the electron is collected. During this interval the effect of the positive ion is negligible, as its transit time is about 10^3 that of the electron. The potential now is

$$V(t) = \frac{q_+(t) - e}{C} \quad . \qquad (11)$$

The important fact to note is that the expected final potential of $-e/C$ is not attained when the electron is collected, but only when the positive ion ceases to induce a charge, i.e., when the ion strikes the high-voltage electrode.

The collector potential for the process just described is sketched in Fig. 22. The pulse profile shown makes the simplifying assumption that n ion pairs were formed at a point x_0; actually the ionization is produced along a track, and the qualitative pulse shape in the figure will be distorted by the spacial distribution of ion pairs. Electron diffusion will tend to obscure the sharp changes in slope. From the discussion of ionization in gases it will be apparent that the presence of an electronegative gas such as oxygen will seriously distort the pulse.

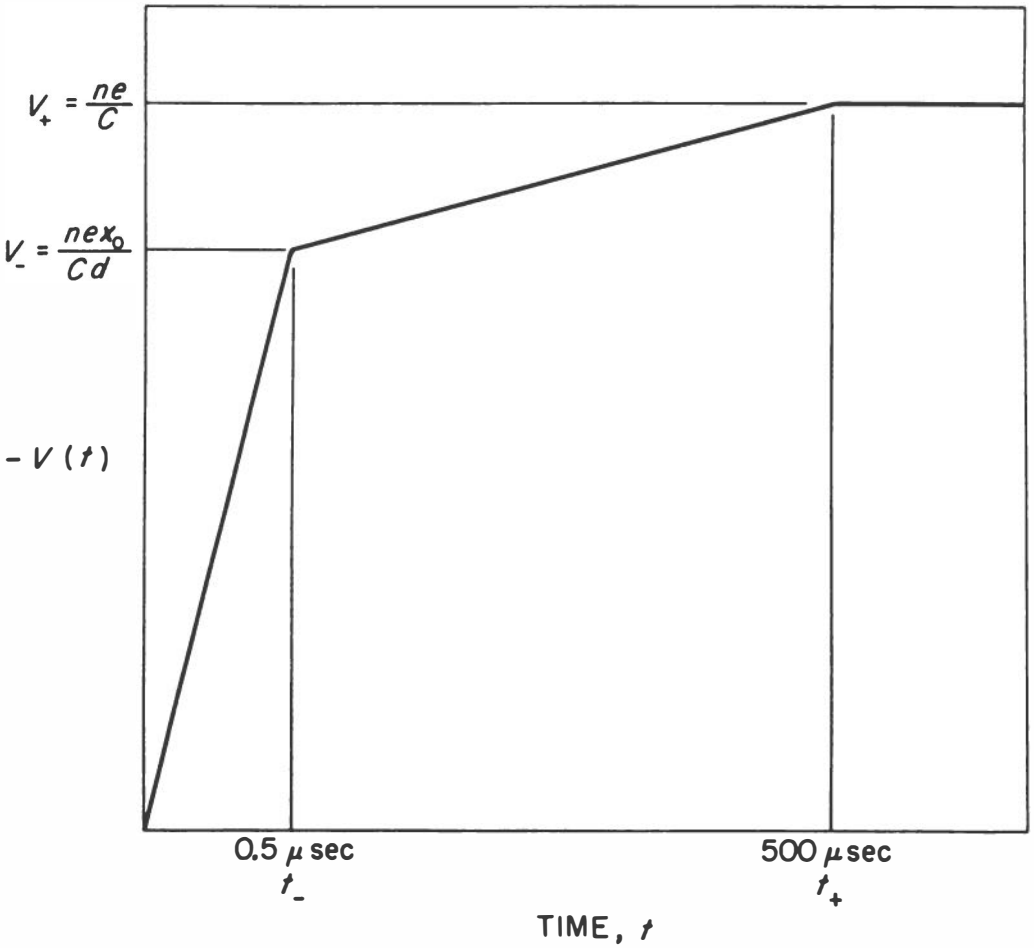

Fig. 22. Idealized voltage pulse in a parallel-plate ionization chamber with plate spacing d, after production of n ion pairs a distance x_0 from the collecting electrode. The electrons are collected at t- and the positive ions at t+. Note that the time scale is distorted to show the initial rise.

As seen in Fig. 22 the potential due to electron collection depends on the location of the ion pair at t = 0. This is not especially important if only counting is required, for the pulse must only be large enough to be recorded. However, some of the important applications for ionization chambers require a pulse whose height is proportional to the number of ion pairs. At first glance it may seem that one should amplify the pulse corresponding to the total ionization, i.e., V_+ of Fig. 22. Although this approach has been used very successfully, the amplifier required for broad, slow-rising pulses is prone to be rather noisy and is very sensitive to microphonics

and power-supply hum. The tolerable rates are only a few per second, because of the danger that the pulses can "pile up." The slow rise time makes timing very uncertain, so that coincidence techniques are not very applicable (see discussion of electronic equipment in Section VI).

To avoid some of the difficulties encountered when total ionization pulses are collected, only the portion of the pulse due to electron collection is employed. Figure 22 shows that the electrons are collected in a much shorter time; it now remains to avoid the variation in pulse height with position of the ionized track. Two methods are used: either the collecting electrode is made very small, or it can be shielded by a grid.

The addition of a grid to a parallel-plate chamber is the most desirable technique for removing the effect of positive-ion induction.[38,41,44] Such an arrangement is shown in Fig. 23. The sample is placed on the high-voltage electrode; the gas pressure and geometry are so arranged that all of the ionization is produced in the region between the grid and the high-voltage electrode. The grid shields the collecting electrode from the influence of the positive charges, but the electrons are accelerated toward the collector. Then the charge at the collector is equal to the total ionization induced by the primary particle.

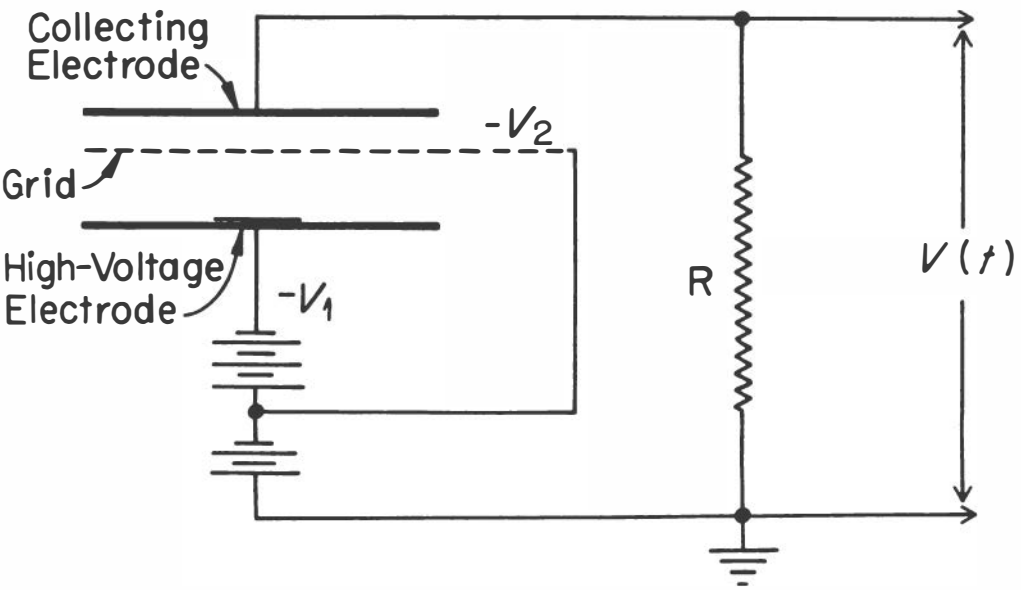

Fig. 23. Schematic diagram of a gridded ionization chamber.

4. Design Considerations

Because complete saturation can be attained with rather modest electrical fields, it is possible to design an ionization chamber to suit almost any experimental arrangement. For current chambers the parallel-plate geometry is preferred, because it is the easiest design to analyze mathematically. Coaxial cylinder chambers are very easy to construct, and most of the ionization chambers in radiation survey instruments are of this type. Pulse-type chambers present a less critical design problem, because regions of weak field are of less concern than for current chambers.

In current chambers the placement and construction of the insulators are matters of the greatest importance, since the current flowing through the insulator should be negligibly small compared with the current flowing through the conductor it supports. Even materials of high resistivity may develop serious leakage currents if the surfaces are permitted to acquire a charge from mechanical stresses; from rubbing one surface against the other; or from the electric field, which can induce an image charge or cause ions from the active volume to be collected on the insulating surfaces.[37]

On the other hand, ordinary surface leakage is not very important in fast pulse chambers at voltages of 1 or 2 kv. Small leakage currents can be tolerated, since the electronic system sees only fast transient signals; naturally, any corona discharge or other source of erratically changing leakage will cause bursts of spurious counts to be recorded.

Current chambers should always use guard rings. As shown in Fig. 24, the guard ring serves two purposes: (a) When the guard ring is grounded, any high voltage leakage is passed to ground instead of to the collector. Since only a small potential difference appears across the collecting electrode insulator, the collector leakage current is greatly reduced; (b) the active volume of the chamber is defined by the guard ring.

Guard rings are not always required in pulse chambers and in some cases may lead to spurious counts. For example, the sensitive volume of a current chamber may be defined by a guard ring; but if the same chamber is operated in the pulse mode, ionization produced in the volume between the guard ring

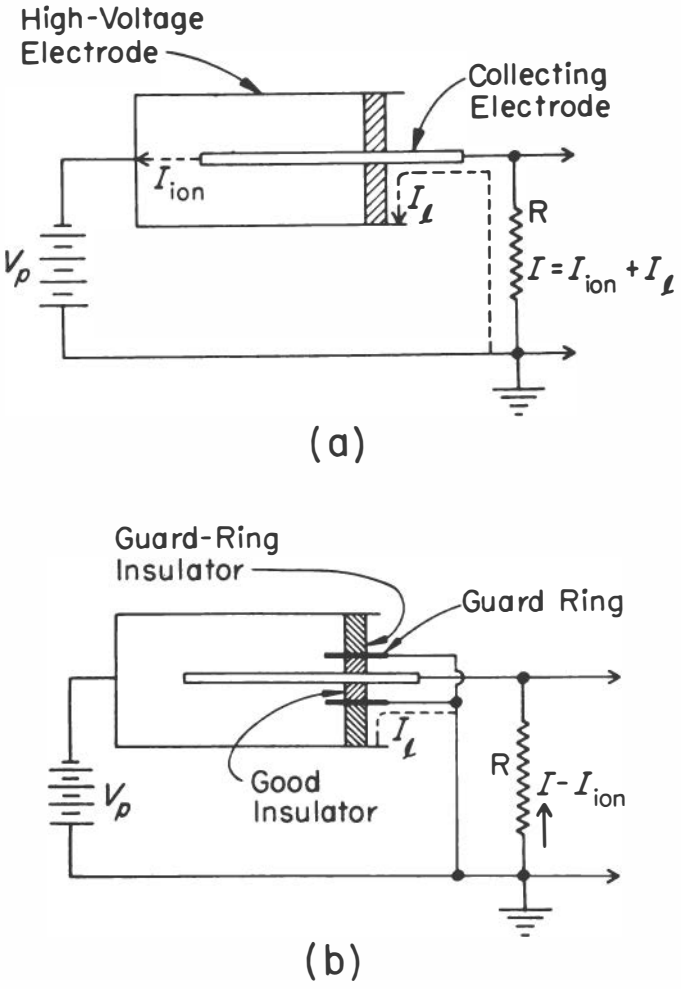

Fig. 24. Importance of guard rings in a cylindrical ionization chamber. (a) Without a guard ring, the measured current through load resistance R is the sum of the ionization current and the leakage current. (b) A grounded guard electrode ensures that the high-voltage leakage current will not pass through the load resistor, so the current through R will be due only to ionization.

and high-voltage electrode can induce on the collector a pulse of detectable amplitude.

5. Counting and Assay Applications

Ionization chambers are widely used for measuring the strengths of sources of heavy charged particles. Very simple detectors can be made for routine alpha counting if the energy

distribution is not required. Usually a spherical collecting electrode concentric with a cylindrical high-voltage electrode will suffice. To avoid random summing of low-amplitude pulses when a high beta- or gamma-ray activity is present in the alpha-particle source, a short clipping time is needed. A useful shortening of the detector rise time can be obtained by increasing electron drift velocity; in argon, a common filling gas, the rise time is improved by the addition of 5% CO_2.

The energy released in fission is nearly forty times that for a 5-Mev alpha particle, and so fissions may be counted to the exclusion of other events. Parallel-plate pulse chambers are widely used for measuring fission cross sections and for intercomparison of fissile sources. If the number of alpha particles per fission event is very high, then the "pileup" of alpha pulses will cause a troublesome background; in such cases it would be advisable to use a detector with a more rapid response, such as, for example, a gas scintillation counter[5] or a semiconductor radiation detector (Section IV., below).

Ionization chambers also may be used for neutron detection. Fission chambers containing U^{235} are widely used as neutron-sensitive devices in reactor control and personnel protection. In some applications, chambers are filled with BF_3 gas, or lined with boron or lithium. The ionization is produced by the alpha particles and recoil nuclei from the (n,α) reaction on B^{10} or Li^6.

Low-energy beta emitters may be introduced as gases into a calibrated chamber for quantitative assay (Section IX.5.). Ionization chambers may be used for relative assay of either gas or solid samples, even if the particles are not completely stopped in the gas.[45] In this application the chamber must be calibrated for the particular beta activity and type of source mounting.

Current ionization chambers are particularly well suited to the assay of gamma-ray emitters. A chamber designed with the proper regard for insulator considerations and mechanical rigidity should retain its calibration to within a fraction of a per cent for years. Vibrating-reed electrometers are capable of measuring the saturation current with high precision (~0.05%). If standard gamma sources of known disintegration rate are used for efficiency calibration, the chamber may be used as a precise secondary standard. Figure 25 shows the

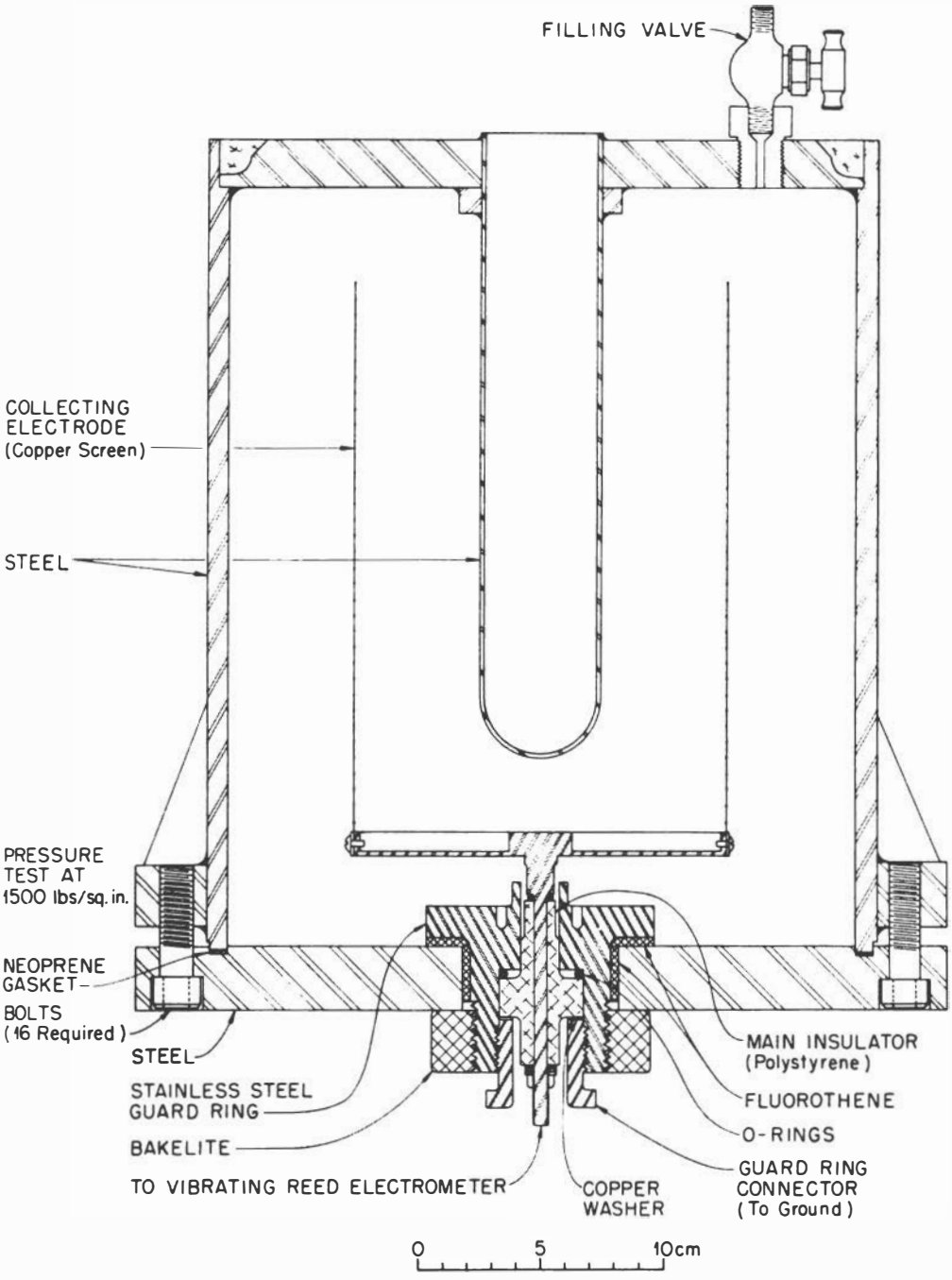

Fig. 25. Design for a high-precision ionization chamber for secondary standardization of gamma-ray emitters. The chamber is filled with dry argon to a pressure of 40 atmospheres. Samples are introduced via the re-entrant tube located inside the cylindrical collecting electrode (Stephenson[46]).

details of such a gamma-ray assay chamber, which is filled with 40 atmospheres of dry argon for high gamma-ray efficiency.[46] Sources may be loaded as solids or as liquids in small bottles, which makes the arrangement free of complicated sample-preparation procedures. Because of the high sensitivity of the chamber, it is necessary to enclose it in a 4-in.-thick lead housing as a means of reducing environmental background effects.

6. Energy Spectra

In several laboratories, gridded ionization chambers are used routinely for analyzing energy spectra of charged particles, especially alpha particles from radioactive samples. This method has been especially important in research on the trans-uranium elements. Good energy resolution (better than 1%) can be attained with large-area sources; background effects are very low; and the high geometry (nearly 50%) yields a high efficiency. The present "state of the art" has been reviewed by Hanna.[47] Since the advent of the simple, high-resolution semiconductor detectors, many of the favorable arguments for grid chambers have been vitiated; however, the ionization chamber is still useful where both large sources and high geo-metrical efficiency are required.

IV. SEMICONDUCTOR RADIATION DETECTORS

Basic understanding of the physics of semiconductors has evolved, for the most part, during the years following the invention of the transistor in 1948. The technology of semi-conductor devices has proceeded hand in hand with the advances in basic science, and this combined effort of theorists and technologists has made a significant contribution to the detection and measurement of nuclear radiation. In this section we will discuss the use of p-n junctions and surface barriers as charged-particle detectors, an application which promises to become the most important innovation in radiation detectors since the development of the modern scintillation counter.

1. Principles and Description*

The semiconductor radiation detector behaves quite analogously to the gas ionization chamber, except that the charge is carried by electrons and electron vacancies (holes), instead of by electrons and positive ions. Because of this similarity the device is often termed a solid-state ionization chamber. The use of a solid as a detector is very attractive, because the sensitive layer can be very thin and yet possess a high stopping power. Another advantage results from the low energy to produce one hole-electron pair (3.5 ev in Si): nearly eight times as much charge is produced for a given energy loss in silicon as in argon gas, which leads to small statistical fluctuations in the number of pairs and improved energy resolution over gas-filled counters. The intrinsically high speed of the device is due to the high mobility of the carriers in the electric field, coupled with the short distance between electrodes.

A. Introduction to Semiconductor Theory. Except at very low temperatures, a highly purified semiconductor exhibits intrinsic conductivity, as distinct from impurity conductivity of specimens which contain foreign atoms at some of the lattice sites. The electronic band scheme which explains this behavior can be discussed with reference to Fig. 26. At absolute zero the conduction band is vacant, while the valence band is filled. As the temperature is raised, electrons in the valence band are transferred by thermal activation across the energy gap and into the conduction band. Both the vacancies (i.e., holes) in the valence band and the electrons in the conduction band contribute to the electrical conductivity and are called carriers.

Apart from the intrinsic method of carrier excitation, electrons and holes may be introduced extrinsically from impurities or imperfections. Consider in particular the effect of impurities on silicon and germanium, which crystallize in the diamond structure with the chemical valence four. If a pentavalent atom such as P, As, or Sb is substituted for a Si

*For an introduction to the theory of semiconductor radiation detectors, see Brown,[48] and for an introduction to semiconductor devices in general, see Jonscher,[49] Shive,[50] and Henisch.[51]

atom, there will be one valence electron left over. Such a pentavalent impurity is called a donor, because the energy level of the extra electron lies near the energy of the conduction band (see Fig. 26); at most temperatures there is a

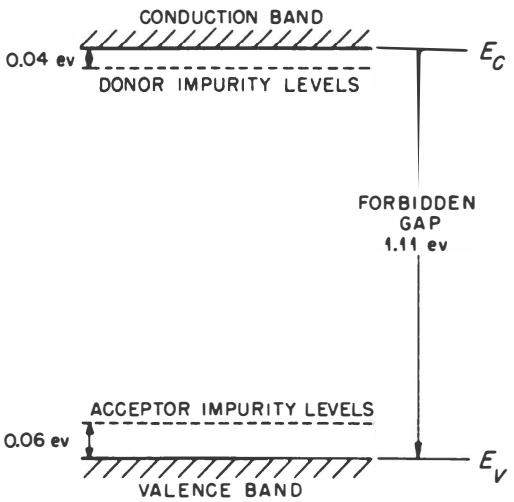

Fig. 26. Electronic band scheme for silicon.

high probability that the electron will be raised into the conduction band. Since the conductivity in this case is by negative charges, the material is said to be n-type. A trivalent atom such as B, Al, Ga, or In is called an acceptor because it can take on an electron from the valence band, leaving a hole; the resulting conductivity can be ascribed to the motion of the positive holes, and the material is said to be p-type.

The Fermi-Dirac probability distribution function gives the probability that a given state is occupied at a particular temperature. The energy about which the probability curve is symmetrical (i.e., the probability = 1/2) is called the Fermi energy or the Fermi level. Without resorting to a mathematical treatment, it is sufficient to state qualitatively that in a p-type semiconductor, the Fermi level lies in the energy gap, near the valence band; on the other hand, because n-type material contributes a large number of electrons into the conduction band, the Fermi level is displaced to an energy near the conduction band.

The process of stopping a charged particle in a semiconductor results in lifting electrons from the valence and

other low-lying, occupied bands to higher, unoccupied bands. Thus, electrons appear in nominally unoccupied bands, and holes are created in nominally full bands. Interactions between electrons and holes cause the electrons to fall to the lowest available levels in the conduction band, while the holes rise to the highest levels of the valence band. The many states of this process, which are complete in about 10^{-12} sec, result in an overall expenditure of 3.5 ev to produce one hole-electron pair in Si. It may be noted that this is about three times the 1.1-ev energy gap in Si, which is the minimum energy to produce a hole-electron pair. The additional energy is believed to be lost through strong coupling between electrons and lattice vibrations of the solid.

The energy to produce one hole-electron pair in a Si detector is independent of particle type, within the accuracy of existing measurements. This is a notable advantage over the usual NaI(Tl) or CsI(Tl) scintillation spectrometer, for which the light output per Mev of energy transferred to the crystal depends greatly on the ionization density of the heavy particle involved. Recent data on the response of surface barrier and diffused junction diodes to fission fragments does give some evidence for a defect. It is likely that this isolated case of nonproportionality of pulse height with energy involves a failure to collect all the current carriers formed in high density by the intensely ionizing fragments.

The reader quite reasonably might ask why detectors are not made from materials with a smaller forbidden gap and hence a smaller energy requirement for producing a hole-electron pair. In general, a material with a small forbidden gap can only be used at low temperatures; otherwise, thermal excitation of carriers will obviate its usefulness. Good low-temperature detectors of Ge(w = 2.9) have indeed been made.[52]

B. Production of High Fields in a Semiconductor. It is easy in principle to arrange the solid-state equivalent of a uniform-field, parallel-plate ionization chamber; however, due to the small electrode spacing and the necessity for a high electric field to collect all of the charge, the resistivity of the material must be very high. Even the highest resistivity material passes such a large current that the power dissipation at several thousand volts/cm would reach alarming proportions. More important are the random fluctuations in the current,

which would be very large in proportion to the minute signal arising from the collection of hole-electron pairs at the electrodes. Thus, it is necessary to find some other way of sustaining a high electric field inside a solid without the use of high applied voltages and without requiring material of very high resistivity.

p-n Junctions. One way in which the necessary field may be obtained is by means of a reversed-biased, p-n junction. This device is fabricated from high-resistivity p-type material (sometimes called π-type), into which a small amount of donor impurity such as phosphorus has been diffused. A high donor density exists in this surface layer which is only a micron or less in thickness. The equilibrium condition for such a situation is shown in Fig. 27(a). The electrons at the n-type surface tend to diffuse to the left, and the holes in the p-type bulk material tend to diffuse to the right. Thus, the p-type region acquires a negative charge and the n-type region becomes positively charged, until the two regions are aligned about the constant Fermi level energy of the system. The result of this equilibrium is that a potential barrier is established which opposes any further flow of electrons or holes across the junction.

A space-charge region or depletion layer now exists, in which the acceptors are completely filled and the donors are completely empty. There must be an overall balance of positive and negative charge. Since the density of acceptors is low in the high-resistivity p-type material, the space charge region extends much further into the p-type region than into the n-type layer. The potential difference is about 0.6 volt, and may extend over 10^{-3} cm. The resulting electric field is not uniform but averages several hundred volts in Si at room temperature.

If a voltage is applied to the junction by connecting the negative terminal to the p-type region and the positive terminal to the n-type region, the junction is said to be reverse-biased. As this reverse bias voltage is increased, the barrier height increases and the space-charge region is extended [see Fig. 27(b)]. The exhaustion-layer theory of Schottky[53] has been very successful in accounting for the properties of potential barriers and space-charge regions in semiconductors. The nomograph of Fig. 28 is useful for applying the Schottky theory to practical silicon diodes. If the applied bias voltage and the resistivity of the base material (p-type silicon in the

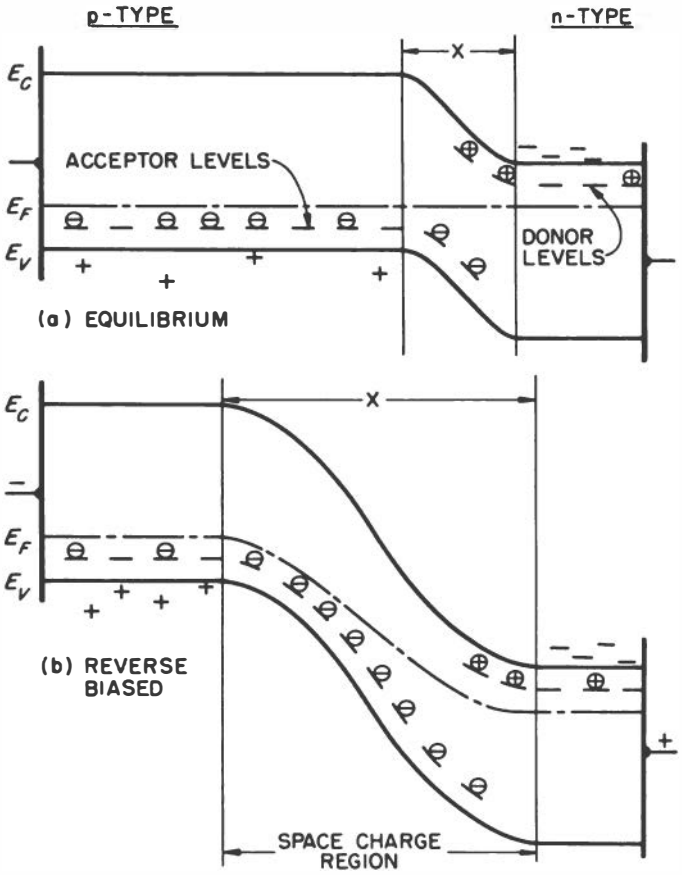

Fig. 27. Band scheme for a p-n junction. E_F represents the energy of the Fermi level; E_C and E_V indicate the lower edge of the conduction band and the upper edge of the valence band, respectively.

case just described) are known, the barrier depth x may be quickly determined. Since the depletion layer is the only region containing a high field for collection of charge, the experimenter must be able to estimate x in order to be certain that incident particles will be stopped within the sensitive part of the counter.

Note that the nomograph in Fig. 28 includes values for the dynamic capacitance in pf/cm². This capacitance arises because the space-charge region resembles two charge sheets of finite thickness, separated by a thin, high-resistivity layer, the barrier itself.

A modification of the p-n junction detector, which promises to yield sensitive regions deep enough even for beta particles

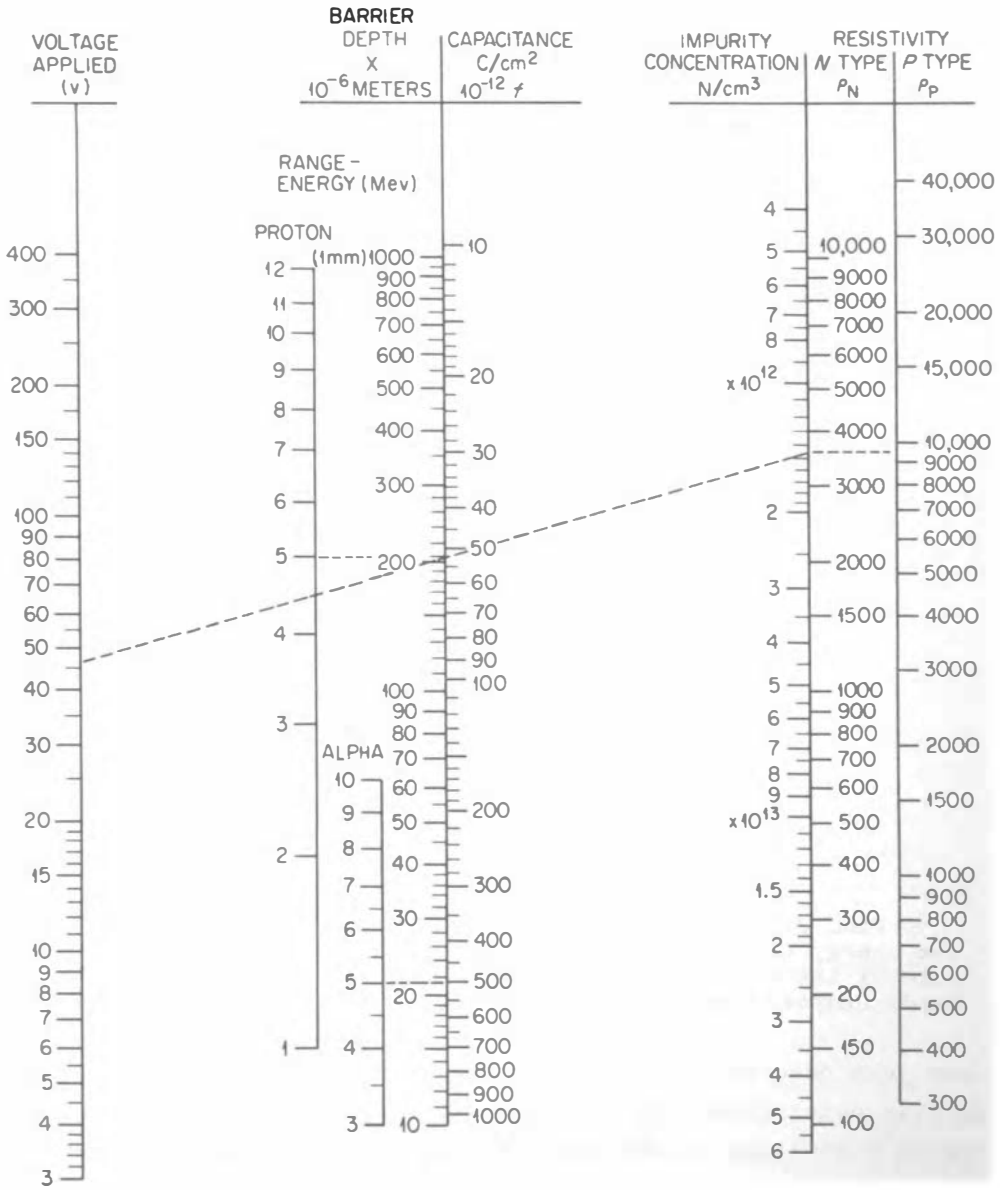

$$X^2 = V.\frac{1}{N} \cdot 1.326 \times 10^{15},\ C/A = 1.061 \times 10^4,\ \frac{1}{X} \cdot \rho = \frac{1}{N\mu e}$$

$$\mu_N = 1200\ \text{cm}^2/\text{volt}\cdot\text{sec},\ \mu_P = 450\ \text{cm}^2/\text{volt}\cdot\text{sec}$$

Fig. 28. Nomograph which relates the applied reverse bias voltage, barrier depth, dynamic capacitance, and impurity concentration for a Schottky-type barrier in silicon. The impurity concentration may be found by using the resistivity in ohm-cm of the base material used. Also included are ranges of charged particles in silicon corresponding to particular barrier depths (Blankenship and Borkowski[54]).

of several Mev, makes use of the "ion-drift" technique investigated by Pell.[55] A junction is formed on p-type silicon by diffusing lithium into the surface; the lithium finds its way into interstitial positions and acts as a highly mobile donor. A plot of the donor and acceptor concentrations in the junction are shown in Fig. 29(a). If reverse bias is applied to this junction, the electric field in the region around the point c will exert a force which will move the positively charged Li^+ ions from the Li-rich side of the junction to the Li-deficient side. This effect requires that the temperature be sufficiently high to impart appreciable mobility to the Li^+ ions. The result of such an ion drift is shown in Fig. 29(b). Over a considerable region the donor concentration has been adjusted to compensate precisely for the acceptor concentration; in effect, a region of intrinsic silicon has been formed. Pell[55] has shown that x^2 is approximately proportional to the time of drift at constant temperature and bias voltage.

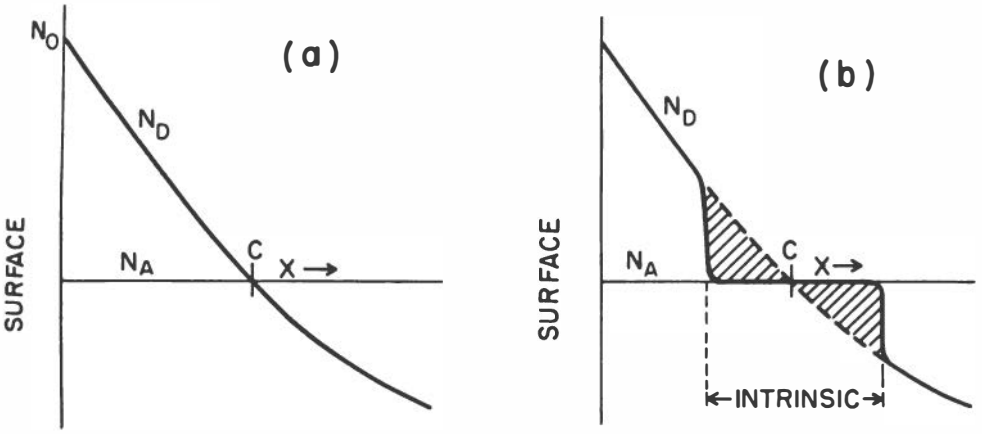

Fig. 29. Illustration of the ion-drift technique. (a) Density of donor and acceptor atoms as a function of depth from the surface, after forming the p-n junction. (b) Following ion drift, the donor concentration equals the acceptor concentration over a significant region (Pell[55]).

Elliott[56] has reported on the fabrication and evaluation of detectors made by ion drift. He was successful in producing detectors with x = 0.338 cm, which corresponds to the range of 96-Mev alpha particles, 24-Mev protons, or 1.7-Mev electrons. A Li-drifted diode having a depletion layer 0.20 cm thick (or an electron range of 1.1 Mev) gave an energy resolution of 2.5% full width at half-maximum at 624 kev electron energy; most of

this width was due to electronic noise. The ion-drift technique therefore appears to be a very promising method for attaining thick depletion layers at room temperature.*

Surface Barriers. A second general class of semiconductor device which can build up a high electric field for the collection of charge is the surface barrier detector, which is usually made from high-resistivity, n-type silicon. Although the detailed mechanism is not well understood, the nature and formation of the surface barrier is believed to arise from surface states, whose existence is well established for silicon and germanium.[57]

As shown in Fig. 30(a), the surface states are able to trap electrons from the crystal until the Fermi level at the surface is equal to the Fermi level in the interior. The high density of electrons on the surface and the positive charge on the semiconductor which yielded the electrons combine to distort the energy levels E_V and E_C near the surface, and a potential barrier results. The positive space charge within the barrier arises because the donor sites are nearly completely ionized, and there are few if any electrons to compensate. Further, the space charge is enhanced near the surface by the presence of minority carriers (holes). Note that in establishing the conditions for a surface barrier, the Fermi level approaches the top of the valence band just as it would for a p-type semiconductor. The region bounded by the surface and

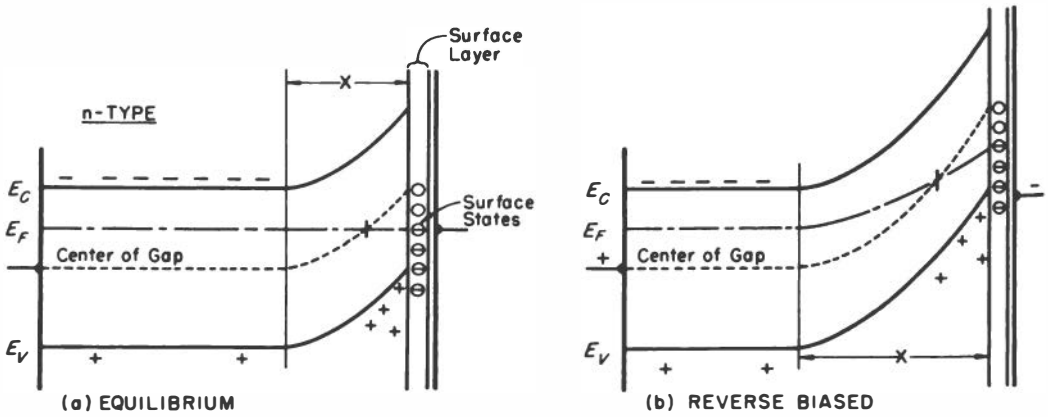

Fig. 30. Electron-energy-band scheme at the surface of n-type silicon, showing the formation of a surface barrier.

*Developmental lithium ion-drift detectors are available from Solid State Radiations, Inc., 2261 South Carmelina Avenue, Los Angeles 64, California.

the point where the Fermi level crosses the center of the gap is often called an inversion layer, because its properties closely resemble a semiconductor of the type opposite to that of the interior. In a sense, therefore, the inversion layer forms a p-n junction with the bulk material.

With reverse bias applied [Fig. 30(b)], the depletion region widens very much as was observed for the p-n junction. In fact, the theoretical treatment used to obtain the nomograph in Fig. 28 does not distinguish between barriers formed at p-n junctions or at surfaces.

C. Collection of Charge. Many of the general remarks on the operation of gas ionization chambers apply equally to the semiconductor type as well. It will be recalled that, in gas ionization chambers, the low mobility of heavy positive ions gives rise to several problems associated with the collection of charge; on the other hand, the semiconductor detector possesses the great advantage that both the hole and the electron are highly mobile current carriers. In silicon at room temperature the electron mobility μ_n = 1200 cm²/volt-sec and the hole mobility μ_p = 500 cm²/volt-sec. This situation makes it possible to collect all the charge in a short time, regardless of the location of the event within the depletion layer, and so the output pulse height is largely independent of such geometrical effects, although the rising portion of the pulse may show some variation in shape.

The charge q collected for an average energy $\bar{E}$ dissipated in the sensitive region is

$$q = e \frac{\bar{E}}{w} \eta , \qquad (12)$$

where w is the energy to produce one hole-electron pair (3.5 ev for silicon), and η is the collection efficiency. In a good diode, it should be possible to increase the bias to the saturation value (to a bias for which η = 1).

Even when the bias is sufficient to sustain a depletion layer deep enough to contain the entire charged-particle track, the charge collection still may not be complete. This loss of charge carriers may occur in two ways. First, holes and electrons can be trapped by structural imperfections and chemical impurities which have significant capture cross sections for the current carriers. An electron, for example, may be immobilized at one such location for a period of time and then

be released; it may go through this process several times on its way to the positive electrode. The charge collected in such a case will consist of a band of pulses, randomly distributed in time but with an integral of one electronic charge. Fortunately, this effect is usually not large, and so it is unnecessary to use very long clipping times in the amplifier to be certain of complete charge collection from traps.

The movement of carriers through the field can also be affected by recombination. The electrons and holes produced along a charged-particle track will drift in opposite directions in the electric field, and so before the two charge clouds separate, they must pass through each other. During this time recombination centers are being exposed to both electrons and holes, and occasionally the conditions are met for the elimination of one hole and one electron at one of these sites.

Both trapping and recombination effects depend upon the presence of impurities in the high field region. The most important regions for charge collection are those with high electric fields; in semiconductor detectors the high electric field is at the surface. Unfortunately, the surface region is most likely to contain impurities, especially in p-n junctions formed by high-temperature diffusion. Surface-barrier diodes and junctions formed at low temperature have advantages in this respect.

Recombination and trapping effects should be relatively small for work with electrons and most heavy charged particles. However, fission fragments, which produce intense ionization along a very short track, exhibit measurable loss of charge. The loss of charge by recombination and trapping has been investigated and reviewed by Miller and Gibson.[58]

The signal voltage appearing across the detector is readily obtained from the charge q, and the sum of the barrier capacitance C_b and the stray capacitance C_s:

$$V = q/(C_b + C_s). \qquad (13)$$

Note that for a strictly proportional relationship between V and q, both C_b and C_s must be constants.

2. Fabrication Techniques

Semiconductor radiation detectors resemble conventional photovoltaic cells, and the usual semiconductor fabrication

methods[59] are followed. In this section, emphasis will be given to silicon diodes, because they are suitable for room-temperature operation; however, excellent detectors for operation at liquid-nitrogen or liquid-helium temperatures have been made by using germanium as the base material.[52]

A. Diffused Junctions. A typical diffused junction diode is shown in Fig. 31(a). The general procedure to be described here resembles the technique of Donovan.[60] Wafers of p-type silicon are cut to squares 5 x 5 mm, and about 1 mm thick, using a diamond saw; they are then lapped and etch polished.

The heavily doped n^+ layer is prepared by phosphorus diffusion. The phosphorus may be introduced by painting a suspension of P_2O_5 in an organic liquid on the top surface and heating for 10 minutes at 900°C. A more uniform layer, which is also freer from trace impurities, can be diffused by exposure to gaseous P_2O_5 at 900°C for a few minutes. In both cases, the resulting n^+ layers are about 0.1 micron thick.

The sensitive area desired is masked by painting with Apiezon W wax dissolved in trichloroethylene. A deep etching is made which removes not only the excess n^+ material, but also the p-type substrate to a considerable depth. This leave the so-called "mesa" configuration shown in the figure. Junction edges must be protected from ambient effects either by a covering of wax or an oxide layer.

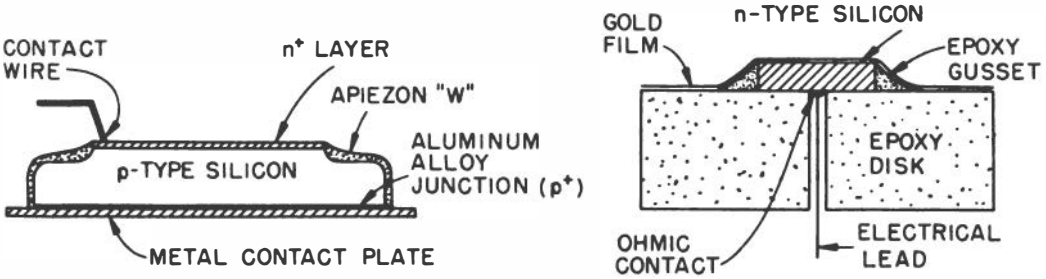

Fig. 31. Sketches showing semiconductor radiation detector construction (not to scale). (a) p-n junction detector. (b) Surface barrier detector.

A metal contact to the high-resistivity p-type silicon must be carefully designed, otherwise an injecting contact may develop, producing erratic results. One of the simplest contacts is made by amalgamating a metal plate to the silicon with indium amalgam. If a pressure contact is to be used, an alloy junction

is made by alloying an acceptor metal such as aluminum with the high-resistivity base. This may be done immediately following the phosphorus diffusion. About 0.05 micron of aluminum is evaporated onto the lower face of the wafer, followed by heating to 650°C for a few minutes. This forms a heavily doped, or p^+ layer, to which a pressure contact may be made with ease. During the final etching, both the sensitive n^+ face and the p^+ alloy must be protected by wax.

Because of the heavy doping of the n^+ layer, an ohmic contact to it is readily made. A gold, or even a copper wire is put in pressure contact with the n^+ layer. The contact is improved if a 0.01 μfd capacitor, charged to several hundred volts, is discharged through the diode in the forward bias direction. This welding operation is known as "forming," or to the initiated as "zapping" the diode.

Junction detectors similar to the design just described may be obtained from several manufacturers.*

B. Surface Barriers. The surface-barrier detector shown in Fig. 31(b) resembles the design of Blankenship and Borkowski,[54] with some modifications by Chetham-Strode, et al.[61]

The wafers of n-type silicon are cut to about 5 x 5 x 1 mm and then lapped. The lapped wafer is nickel plated,[59] and the ohmic contact is made by soldering a wire to the nickel. The solder joint is painted with Apiezon W wax, and the entire crystal is immersed in the etching bath. After the etching is complete, the wafer is laid on an epoxy disk, with the electrical lead protruding through a small hole. Mounting is accomplished by flowing a smooth gusset of epoxy resin around the wafer so that all edges are protected. A thin layer of gold (~100 μgm/cm²) is then deposited by vacuum evaporation over the entire top face of the assembly, to form a conducting layer. Electrical connection to this layer is made by pressure contact to the top face of the epoxy disk. Lower leakage currents and higher

*Some manufacturers are:

Harshaw Chemical Company, 1945 East 97th Street, Cleveland 6, Ohio.

Hughes Aircraft Company, P. O. Box 90515, International Airport Station, Los Angeles 45, California.

RCA Victor Company, Ltd., Montreal 30 Canada.

Solid State Radiations, Inc., 2261 South Carmelina Avenue, Los Angeles 64, California.

inverse voltage breakdowns will be obtained if the finished detectors are baked for 48 hours at 110°C. Because of their sensitivity to ambients, surface barrier detectors should be stored in a vacuum dessicator before use.

Silicon surface barrier detectors similar to the type just described are available from commercial sources.*

C. Guard-Ring Detectors. Surface leakage currents at the edge of a semiconductor radiation detector are often much greater than leakage currents through the bulk, and so they constitute an important source of noise. This edge leakage becomes quite serious when it is desired to fabricate detectors of large sensitive area, because the increase of exposed surface area causes an attendant increase in the detector noise. Also, the leakage noise increases with the reverse bias applied, and the noise may limit the usable bias to an unacceptably low value in cases where a deep depletion layer, and hence a high reverse bias, is required.

As was mentioned earlier, some form of edge protection is required; various materials have been suggested for this purpose, e.g., Apiezon W, epoxy resins, oxide films, and silica or glass films.

A technique which promises to be very useful in some applications is the use of a guard ring, similar in principle to the guard ring of a gas ionization chamber (Section III.4., above). A guard-ring p-n junction detector used by Hansen and Goulding[62] is shown in Fig. 32. The sensitive detector area is the center

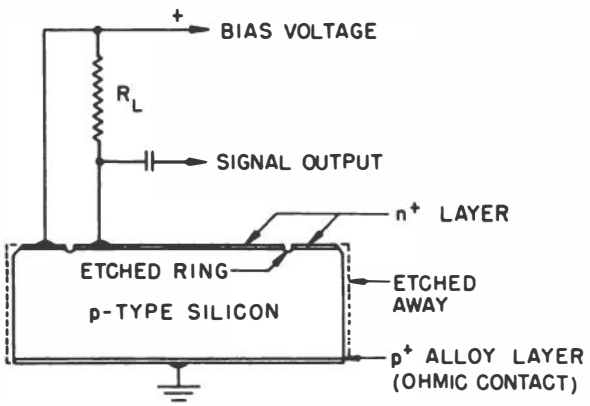

Fig. 32. Guard-ring details for a p-n junction radiation detector (Hansen and Goulding[62]).

*For example, from Oak Ridge Technical Enterprises Corp., P. O. Box 524, Oak Ridge, Tennessee.

disk-shaped region defined by the etched ring. The guard ring formed at the periphery is connected directly to the bias-voltage source; therefore, leakage currents at the edge of the detector flow from the bias supply to ground and do not pass through the load resistor R_L. Since the potentials of the guard ring and center disk differ only by the amount of the signal voltage, leakage across the etched ring is extremely small. For best results, however, good surface treatments must be used on all etched surfaces.

Prototype versions of guard-ring p-n junction detectors are now available commercially.*

3. Application to Spectrometry

A. Electronics. A typical electronic system for use with a silicon surface barrier detector is sketched in Fig. 33. The bias supply must be well filtered, and it is usually helpful to monitor the leakage current and the rms noise as the bias voltage is varied.

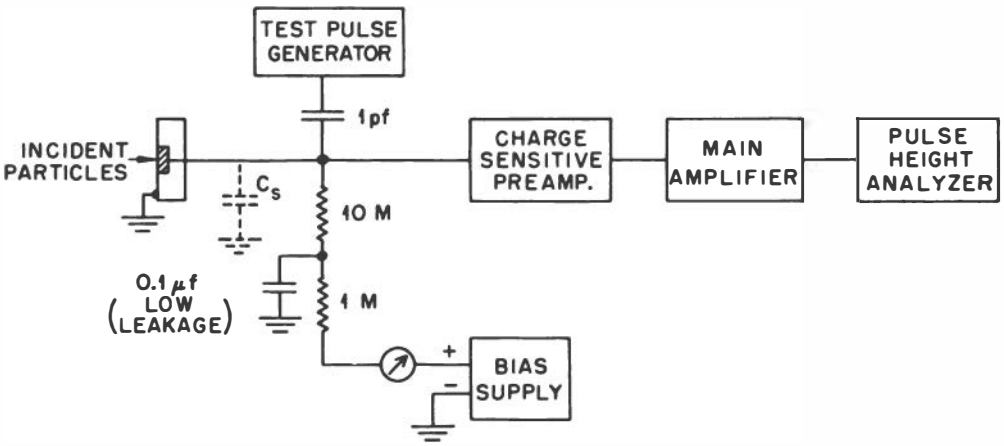

Fig. 33. Functional block diagram of equipment used with a surface-barrier detector.

Because signals from the detector are of such low amplitude, the preamplifier should be very carefully designed for low input noise. It is also recommended that the preamplifier be of the "charge-sensitive" type (Section VI.2.D., below),

*Solid State Radiations, Inc., 2261 South Carmelina Avenue, Los Angeles 64, California.

which produces an output pulse whose amplitude is proportional to charge and not voltage. A voltage-sensitive amplifier will reflect any variations in the input capacitance resulting from variations in the barrier properties (cf., Eq. 13); such irregular changes in capacitance can occur but are not serious if the amplifier is charge sensitive.

A test-pulse generator with low-impedance output may be used for checking the operation of the system. When used as shown in Fig. 33, the generator may be calibrated in terms of energy and will, for a given generator amplitude setting deliver the same amount of charge to the preamplifier even though the input capacitance may vary greatly. Its output is a useful substitute for a detector pulse. The noise of the system with an equivalent capacitance substituted for the detector may be measured by injecting an amount of charge corresponding to some given energy, and from the width of the peak obtained the amplifier noise may be calculated. The equivalent noise from such a measurement typically is 3-10 kev full-width at half-maximum.

The clipping time of the main amplifier may be chosen for optimum signal to noise ratio, since the collection time is extremely rapid compared to gas ionization chambers. Recommended clipping times[54] are 0.5 to 2 μsec.

If the sensitive depth is determined with particles of known energy, it is found[63] that the measured depth exceeds the value of x obtained from Fig. 28. Further, the experimental value increases with an increase in the clipping time. This behavior arises because the electron-hole pairs created outside the space charge region do not contribute to the current immediately. They diffuse about in the field-free region and may reach the edge of the space-charge region, where one of the carriers will be swept across and collected. Since this is a slow process compared with the normal collection of charge formed within the field, the probability of collecting charge by diffusion is enhanced by slowing down the amplifier response. Naturally, this is an artifact and is of no practical importance if the space-charge region always extends beyond the incident particle range.

B. Experimental Arrangement. Semiconductor detectors have been applied to the study of many types of charged particles. Perhaps the most successful application of interest to chemists is in high-resolution alpha spectroscopy, although

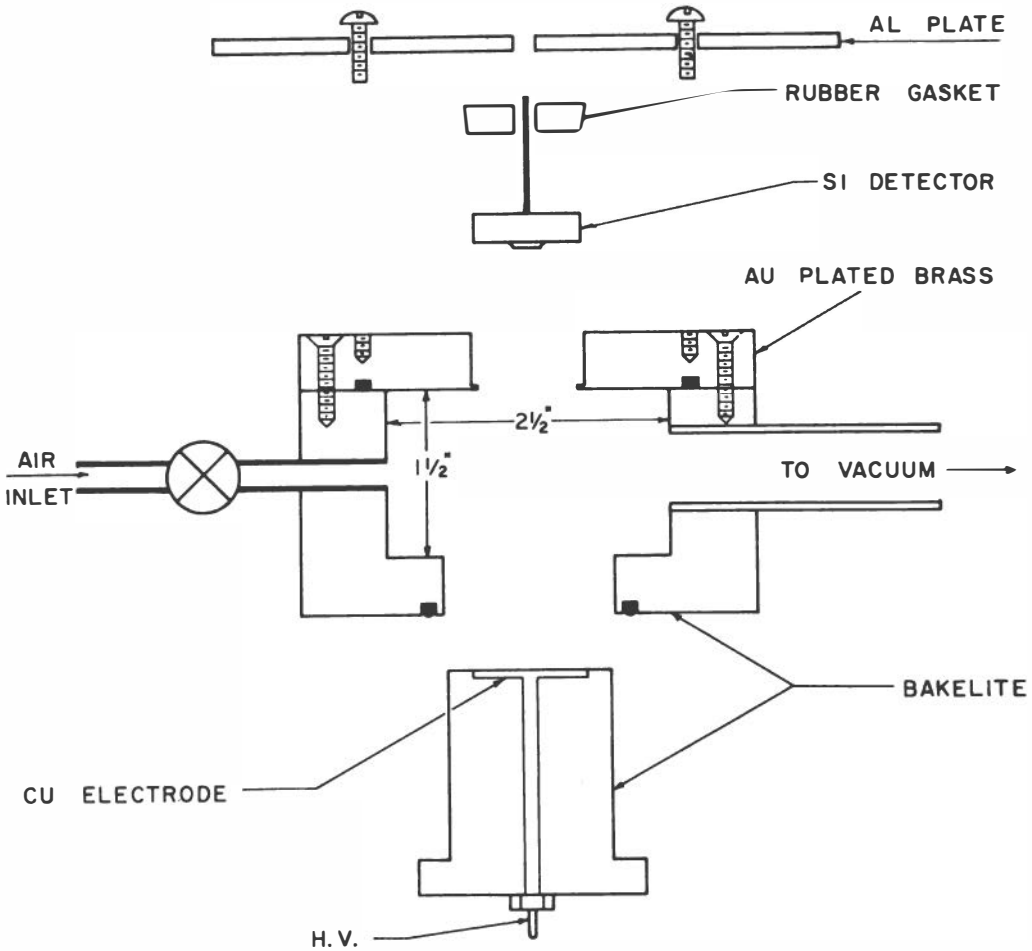

Fig. 34. Exploded view of a chamber for study of alpha-particle spectra with a surface-barrier detector (Chetham-Strode, et al.[61]).

recent advances in technique indicate that these detectors may eventually find even more widespread use in electron and beta-ray energy studies.

Figure 34 shows the counting chamber designed by Chetham-Strode, et al.,[61] for precision alpha spectrometry with silicon surface-barrier detectors. The relatively large internal dimensions were chosen to remove scattering surfaces from the source and detector. The detector was recessed so that the sensitive part of the detector could not "see" the scattering surfaces. Since the surface-barrier detector is rather sensitive to air ambients, and the alpha-particle energy is degraded by air, provision was made for evacuating the chamber.

The technique to be followed was treated in detail by Chetham-Strode, et al.,[61] who discussed the problem of eliminating background counts in order to realize the inherently low background possible with silicon detectors. Materials of construction used in the counting chamber should have very small alpha contamination. In cases where the recoil daughter nuclei formed in alpha decay are radioactive and may contaminate the silicon detector these authors suggest introducing a low gas pressure into the chamber to slow the recoils to an energy such that they can be returned to the source plate by application of an electric field.

An alpha spectrum of Cm^{244} obtained with a surface barrier detector is shown in Fig. 35. The full-width at half-maximum counting rate is only 16 kev, and so the two main alpha groups, 43 kev apart, are well resolved. In addition to the groups shown, a third group, 142 kev below the intense peak (α_{142}) is known[64] to be present in an abundance of 0.017%. Since the resolution is adequate it would be hoped that measurement of such low-abundance groups could be accomplished on sources with too low an intensity to measure by magnetic deflection. Such weak alpha groups may often be obscured by a non-gaussian, low-energy tail on the peaks. The height of this tail at the expected position for the α_{142} peak of Cm^{244} is 0.15% the height of the α_0 peak. From information available to date, it appears that a substantial portion of this tail is associated with processes within the detector and not with environmental effects such as source properties, scattering, or energy loss in the gold detector film.

V. GAS MULTIPLICATION COUNTERS

1. Introduction

The operation of an ionization chamber depends upon the collection of the charge produced when an ionizing particle traverses the sensitive volume. Any enhancement of the electrical signal produced must be done in the electronic amplifier system, as the chamber possesses no internal amplification properties. On the other hand, proportional counters and Geiger counters make use of gas multiplication, which enables them to produce output pulses many times larger than would be

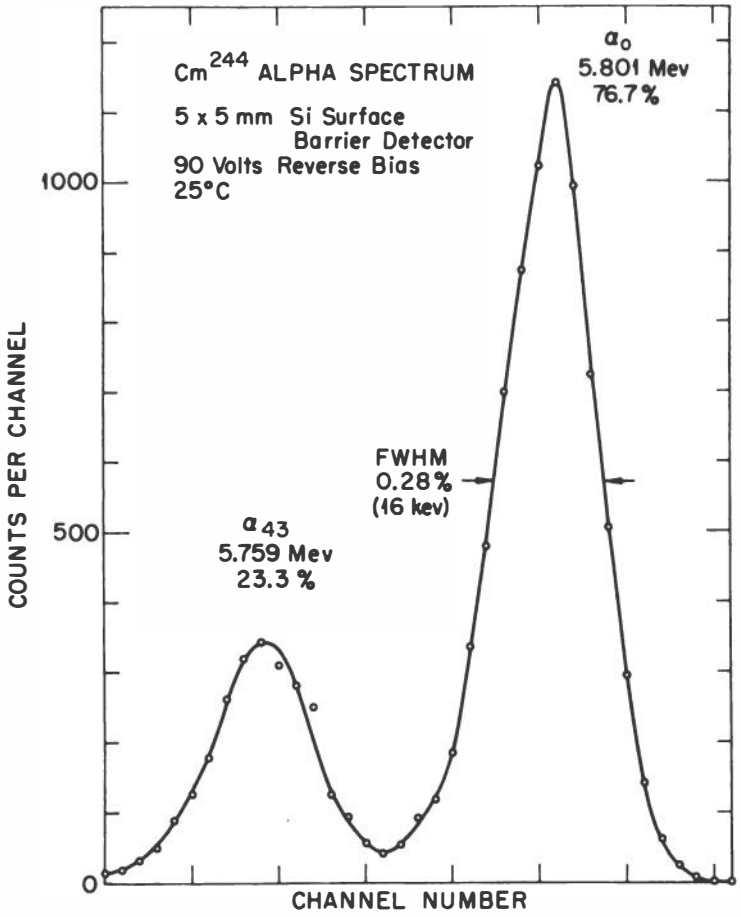

Fig. 35. Pulse-height distribution measured with a 5 x 5-mm silicon surface-barrier detector at 25°C and 90 volts reverse bias. The energies and abundances of the alpha groups to the ground and 43-kev states of the Pu^{240} daughter nucleus are literature values (A. Chetham-Strode, Oak Ridge National Laboratory).

obtained if only the primary ionization were collected.

The distinction between simple ionization chambers and gas multiplication counters may be seen by considering the number of ion pair collected (or pulse height) as a function of applied voltage. For example, Fig. 36 shows the behavior of a gas-filled counter with coaxial electrodes; the inner electrode is a fine wire, which serves as the anode. As was shown in Section III.2., the number of ion pairs collected rises with applied voltage, until a saturation region (B of Fig. 36) is reached. When the voltage is advanced beyond region B, the electrons acquire sufficient energy near the anode to produce

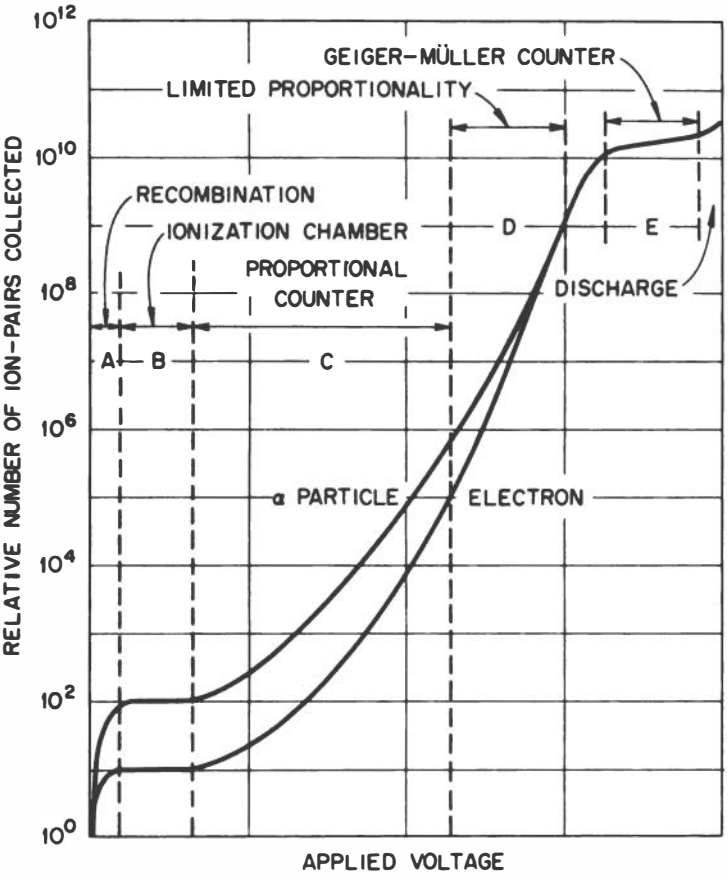

Fig. 36. Illustration of the relative number of ion pairs collected in a counter as a function of the applied voltage, showing the relationship between the ionization chamber, proportional counter, and Geiger-Müller counter regions of operation.

additional ionization of the gas by collision, and the pulse height rises. Throughout region C, each electron produced initially will produce an avalanche of m secondary electrons; m is called the gas multiplication. Region C is referred to as the proportional counter region, because the pulse size is proportional to the initial ionization; hence, the pulse height from the alpha particle of Fig. 36 remains a factor of 10 higher than the electron pulse height. This suggests that alpha particles can be counted in the presence of electrons which usually have a lower energy: a pulse-height discriminator (cf., Section VI. below) may be set to reject the low-amplitude electron pulses and count only the alpha particles.

Eventually, a further increase in voltage creates such a

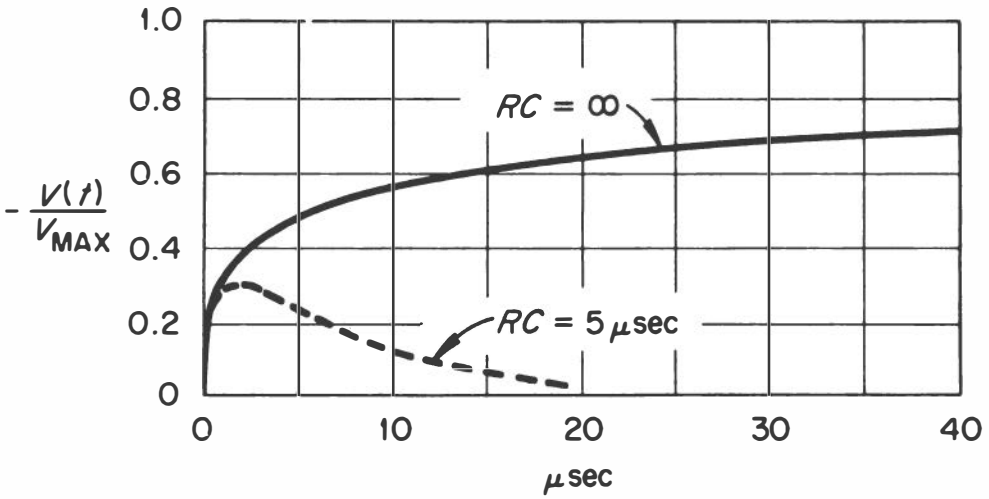

Fig. 37. Shape of a proportional counter pulse. The dotted curve shows the shape obtained with an input time constant RC = 5 μsec (Staub[44]).

density of secondary charges near the anode that the positive-ion space charge from one primary electron begins to interfere with the formation of an avalanche by a neighboring electron. This effect leads to the situation in D of Fig. 36 where the different amounts of primary ionization produce slightly differing pulse heights, but the strict proportionality is lost.

Region E is the Geiger-Müller region, in which the detector produces a pulse of almost constant height, regardless of the initial ionization. In this mode of operation the discharge is not localized, but rather a single electron initiates an avalanche which propagates throughout the anode's length. Although the Geiger-Müller counter, or Geiger counter as it is often called, cannot be used for spectrometry, its large-amplitude output pulse makes it useful for many applications where simple counting will suffice.

2. Proportional Counters*

Proportional counters are especially useful where pulse counting of beta radiation is required. Because of their shorter resolving time, proportional counters can be used at much higher counting rates than a Geiger counter, and they

*See references 39, 40, 41, 65, 66, and 67.

exhibit excellent long-term stability. When used as a spectrometer for low-energy beta rays and X-rays, the proportional counter is capable of much better resolution than a scintillation spectrometer.

A. Conditions for Gas Multiplication. To achieve gas multiplication it is necessary to provide an electric field strength capable of accelerating the primary electrons to an energy sufficient to produce additional ionization. In a typical geometry, the anode is a fine wire of radius a, coaxial with a cylindrical cathode of radius b. The electric field strength $\mathcal{E}$, at a radial distance r, and an applied voltage V, is

$$\mathcal{E} = \frac{V}{r \log_e (b/a)} . \qquad (14)$$

It is apparent from Eq. 14 that the high field is confined to the region near the central wire; hence, most of the gas multiplication occurs within a few mean free paths of the anode. Since the electrons move such a short distance before they are collected, the voltage pulse which appears on the anode arises from induction by the positive ions as they move away from the central region. The formation of a voltage pulse in this way is not as slow as might be expected, because the positive ions move through most of the voltage drop while still in the high-field region near the central wire. The time to collect all of the ions depends on the geometry, applied voltage, the gas chosen, and its pressure;[41] generally, collection times are a few hundred μsec.

The pulse shape[44] for a single ion or a group of ions produced at the same place is shown in Fig. 37. The output voltage rises very rapidly at first, being nearly linear with time; later, the pulse shape becomes logarithmic. In the example of Fig. 37, the pulse reaches half of its maximum amplitude in about 5 μsec; the total collection time in this case would be 590 μsec. If the time constant is reduced to 5 μsec, the maximum pulse height drops to about 1/3 of the former value but is much narrower. By "clipping" or "differentiating" the pulses in this way, the pulse width can be made small enough to permit high counting rates (c.f., Section VI.2.). Note that in this procedure all pulses are reduced by the same factor, since the final pulse height in a proportional counter does not depend on the location of the primary ionization. However, there will be

some variation in the rising part of the voltage pulse if the primary electrons are distributed radially through the chamber, since the primary electrons will then require a varying amount of time to drift into the multiplication region. For this reason, it is customary to integrate the signal with a time constant equal to several times the signal rise time to reduce the effect of rise time variations on output amplitude.[68]

The gas multiplication factor for a proportional counter may vary over a wide range. Actual values for particular filling gases are obtained experimentally as a function of applied voltage, chamber geometry, and gas pressure. Usually, gas multiplications range from unity up to about 10^4, with values as high as 10^6 possible for events with low primary ionization; the onset of nonproportionality is observed to occur with particles of high primary ionization at lower multiplications than minimum ionizing particles (see Fig. 36).

B. Construction and Use. Many practical forms of proportional counters have been employed. The design chosen usually depends on the application - for spectroscopy, the requirements may be quite exacting, while for beta counting, the design is not so critical.

When the proportional counter is to be used for spectroscopy of low-energy electrons or X-rays, the electric field should be uniform and the electrical noise generated by insulator leakage must be very small. The former requirement can best be met by using a cylindrical geometry, and then only if the central wire diameter is very uniform. It can be seen from Eq. 13 that small variations in the diameter of the central wire will cause large variations in the electric field strength. Any practical design will lead to some distortion of the electric field at the ends, the so-called end effect. However, if the radiation to be analyzed can be collimated so that only the center portion of the sensitive volume is illuminated, then the end effect will not be very serious, providing that the counter tube is long with respect to its diameter. Such a design is shown in Fig. 38; low-energy X-rays are permitted to enter the counter through a beryllium window, midway along the wall.

Occasionally it may be inconvenient to make a long counter; a considerable latitude in dimensions is possible without field distortion if electrically insulated field tubes[66] are placed

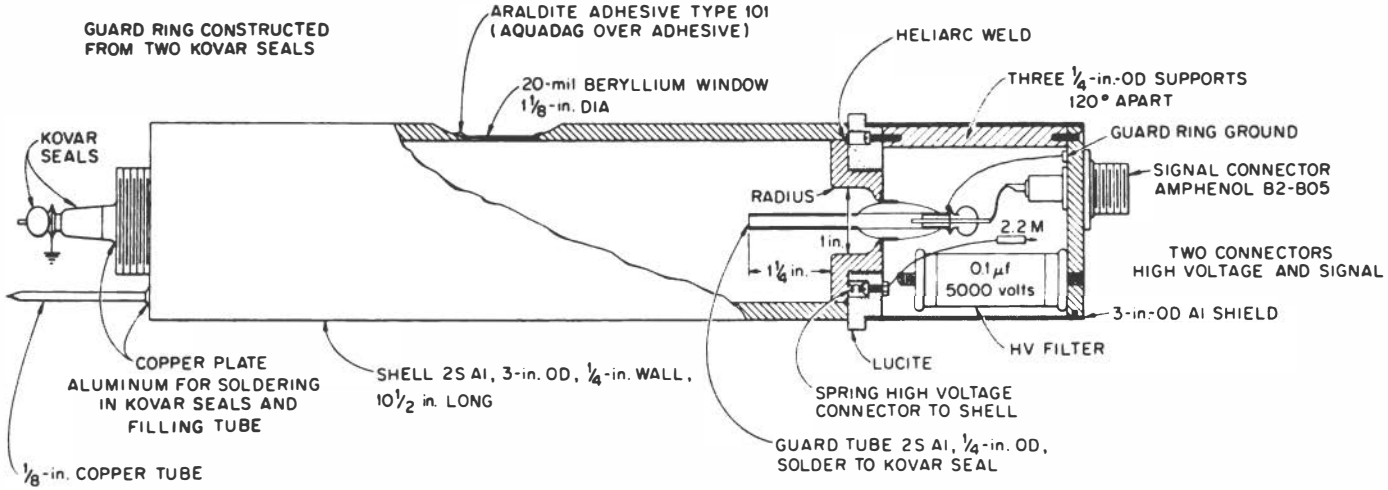

Fig. 38. Proportional counter for X-ray spectrometry, showing details of construction (C. J. Borkowski, Oak Ridge National Laboratory).

over the guard tubes. Their voltage is adjusted so that the lines of force are radial at the end of the sensitive volume.

Figure 38 also serves to illustrate how the requirement of low leakage noise is met. First, a guard electrode is used in the same way as for ionization chambers. Also, the anode is operated at ground potential, so there is no need for a high-voltage blocking capacitor, which often can become a source of noise.

Because they are so much more convenient and reliable than Geiger counters, most routine beta assay work is performed with proportional counters. Often it is neither practical nor necessary to approximate a cylindrical geometry for an end-window counter; in this case, the design of Fig. 39 is useful. A wire loop is the anode and may be placed inside a cylinder as shown, or inside a hemisphere [Fig. 51(b)]. These counters are usually

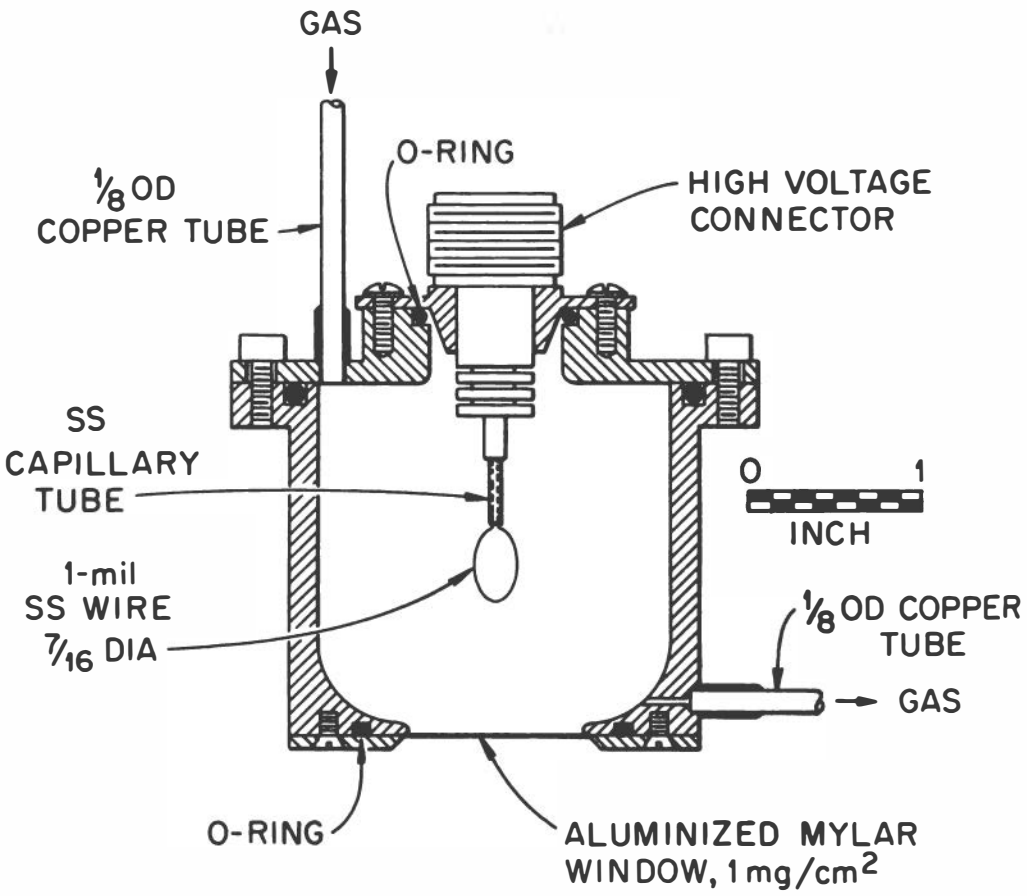

Fig. 39. End-window proportional counter for routine beta-ray counting.

operated at one atmosphere pressure of filling gas, which flows continuously. If pure methane is used as the counter gas, a rather high voltage (typically 3500 volts) is needed; a mixture of 90% argon and 10% methane ("P-10 Gas") permits operation at about half the methane voltage.

In a flow counter the window may be eliminated entirely. This is especially helpful in the counting of alpha particles and low-energy electrons. The sample is introduced into the chamber by means of a slide.

The 4π counter has enjoyed increasingly widespread use in the standardization of radioactive sources (c.f., Section VIII.2.D.). A useful version of this type of counter is shown in Fig. 40. Two identical proportional counters view the source with almost an exact 4π geometry. The chambers are of the "pillbox" type with 1-mil stainless steel anode wires. When used for absolute beta counting, the anodes of the two halves are connected together and operated as a single counter. A slide is provided for rapid changing of samples. The carrier-free source is mounted on a thin plastic film, metallized to ensure electrical conductivity; thus, the source film cannot acquire an electrostatic charge but remains a part of the ground plane dividing the two counters.

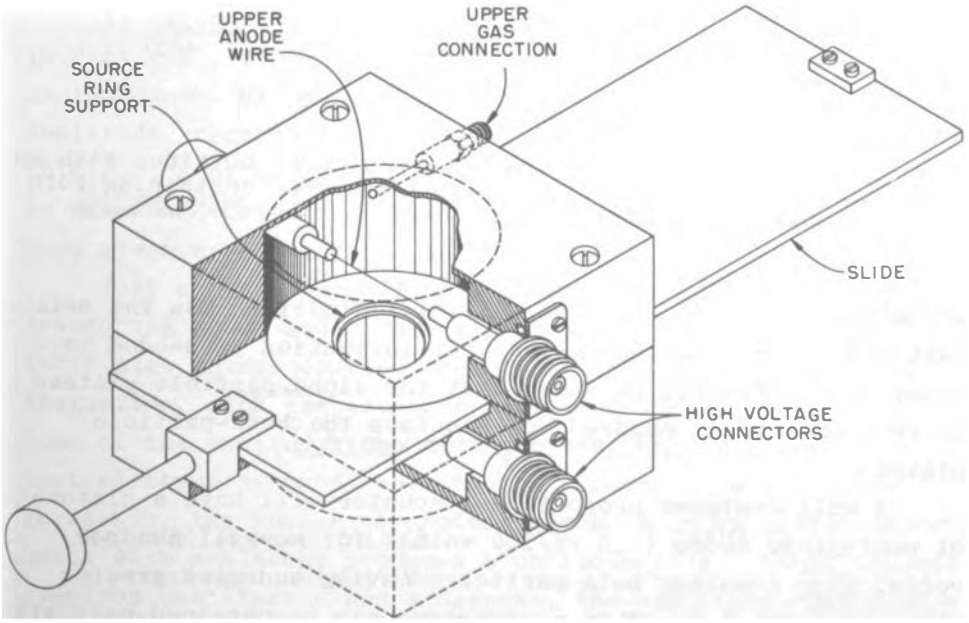

Fig. 40. Proportional counter for 4π beta counting (Oak Ridge National Laboratory Model Q-1632).

C. Plateau Characteristics. For alpha and beta counting the required voltage sensitivity is about 1 mv. This is obtained, for example, if the amplifier voltage gain is 250, and the scaler or other recording equipment records all pulses above 0.25 v. As the voltage is increased, the counting rate rises until all particles yield a pulse large enough to count; increasing the high voltage still further produces an essentially constant counting rate, since all particles are now being recorded. This region of almost constant counting rate is called the plateau.

In Fig. 41 is shown a counting rate-voltage curve obtained with a source containing both an alpha and a beta emitter. The

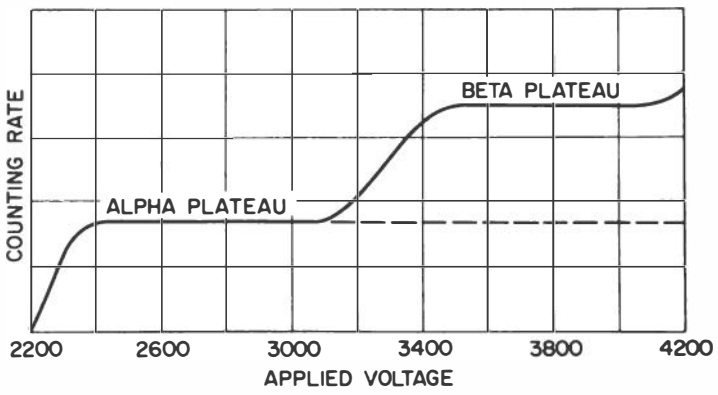

Fig. 41. A counting rate-voltage curve obtained with an end-window proportional counter, and a source containing both an alpha and a beta emitter.

alpha particles deposit more initial ionization than the beta particles, and so a smaller gas multiplication is needed to count them. The figure shows that the alpha-particle plateau is reached several hundred volts before the beta-particle plateau.

A well-designed proportional counter will have a plateau of negligible slope (< 0.2%/100 volts) for several hundred volts, when counting beta particles having energies greater than about 200 kev. This performance can be obtained only with an amplifier having low noise and good overload properties. (See Section VI.2., below).

3. Geiger Counters*

The Geiger counter once was the most popular type of radiation detector, since it was capable of detecting any ionizing radiation with adequate sensitivity, and because of its large pulse size, it did not require a high-gain amplifier. Now, however, Geiger counters are not often used in laboratory counting for a number of reasons: their plateaus have a greater slope than proportional counters, and so a Geiger counting setup is not as stable as the proportional type; they possess a long dead time which arises from the mechanism of the discharge, and cannot be reduced; finally, they produce a pulse of constant amplitude regardless of the initial ionization, and therefore cannot distinguish between alpha and beta particles. Geiger counters can be made into very rugged assemblies, and, because they require only very simple ancillary equipment, they are widely used for survey devices and other field applications.

In general appearance the Geiger counters resemble their relatives, the proportional counters, but they differ in the nature of the filling gas and the pressure. Design requirements for a Geiger counter are rather critical, and a cylindrical geometry is almost always used because the necessary parameters are easily controlled.

A. Mechanism of the Geiger Counter. As mentioned above in Part V.1., if the voltage applied to a proportional counter is increased, all pulses eventually become of the same high amplitude, regardless of the initial ionization (see Fig. 36). This region of operation is called the Geiger region, and will be discussed briefly. Detailed treatments of the subject have been given by Wilkinson[41] and by Korff.[69]

Just as in a proportional counter, the electrons drift toward the anode and become accelerated in the electric field Their high energy enables them to release more electrons by ionization, each new electron releasing further ionization. Some of the excited atoms emit photons, and occasionally a photoelectron is produced. As the electric field strength increases, the number of photons produced in an avalanche grows until each avalanche produces a photoelectron. Since a single electron can start a new avalanche, the avalanche region spreads until it envelops the entire central wire.

*See references 39, 41, 65, and 69.

As in a proportional counter, collection of all the electrons is a fast but small contribution to the voltage pulse. The larger part comes from electrostatic induction by the positive-ion sheath as it crosses the high-field region on its way to the cathode.

If a positively charged rare-gas ion strikes the cathode, a secondary electron may be produced. This additional electron will result in another discharge unless provision is made to prevent multiple discharges by quenching. Almost all modern Geiger tubes are self-quenching; that is, they contain some polyatomic gas which brings a halt to the process when the positive-ion sheath reaches the cathode. Argon-filled Geiger tubes frequently use alcohol as the quenching gas; in such a tube, an argon ion makes frequent collisions with argon atoms and alcohol molecules on its way to the cathode. The probability is very high that an argon ion will be neutralized in an encounter with an alcohol molecule, but the opposite transfer of charge is not energetically possible. Therefore, the positive-ion sheath which finally reaches the cathode is composed only of alcohol molecular ions. These ions cannot release secondary electrons; instead, they become neutralized at the cathode surface and dissociate harmlessly. The organic gas eventually becomes depleted after about 10^9 counts have occurred, and the counter is no longer usable. The consumption of quenching gas increases with operating voltage.

The life of Geiger counters has been extended greatly through the use of halogens as quenching gases. A common filling is about 0.1% chlorine in neon. The quenching mechanism is the same as just described for organics, except that after the diatomic chlorine molecules dissociate at the cathode, they eventually recombine; thus, the quenching gas is continually replenished. This makes it possible to operate the tube at very high voltages without harm, and so very large signal pulses are obtainable.

B. Plateaus. The counting rate-voltage plateaus for Geiger counters do not, as a rule, have a very small slope. The organically quenched tubes exhibit plateaus 200-300 volts long, with a slope of 1-2% per 100 volts. Because of the organic quenching gas, their life is limited to only about 10^9 counts, and therefore should not be subjected to high counting rates for extended periods. The halogen-quenched tubes are character-

ized by shorter plateaus (100-200 volts), and steeper slopes of 3-4% per 100 volts. Halogen-quenched tubes have a much longer counting life, extending to perhaps 10^{11} counts. An early objection to the halogen-quenched tubes was that, because of the large anode used, the detection efficiency was not uniform over the window area. Recent improvements in design have largely eliminated this effect and have improved the plateau performance to the extent quoted above.

C. Resolving Time. Although the time constant of the counting equipment may be made quite short so that only the initial part of the output pulse is utilized, the Geiger tube does not immediately recover from the discharge. Unlike the proportional counter, the positive ions form a nearly cylindrical sheath around the anode, which profoundly disrupts the electric field and prevents the initiation of new avalanches near the anode. This situation prevails until the ion sheath has migrated out of the high-field region. The time interval during which the tube is completely insensitive to additional ionizing particles is called the dead time; the time interval which follows is called the recovery time, because once the tube begins to count again, it requires a considerable period before the pulse size regains the original amplitude. This is illustrated in Fig. 42.

In a practical measuring system, it is necessary to know the resolving time, or average time interval for which the

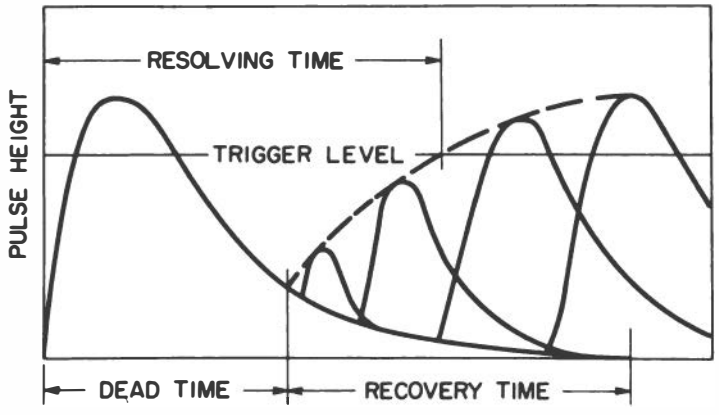

Fig. 42. Illustration of pulse shapes in a typical Geiger tube operating at a high counting rate. The dead time and recovery times are determined by the Geiger tube characteristics, but the resolving time depends on the triggering level of the electronic recording system.

recording equipment is insensitive. For a system which has the sensitivity to count all pulses, the resolving time will be equal to the dead time. Figure 42 shows that a system which triggers on high-amplitude pulses will exhibit a resolving time greater than the dead time. Typical dead times for Geiger tubes are from 100 to 300 μsec.

Corrections applied to counting data because of the resolving time are especially large and, therefore, important when using Geiger tubes. A precise value for the resolving time of a particular tube can be determined only by experiment. Such a determination can be made by using the multiple-source comparison method.[70] Another method which offers some advantages is to count repeatedly a sample of some short-lived nuclide as it decays from a high rate to a very low rate. The known half life may be fitted accurately to the points at low rates, for which the corrections are small or negligible, and the decay curve is extrapolated to time zero. The differences between the decay curve and the experimental points may be used to construct a correction curve directly or to compute the resolving time.

The uncertainties in applying a resolving-time correction may be avoided by fixing the resolving time of the detection system electronically at a value somewhat greater than the Geiger-tube dead time.

Once the resolving time τ is known, the corrected counting rate N_0 can be approximated for any measured rate N, by

$$N_0 = \frac{N}{1 - N\tau} \quad . \tag{15}$$

The time unit for τ, N, and N_0 must be the same.

VI. AUXILIARY ELECTRONIC INSTRUMENTATION

1. General Introduction

So far, this monograph has been concerned with the detectors used in a nuclear measurement system. From time to time it has seemed advisable to remark upon some of the considerations which are important in selecting the electronic accessories to be used with a particular detector. The ensuing

discussion will be devoted to a more general treatment of some of the available electronic equipment.

These devices will not be treated in detail, but rather their nature and application will be described in the hope that an experimenter will be guided to select the measuring system best suited to his needs.

A nuclear measuring system capable of performing a variety of tasks is diagrammed in Fig. 43. If integral counting is the only requirement, the pulse-height selector may be set to produce an output pulse for every input pulse whose amplitude exceeds a desired value. The scaler may record the number of pulses in a standard time interval, or the counting-rate meter may be used to indicate continuously the average counting rate. Should the experiment require data on the pulse-height distribution, the amplifier signals are fed to a pulse-height analyzer for sorting and information storage.

Before describing the various components themselves, it may be noted that transistorized electronic devices are now available which are essentially equivalent to equipment using vacuum tubes. Thus, linear amplifiers, scalers, and pulse-height analyzers generally may be obtained in either transistorized or vacuum-tube versions. On the basis of experience to date, it appears that transistorized units are to be preferred, even though they may be considerably more expensive in some cases. The chief advantage of transistor circuits is their greater reliability; less maintenance is required, a particular benefit for laboratories not equipped with extensive repair facilities. Other advantages of transistors are small size and low-heat dissipation.

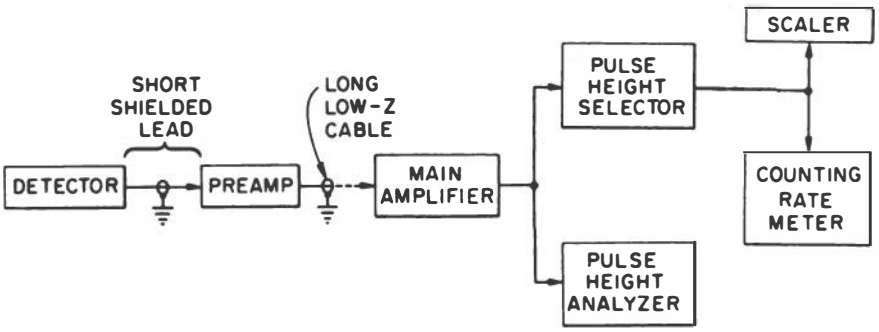

Fig. 43. Typical nuclear measuring system, with provisions for either integral counting or differential pulse-height analysis.

2. Amplifiers*

The signal from a radiation detection is produced by delivering an amount of charge q onto an input capacitance C. Typical values for the output voltages (given by q/C) from several detectors are listed in Table 4. It is readily seen

TABLE 4. DETECTOR PULSE CHARACTERISTICS

Detector	Typical Output Signal[a]	Energy Dependent	Rise Time
G-M	0-10 volts	No	Slow
Proportional	0-100 mv	Yes	Slow
Pulse Ion Chamber	0-3 mv	Yes	Slow
Semiconductor	0-25 mv	Yes	Fast
Scintillation	0-2 volts	Yes	Fast

[a]For a circuit capacitance of 20 pf.

that the pulse heights obtained are very small, and so an amplifier is needed between the detector and measuring apparatus. For spectrometry, where a precise analysis of the pulse-height distribution is to be made, vacuum-tube amplifiers with positive output pulses of 0-100 volts are often used; by contrast, transistorized amplifiers generally produce negative output pulses in the range 0-10 volts.

To accommodate a wide range of detector operating conditions, vacuum-tube amplifiers for scintillation and proportional counters commonly have a maximum gain of 5,000 to 50,000, with attenuators for setting the gain over a range of at least a factor of 100. Transistorized amplifiers require a voltage gain only about 0.1 as great.

The word amplifier as used here will be taken to mean a linear amplifier, i.e., one whose output amplitude is quite accurately proportional to the input amplitude. However, there are counting applications where nonlinear operation may be desired if the particular amplitude dependence can be kept reproducible and stable.

*See references 37, 68, 71, and 72.

A. Pulse Shaping. The generalized detector waveform shown in Fig. 44(a) defines the terms often used to describe such pulses. The rise time t_r depends on the particular

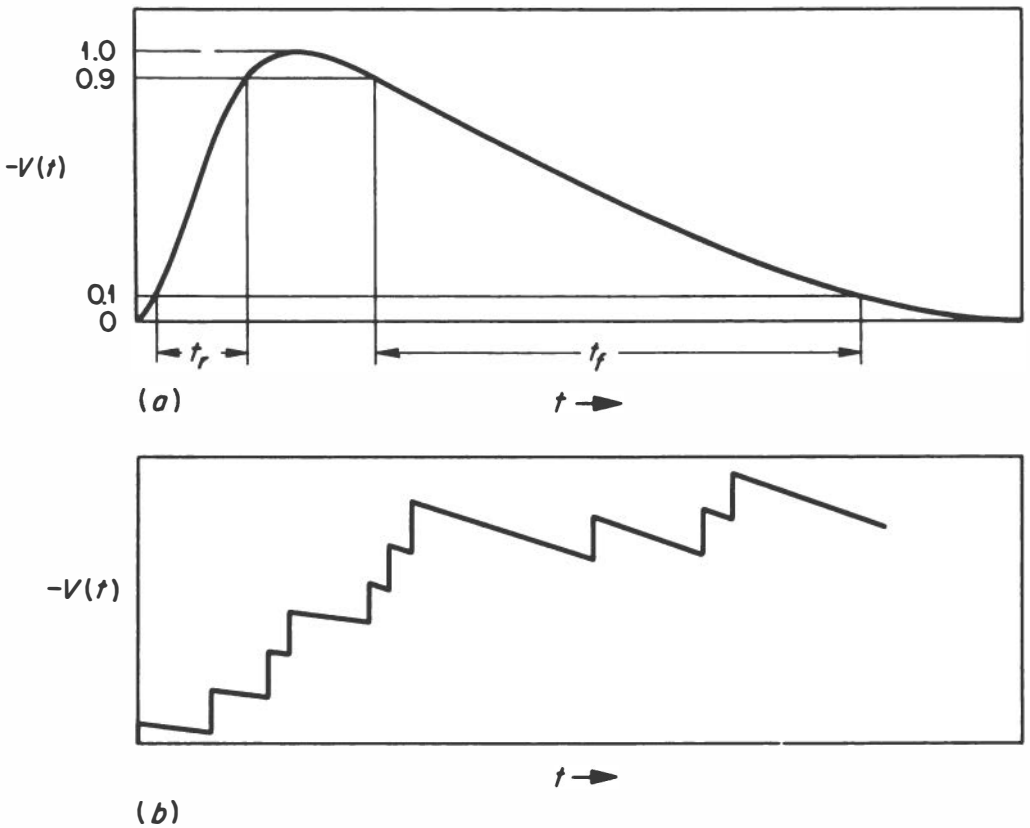

Fig. 44. Radiation detector pulses. (a) Single pulse plotted on an expanded scale to show definitions of rise time t_r, and fall time, t_f. (b) Pulses appearing at the input of an amplifier. All pulses have the same fast rise time, followed by a slow fall time. The high pulse rate causes the pulses to sum.

detector; for example, the rise time of a scintillation detector pulse depends on the decay time of the fluorescent light and the photomultiplier characteristics. The fall time t_f of the pulse depends on the load resistance R and the capacitance C of the signal lead to ground: $t_f = 2.2\ RC$.

Usually the fall time must be quite long relative to the rise time; this leads to the situation sketched in Fig. 44(b), which shows the pulses appearing at the input of an amplifier, all with the same characteristic fall time. Because of the high

rate, the "tail" of one pulse does not decay to the base line before another pulse appears. Such a state of affairs will not permit an accurate pulse-height analysis to be made. Further, since the useful information is contained in the leading edge of the pulse and its top, the tail only complicates the problem to no purpose.

The desired early portion of the detector pulse is extracted by using a clipping, or differentiating circuit.[37,74] Several electrical networks will perform the mathematical operation of differentiation; the most obvious approach is to use a single coupling stage in the amplifier whose RC product (or time constant) is much less than the others. This system suffers from two defects: there is a signal present in the amplifier long after the peak is reached [Fig. 45(a)], even though the fall time now is about 100 times faster than for the detector pulse; therefore, the clipping is not complete. In addition, practical amplifiers have many stages, and so there are, in effect, many differentiating circuits. An analysis shows that when only one RC time constant is short, every output pulse will be followed by a low-amplitude signal of opposite polarity (undershoot), which lasts for a very long time and whose area equals the area of the signal pulse. If additional pulses are processed during the recovery from an undershoot, the amplitude of such signals may be seriously altered. Further, the average voltage or base line will no longer be zero but will vary with changes in counting rate.

Clearly, it is desirable to reduce the duration of the undershoot so that the probability of pulse overlap is small. If two time constants in the amplifier are equal to each other and are smaller than the remaining networks, then the undershoot will have the largest amplitude and the shortest duration. This pulse shaping is known as double differentiation or double clipping; a typical waveform is shown in Fig. 45(b). Although the areas under the main pulse and its undershoot are equal under the conditions of Fig. 45(b), the amplitudes are not. As a result, there may be serious difficulties if the amplifier is driven out of its linear range by very large detector pulses. For example, when the amplifier is set for high gain in order to study low-energy radiation, then high-energy pulses which are also detected will drive the amplifier to its saturation output value. Under this overload condition, it is unlikely

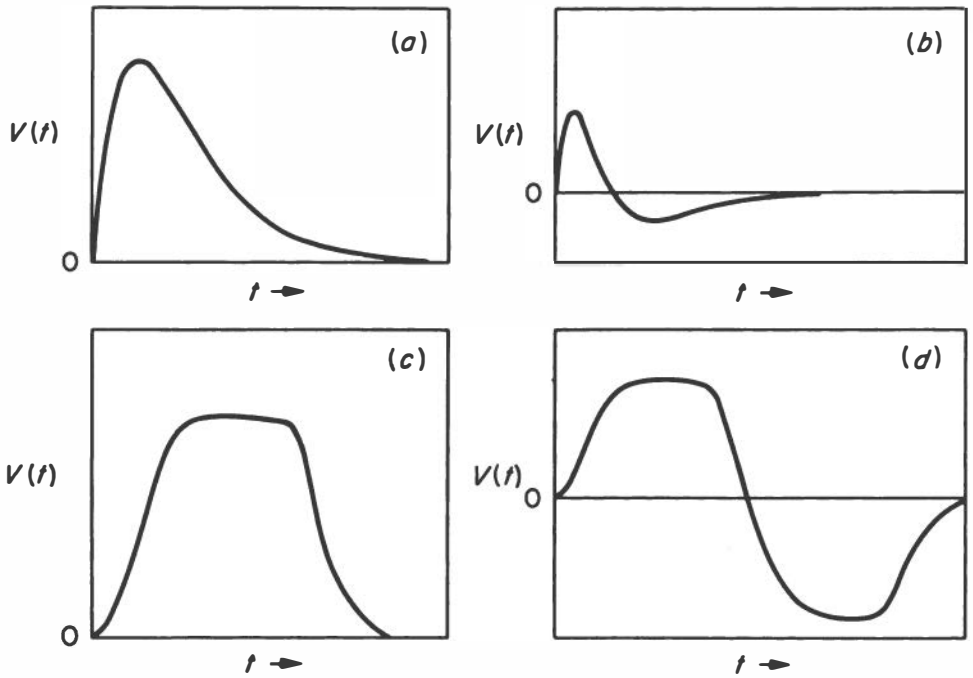

Fig. 45. Output pulses from amplifiers using (a) RC clipping, (b) Double RC clipping, (c) Single delay-line clipping, and (d) Double delay-line clipping.

that the undershoot will be distorted in the same way as the main pulse, and so at high counting rates, base line shifts can still occur.

Clipping with a delay line is to be preferred over the RC clipping techniques just described. An example of an amplifier which uses a shorted delay line clipper (with provisions for RC clipping if desired) is the Oak Ridge National Laboratory Model A1D, designed by Bell, Kelley, and Goss, and described in reference 39; the A1D output waveform is sketched in Fig. 45(c). The advantages of delay-line clipping over RC clipping are: the pulse is almost rectangular, and so the long tail characteristic of RC clipping is eliminated; also, the top of the pulse is more nearly flat, a desirable circumstance when certain types of pulse-height analyzers are to be employed. A disadvantage is that the delay-line circuits often used give rise to a small undershoot, which causes a base line shift at high counting rates.

The best pulse shape for most work is obtained by double clipping with delay lines. The symmetry of such a pulse, shown

in Fig. 45(d), leads to excellent overload and counting rate properties, since the area balance between positive and negative halves is essentially unchanged by overload. Double differentiation as a means of pulse shaping in a linear amplifier was proposed by E. Fairstein and R. A. Dandl. Practical applications of this technique are the Oak Ridge amplifiers model DD-2[75] and model A-8.[76] A transistorized design by Goulding, et al.,[77] has recently appeared.

The overload performance of an amplifier is extremely important in modern experiments, where it may be necessary to study low-energy radiations in the presence of a high-energy background. For example, the gain of an amplifier may be set so that maximum output is obtained for 50 kev of energy detected; if 5-Mev detector pulses are also present, they are said to drive the amplifier to 100 times overload. Such harsh treatment can lead to blocking, or a temporary amplifier paralysis following an overload pulse. Naturally, if high counting rates are to be tolerated, the amplifier should recover quickly after an overload. Double delay line differentiation and careful attention to blocking make it possible for the A-8 to recover after a 4000 times overload in less than 10 μsec, with no positive base-line excursion after the main pulse.

B. Noise. The extent to which amplifier noise is important will depend on the kind of measurement being made. If the amplifier is part of a simple counter, noise introduces spurious counts; thus, the lowest amplitude of usable signal is approximately equal to the noise level. If the amplifier is part of a spectrometer, the noise signals are not counted directly but appear as a broadening influence on spectral lines. As mentioned in Section IV.3.A., the noise is often stated in energy units such as kev. This is an experimenter's way of expressing the more fundamental noise unit, the equivalent charge,[78] which is a convenient concept because nuclear detector signals consist of bursts of charge collected on the input capacitance. By the use of units of charge instead of voltage, the capacitance need not be known.

The main sources of noise in a well-designed amplifier are those arising from the thermal motion of electrons in the input grid resistor and the noise from the input tube due to flicker effect, grid current, and shot effect. The last two of these

are usually the dominant contributions. The general trend is that noise increases with input capacitance. For more details, the reader may consult the recent reviews by Fairstein[37,78] and the earlier book by Gillespie.[68]

In a measuring system, sources of noise other than those associated with the amplifier must be evaluated. The photocathode of a photomultiplier tube releases electrons by thermal agitation which appear as random noise; if a scintillation counter is to be useful at low energies (and therefore, low-light intensities), this source of noise is usually far more important that the amplifier noise. At present, noise from the leakage current of a semiconductor radiation detector, rather than amplifier noise, limits the energy resolution of this device.

The noise problem becomes acute when an amplifier must be used for spectrometry with detectors of low output amplitude but with high-energy resolution. Examples of this case would be a semiconductor radiation detector or pulse ionization chamber. These detectors usually are not required to accommodate a large range of signal amplitudes, so overload performance is not very critical. An analysis shows that these conditions can best be satisfied with single RC clipping if the counting rates are not very high. Double differentiation gives a relatively higher noise contribution but may be justified if the counting rates are to be high.

Scintillation detectors produce large signals (see Table 4) but exhibit rather poor resolution. Therefore, the slight worsening of the noise level by double differentiation is negligible. On the other hand, the wide range of detector signal amplitudes requires double differentiation to achieve good overload characteristics.

Presently available transistors cannot equal the low noise performance of vacuum tubes at low input capacitances. With input capacitances of 15 to 20 pf, transistor amplifiers exhibit 3 to 10 times more noise than the best vacuum-tube amplifiers. At input capacitances of about 1000 pf the two systems are equal.[79] The poorer noise level for transistor amplifiers, while serious in the most critical high-resolution applications, is well within the acceptable limits for NaI(Tl) scintillation spectrometry.

C. Window Amplifiers. In many experiments it may not be

desirable to cover the energy range starting at zero. For example, alpha particles from heavy nuclides all have energies greater than about 4 Mev, and thus some way of shifting the amplifier threshold is indicated. This is accomplished by first amplifying the pulses in the usual way and then subtracting a constant amount of height from each pulse. The resulting pulses then are amplified to the required size by an amplifier with good overload properties. Such output amplifiers are variously known as expander amplifiers, window amplifiers, or more recently, as post amplifiers. This technique, especially as regards its application in improving the precision of pulse-height analyzers, is reviewed by Van Rennes;[80] some considerations based on recent developments in alpha spectroscopy were discussed by Fairstein.[78] The Oak Ridge Model Q-2069 amplifier system[81] is a good example of a low-noise amplifier for alpha spectrometry and includes a convenient post-amplifier arrangement.

D. Preamplifiers. An amplifier system usually is divided into a preamplifier and the main amplifier (Fig. 43). It is undesirable to couple the detector to a voltage-sensitive amplifier through a long cable because of the attendant signal losses and the increase in noise level associated with high cable capacitance. The use of a preamplifier mounted on or near the detector provides the shortest possible detector leads. A preamplifier may have a gain ranging from 1 to 30 and should have as its output stage a cathode follower capable of driving long sections of low-impedance cable, such as 93-ohm RG-62/U, with good linearity. This permits the detector and preamplifier to be located 500 feet or more from the complex of measuring equipment with good results.

As was stressed earlier, nuclear particle detectors produce a packet of charge. Until recently, all preamplifiers were of the voltage-sensitive type, i.e., the output pulse height is proportional to q/C. However, it is now realized that a charge-sensitive amplifier is to be preferred in most applications. Since the output is essentially proportional to q alone, the pulse height does not vary with input capacitance, as has already been mentioned in connection with semiconductor radiation detectors (Section IV.3.A.). Therefore, the experimenter is able to alter the input circuit and still retain

approximately the same gain calibration. It is not necessary to compromise on noise specifications, since for the same input capacitance as for a voltage-sensitive amplifier, the charge-sensitive device exhibits nearly the same noise contribution. In view of its convenience, it is likely that most new preamplifiers will be of the charge-sensitive type.

3. Trigger Circuits

Nuclear detection systems make frequent use of devices known as trigger circuits, which produce a pulse of constant height and width for each incoming pulse whose height exceeds a set value. A trigger which is adjusted by a front panel control is called an integral pulse-height selector (PHS) or integral discriminator. As shown in Fig. 43, it may be used to produce pulses of standard height for operating a scaler or counting-rate meter. Also, a PHS is needed in most integral counting work for discrimination against amplifier noise, or low-amplitude pulses from unwanted radiations.

4. Scalers

It is essential that a counting system be capable of accurate counting at high rates. Electromechanical registers can only accommodate counting rates up to 60 per sec, while many experiments demand recording data at rates of 30,000 counts/sec or more. This is accomplished by dividing the number of incoming pulses by a known factor (the scaling factor), so that a register will follow the reduced rate. The electronic device for performing this division is called a scaler.

A. Binary Scalers. The simplest high-speed scaling device is the scale-of-2, often called a binary, because it is a circuit having two stable states representing the binary numbers 0 and 1. The first input pulse transfers the state from 0 to 1; the second event will reset the binary to the 0 state and also generate an output, or carry pulse. Thus, only one output pulse is produced for two input pulses, so for a series of n such stages, a scaling factor of 2^n is obtained.

An array of 4 binaries in cascade to give a scale-of-16 is shown in Fig. 46(a). Each stage is connected to an indi-

cator such as a lamp, which functions when the stage is switched to the 1 state. In Fig. 46(a), the first pulse causes the lamp labeled "1" to light. The second pulse resets the first binary to 0 and sets the second binary to 1; this has the effect of extinguishing the "1" lamp and lighting the "2" lamp. A third pulse causes the "1" lamp to light also; a fourth will extinguish these but will light the "4" lamp, and so on until 15 events have been recorded and all lamps are lighted (1 + 2 + 4 + 8 = 15). The next pulse resets all binary stages, extinguishing the indicator lamps, and produces a carry pulse at the output. This latter pulse can be used to drive a register, or further binaries.

B. Decimal Scalers. When many binary stages are connected in cascade to form a large electronic register, it becomes tedious for the experimenter to translate the binary information into decimal form. Obviously, it is desirable to employ decimal scalers wherever possible. Improvements in electronic components and circuitry during the past few years have made it possible to construct decimal scalers which are as reliable as the binary ones.

A functional diagram for a transistorized decimal scaling stage usable to a pulse rate of 1 Mc is shown in Fig. 46(b). It is composed of four binaries and a "feedback" circuit to modify the scale-of-16 to a scale-of-10 as follows: The first 7 counts are recorded as described above for a binary scaler; on the 8th count, the last binary switches to indicate an "8," but also a short pulse is fed to the second and third binaries, setting up a "2" and a "4," respectively. Thus, on the 8th count the binaries are switched as though 14 (2 + 4 + 8) counts had been received. The 9th count records normally, and on the 10th, all binaries are reset, and a carry pulse emerges from the output.

The leads A_0, A_1, B_0, B_1, etc., sense the state of each binary, and may be used to indicate the number of stored counts. However, indicators cannot be connected directly to these leads; unlike the binary scaler, a translating circuit is required. For visual presentation and automatic recording on punched cards, it is useful to translate the information into decimal form, i.e., the digits 0-9; however, for many automatic recording systems, it is more economical to employ binary-coded decimal (BCD) format, in which the numbers 0-9 are expressed as combi-

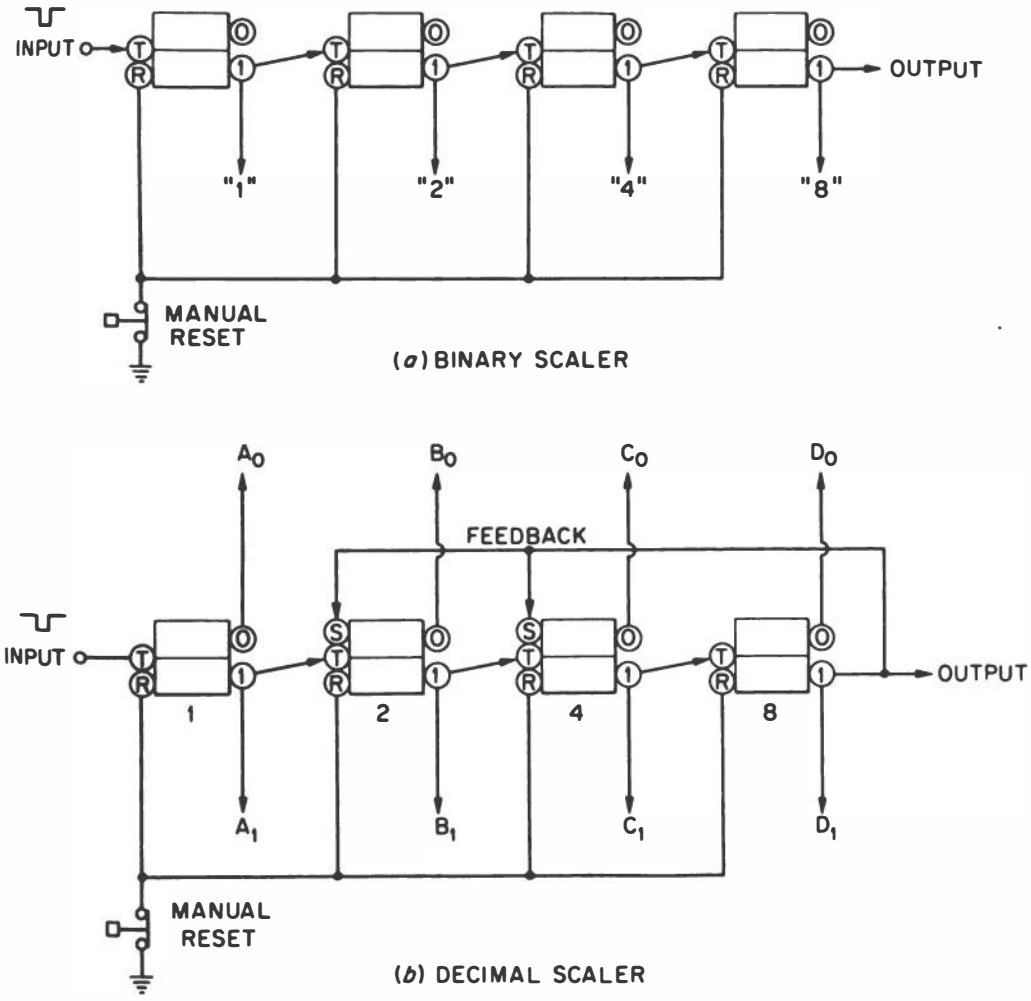

Fig. 46. Functional diagram of scalers. (a) A cascade of 4 binaries, yielding a scaling factor of 16. (b) A scaler made up of 4 binaries wired for decimal counting.

nations of the digits 1, 2, 4, and 8, or 1, 2, 2, and 4. Sometimes the decimal code is called a "10-line" format, and the BCD is called a "4-line" format.

Other reliable decade scalers have been devised and are in everyday use. The cold-cathode, glow-discharge scaler tubes made by several manufacturers (Ericsson Telephone Company, Sylvania Electric Products Company, and Raytheon Manufacturing Company) are capable of operation between 20-100 kc. The electron beam-switching tubes made by the Burroughs Corporation will function above 1 Mc. Often a beam-switching tube is used as a high-speed scaling stage, followed by a series of glow

tubes. The operation and use of some of these devices have been described by Millman and Taub.[82]

5. Counting-Rate Meters

It is extremely convenient to be able to measure the counting rate continuously, without the necessity of counting with a scaler for a measured amount of time. A device which indicates continuously the average counting rate is called a counting-rate meter. This is the indicator most often used on portable survey instruments.

Most counting-rate meters exhibit a linear relationship between output and counting rate. This is obtained by coupling a pulse of constant amplitude from a pulse-height selector onto a "tank," or storage, capacitor which is shunted by a resistor. Each pulse transfers a known charge to the tank capacitor; the steady-state voltage developed across the tank capacitor is reached when the rate of charge loss through the shunt resistor equals the rate of charge input from the pulses. A good quality vacuum-tube voltmeter is used to indicate the voltage across the RC tank circuit. Linear counting-rate meters have been discussed by Elmore and Sands,[72] and by Price.[39]

When wide ranges of counting rate must be measured, a logarithmic response is desirable. Usually this is done by using a logarithmic vacuum-tube voltmeter to read the voltage. It is very difficult to achieve very high accuracy or stability with such a technique, although adequate logarithmic counting-rate meters have been designed for survey purposes. Price[39] has reviewed the various approaches to this problem.

6. Pulse-Height Analyzers

Several of the detectors used in nuclear studies yield pulses whose heights depend on the energy deposited in the detector. This suggests that if these energy-dependent pulses can be sorted according to their height, energy spectra can be obtained. The device for performing this sorting is usually called a pulse-height analyzer.

A simple illustration of the problem is shown in Fig. 47. In (a), a series of pulses from a detector are viewed very much

as they would appear as voltage-time waveforms on an oscilloscope. The example shows the pulse-height scale divided into five channels of equal width. Over the counting interval shown, a five-channel pulse-height analyzer would record no events in channels 1 and 5; two events in channels 2 and 4; and five events in channel 3. Thus, the data from such an analysis may be plotted as the histogram shown in Fig. 47(b); usually, it is more convenient to plot the number of events per channel as a point at each channel number. A smooth curve drawn through these experimental points is easier to interpret.

A. Single-Channel Analyzers. The number of events shown in Fig. 47 is, of course, a ridiculously small sample of a random source of pulses. Although it is more efficient to record the events in all channels at once, it requires only very simple equipment to look through an electronic "window" at a single portion of the spectrum at a time. The window might be adjusted to the width of a channel in Fig. 47(a) and set to the position of each channel shown. At each setting, a count would be taken for sufficient time to obtain a valid statistical sample of the spectrum. The data may be plotted as in Fig. 47(b).

The operation of such a single-channel pulse-height analyzer is simple in principle although fairly complex in practice. Figure 48 shows the general arrangement and mode of operation for three pulses. Two pulse-height selectors (PHS) units are used: a lower PHS is biased to trigger on a pulse of height E, and an upper PHS biased to $E + \Delta E$. The anticoincidence circuit will permit an output pulse only if the lower PHS is triggered without a pulse from the upper PHS. The E dial in the case shown is set at 200 dial divisions; pulse "1" does not have sufficient amplitude to affect either PHS. Pulse "2" falls within the ΔE window, which causes the lower PHS to trigger; as there is no accompanying pulse from the upper PHS, an output pulse is recorded. The third pulse is high enough to trigger both PHS units, so the anticoincidence circuit prevents an output.

Several versions of vacuum-tube single-channel analyzers have been described (see, for example, the reviews by Chase[71] and Van Rennes.[80] Transistorized versions are also in use which are compatible with the transistorized linear amplifiers.[83,84]

B. Multichannel Analyzers. Many applications require

faster data acquisition rates than are possible with single-channel analyzers. A notable example is found in the field of radioactivation analysis, where it has become increasingly important to measure short-lived nuclides for highest sensitivity. Not only is there a great increase in speed and convenience if the pulses are sorted in a single counting interval, but there is also an improvement in the precision of the data obtained, because many instrumental drifts will affect all channels of a multichannel pulse-height analyzer in the same way. For circuits used in these instruments, the reader is directed to the excellent discussion by Chase.[71]

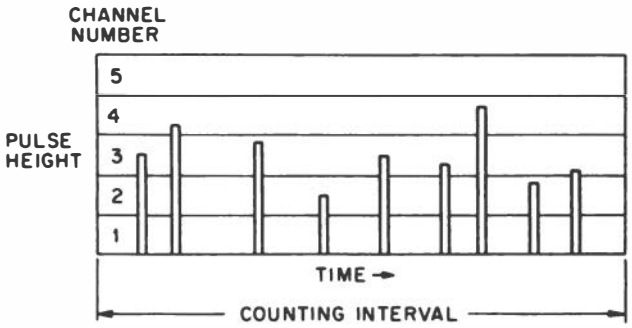

(a) AMPLIFIER PULSES

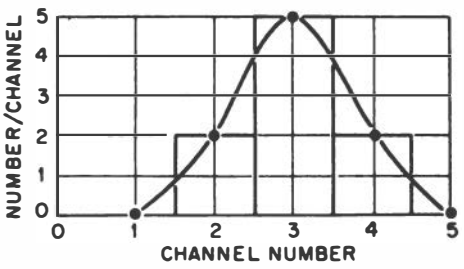

(b) PULSE-HEIGHT DISTRIBUTION

Fig. 47. Illustration of the pulse-height analysis problem. (a) Idealized pulses from a linear amplifier are shown, plotted on a pulse-height scale which is divided into five equal channels. (b) The pulse-height distribution from (a) is shown plotted as a smooth curve through the points.

The most obvious approach to the design of a multichannel analyzer is to construct a number of pulse-height selectors, whose trigger (or bias) levels are progressively increased. Anticoincidence circuitry is provided, so that, in effect, the array consists of a series of single-channel analyzers,

"stacked" up in terms of pulse height. A successful version of this scheme is the 20-channel analyzer designed by Bell, Kelley, and Goss. This analyzer, together with a review of the general problem of pulse-height analysis, is discussed by Van Rennes.[80]

Improvements in detector resolution and the growing need for more automated data recording have created a need for multichannel analyzers with a very large number of channels. The 20-channel analyzer just mentioned costs about $350/channel; hence, a stacked-discriminator type of analyzer is too expensive to build in large configurations. By making use of techniques developed for digital computers, it is possible to construct multichannel analyzers having hundreds of channels

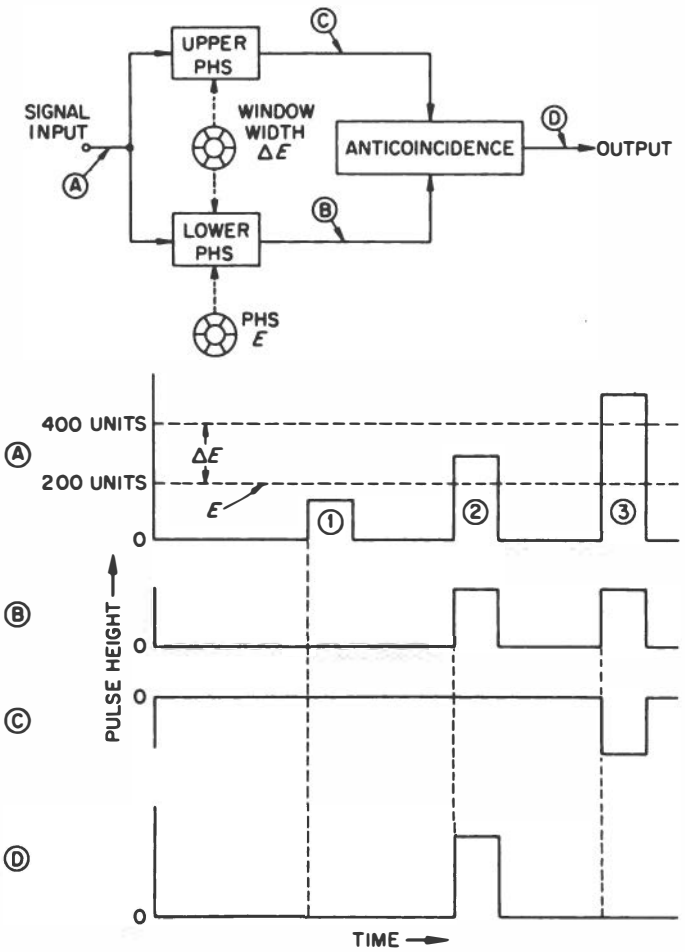

Fig. 48. Functional diagram of a single-channel pulse-height analyzer. Pulse shapes for the different parts of the circuit are shown below the block diagram.

and very large storage capacities per channel. A simplified diagram illustrating the general method of operation of such an analyzer, as well as some of the methods of handling the data, is sketched in Fig. 49.

The heart of the analyzer is the analog-to-digital converter (ADC), which converts the pulse height to a train of pulses. The number of pulses produced determines the channel number in which the pulse is to be stored. These address pulses are counted by the address scaler, which may be either a binary or a binary-coded decimal (BCD) type.

The information is stored in a ferrite-core memory unit, which resembles the memory of a modern digital computer. The memory usually stores data in BCD format, as this is most useful for operating readout equipment. Some of the early instruments used all binary logic, which is more economical but a little more troublesome for the experimenter. Once the address scaler has selected a memory address (channel number), the number of counts already stored in the memory at that address is read out into a scaler called the data register, or add-one scaler. Then, the "store" command is given, the data register increases the old number by one, and the new number is written back into the memory. This memory cycle requires 10 to 20 μsec for most analyzers.

Analysis of a pulse-height distribution in this way requires a rather long time. A typical analyzer might have an 18 μsec memory cycle and a 0.5 μsec spacing between address pulses (2 Mc address pulse rate); this leads to an analysis time for each pulse (during which the analyzer is incapable of recording any further pulses) of $(18 + 0.5\ \nu)$ μsec, where ν is the channel number.

The dependence of the rather long "dead time" on channel number shows that the average dead time is a function of the spectrum under measurement. However, it can be shown that the spectrum shape is undistorted under this condition, and so it is only necessary to correct for the dead time to obtain accurate counting rates. Instead of working with dead time, it is more convenient to count for a given amount of "live time," that is, time during which the analyzer was free to analyze incoming pulses. The device for measuring live time, a live timer, is an electronic clock which counts standard-frequency pulses. When the analyzer is processing a count, the ADC pro-

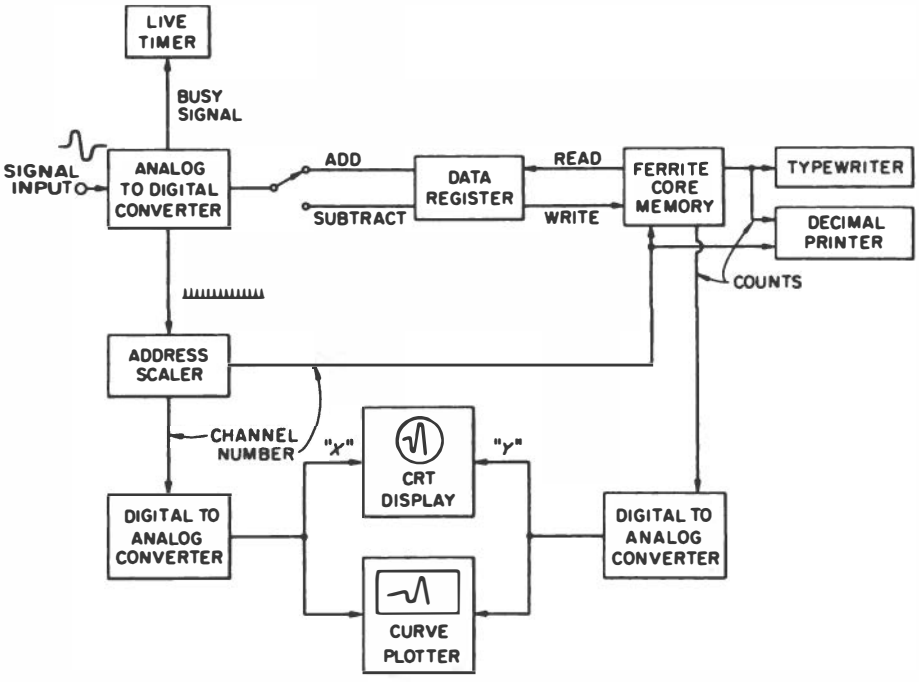

Fig. 49. Multichannel pulse-height analyzer, showing relationships between principal subassemblies and accessory equipment.

duces a busy signal, which stops the clock. Therefore, only live time is recorded.

Because the analyzer operates on computer principles, it has the ability to subtract as well as add. It is quite helpful to subtract background spectra using the analyzer. Some commercial analyzers have provisions for storing a spectrum in one part of the memory; the intensity of this spectrum may be multiplied by normalizing factors and then added to or subtracted from the contents of another portion of the memory.

A variety of readout equipment is possible. The decimal numbers may be recorded by using a typewriter or printer; BCD information may be recorded in computer format on punched paper tape or on magnetic tape. Digital information also may be converted to analog voltages, which are used to display spectra on a cathode-ray tube and may also be used to drive an X-Y curve plotter.

7. Coincidence Measurements

In many nuclear counting problems, it is necessary to decide whether two events are time-correlated. Such infor-

mation may be required for investigations of nuclear decay schemes, for which it may be necessary to know whether two radiations are emitted at the same time. Also in many types of counting, imposing the condition that two events must be coincident in time will serve to discriminate effectively against noise pulses, which are randomly distributed in time. Electronic circuits which make such decisions are called coincidence circuits and produce an output pulse only if all inputs to the device receive a pulse simultaneously.

A. Resolving Time. Coincidence equipments may be classified according to their resolving time. If a two-channel system is used, each channel applies a gate pulse of width τ to the mixer circuit; therefore, to be in coincidence, the two gate pulses must fall within the time interval 2τ, the resolving time. A resolving time of less than a few tenths of a μsec is termed "fast," and longer resolving times are called "slow." With special-purpose photomultiplier tubes and high-speed circuitry, resolving times of less than 10^{-9} sec (1 nanosec) have been obtained. The esoteric subject of fast coincidence measurements in the nanosecond region will not be treated here but has been reviewed extensively by De Benedetti and Findley[85] and by Lewis and Wells.[86] Resolving times of > 50 nanosec are possible, however, with rather conventional equipment.

Short resolving times are required wherever high counting rates are involved, because the random nature of radioactive decay leads to a chance that two uncorrelated pulses will happen to occur within the coincidence resolving time. The random coincidence rate N_r is given by

$$N_r = 2\tau N_1 N_2 , \qquad (16)$$

where N_1 and N_2 are the counting rates in the two channels. Note that, because N_1 and N_2 are related to the disintegration rate N_D by counting efficiencies ϵ_1 and ϵ_2, the random coincidence rate is proportional to the square of the disintegration rate:

$$N_r = 2\tau N_D^2 \epsilon_1 \epsilon_2 . \qquad (17)$$

The relationships of Eqs. 16 and 17 are correct to the first order in most coincidence systems. If the rates N_1 and N_2 are

very high, it may be necessary to make higher order random coincidence corrections. The equations to be used for computing such corrections are discussed by Paul.[87]

A criterion for the feasibility of a coincidence experiment is the ratio of real coincidences to random coincidences. Since the real coincidence rate is given by

$$N_C = N_D \epsilon_1 \epsilon_2 ,$$

then

$$\frac{N_C}{N_r} = \frac{1}{2\tau N_D} . \qquad (18)$$

Thus, the real-to-random ratio increases only as the reciprocal of the first power of the resolving time and disintegration rate.

B. Electronics. A block diagram of a typical coincidence system is given in Fig. 50. The coincidence circuit requires that, to be quantitative, the timing pulses should not "walk," i.e., change their position in time as the pulse height varies. The output from the usual trigger circuits will exhibit such a walk, because low-amplitude pulses will trigger near their peaks, while high-amplitude pulses will trigger proportionately nearer the base line. The output pulses will be distributed through a time range about equal to the amplifier rise time (~ 0.2 μsec for NaI(Tl) scintillation counter systems). A convenient solution to this problem was proposed by Love, who showed that the cross-over point (A in Fig. 50) of the pulse from an amplifier with double delay-line differentiation (Section VI.2.A.) exhibits negligible walk with pulse height, since the point is only determined by the delay-line parameters. Several timing circuits based on this idea have been constructed by Peele and Love,[88] and by Fairstein.[89] Transistorized versions of such a system have also been designed.[83,84]

All pulses are subjected to a fast coincidence (2τ = 0.1 μsec) in Fig. 50. Then, if coincidence measurements are desired between two energy bands, these are selected by the two single-channel pulse-height analyzers. Thus, of all the integral coincidences recorded by the fast unit, only a few will be selected by the analyzers. The slow coincidence unit, which may

have a resolving time of 2 to 5 μsec, imposes these additional pulse-height conditions. As a result of this arrangement, the resolving time of the system is determined by the fast coincidence; the relatively low rates and less sharply timed signals from the single-channel analyzers can be mixed quite accurately with the fast coincidence output in a slow coincidence unit.

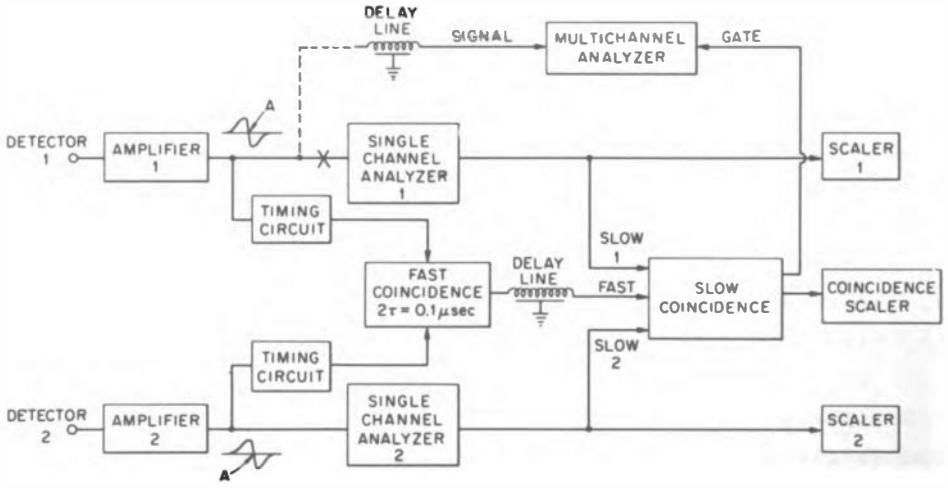

Fig. 50. Coincidence apparatus. For use with a multichannel analyzer, the connection to single-channel analyzer "1" is broken at "X," and the connection shown as a dotted line is used.

Often, it is desirable to include a multichannel analyzer in a coincidence arrangement in order to measure the spectrum at one detector in coincidence with a selected energy from another detector. As shown in Fig. 50, the connection to single-channel analyzer "1" is broken, and a slow coincidence is demanded only between the "Fast" and "Slow 2" channels. With the multichannel analyzer connected to amplifier "1," a coincidence between detector "1" and a count in the window of single-channel analyzer "2" will supply a gate signal which commands the multichannel analyzer to record the pulse appearing at its input.

The ideal arrangement for acquiring coincidence information would record the pulse-height from both Detectors 1 and 2 of Fig. 50 each time a fast coincidence occurred, so that all possible coincidence combinations can be recorded in a single experiment. Further, it is desirable that the number of events corresponding to each possible set of coordinates be sorted and stored in a fast-access memory device (such as a ferrite-core memory). The instrument just described is really a pulse-height

analyzer with two ADC units (Section VI.6.B.), capable of generating an "X" and "Y" address for storing each coincidence event in a matrix whose "Z" axis is the number of events. The concept of a storage matrix leads to the term "three-dimensional pulse-height analyzer" for this device.

A much less versatile but less expensive instrument may be constructed from two ADC units which record the two addresses for each event on magnetic or punched tape as they occur. In this case the data must be sorted by reading the tape with a modified pulse-height analyzer storage unit or with a computer. This procedure is very time consuming and has the disadvantage that because of the additional sorting step, the condition of the data cannot be determined during the experiment, or even very soon thereafter.

The development of the three-dimensional analyzer approach to coincidence spectrometry is still in the early stages but promises to be extremely useful. The general problem was reviewed by Chase[71] and a 20,000-channel, three-dimensional analyzer with a ferrite-core memory was described by Goodman, et al.[90]

A related technique makes use of a signal which inhibits the multichannel analyzer or other apparatus from recording particular events. One application of this anticoincidence arrangement is discussed below in Section VII.2.

C. Delayed Coincidence Measurements. Coincidence techniques are well suited to the measurement of very short half-lives. If delay lines are inserted between the timing circuit and fast-coincidence input, first in one channel and then the other, a delay curve can be obtained, which is just the coincidence counting rate as a function of added delay. This curve will have a width at half-maximum counting rate of 2τ, if the two radiations are prompt; however, should one of the radiations be delayed, the delay curve will be steep on one side but will exhibit a smaller slope on the other side. The analysis of such data to obtain lifetimes of nuclear states is discussed in references 85, 91, and 92.

D. Calculation of Intensities. Quantitative coincidence measurements, especially gamma-gamma coincidence spectrometry, have become essential in the study of nuclear decay schemes. Relative intensities are easily determined, and if the decay scheme includes two or more gamma rays with the same energy, it

may be possible to determine the relative intensity of each by a series of coincidence experiments involving the gamma-ray cascades in question.

It is important to emphasize that all peaks in a coincidence gamma-ray spectrum are not necessarily due to coincidences with the gamma peak on which the single-channel window is set; indeed, an intense coincidence peak may be due to random coincidences (Part A., above), or to true coincidences with events in the single-channel window arising from Compton-electron, gamma-ray scattering, or bremsstrahlung spectra. Thus, it is usually not enough merely to observe that a series of peaks appears in the coincidence spectrum; rather, a quantitative examination of the gamma-ray intensities is required to obtain a meaningful interpretation of the experiment.

Consider first an experiment in which a peak of area $P(\gamma_1)$ due to γ_1 is observed in coincidence with counts of γ_2 in the single-channel window:

$$q_{1,2} = \frac{P(\gamma_1)\ e^{\mu d}}{C_w\ \epsilon_p(\gamma_1)\,\Omega\ \overline{W}_{1,2}(\theta)} . \qquad (19)$$

The quantity $q_{1,2}$, the "coincidence quotient," is the number of events of γ_1, the gamma ray of interest, in coincidence with γ_2, divided by the number of counts due to γ_2 in the single-channel window; $e^{\mu d}$ corrects for absorption of γ_1 in the beta absorber; C_w is the number of counts in the window of the single-channel analyzer; $\epsilon_p(\gamma_1)$ and Ω are the peak efficiency and solid angle for detection of γ_1; and $\overline{W}_{1,2}(\theta)$ is the angular distribution function for the indicated pairs of coincident gamma rays integrated over the face of the crystal.[34]

Although Eq. (19) is useful in many situations, two additional corrections are needed: one to correct for the fact that only a fraction of the counts in the window may be due to γ_2; it is also very important to remove the coincidence contribution from higher-energy gamma rays which give Compton-electron events falling in the single-channel window. When these effects are taken into account, the following expression[93] for $q_{1,2}$ results:

$$q_{1,2} = \left[\frac{P(\gamma_1)\ e^{\mu d}}{C_w\ \epsilon_p(\gamma_1)\ \Omega} - \sum_{\substack{i \\ i \neq 2}} q_{1,i}\ D_i\ \overline{W}_{1,i}(\theta) \right] \frac{1}{D_2\ \overline{W}_{1,2}(\theta)} , \qquad (20)$$

where D_2 is the fraction of counts in the window due to γ_2; from the window width, this fraction can be obtained from the single-crystal spectrum, analyzed as described in Section II.3.D.

The term $\sum q_{1,i} D_i W_{1,i}(\theta)$ corrects for coincidences arising from "gating" events in the window from any gamma ray (γ_i) other than γ_2. Here D_i is the fraction of counts in the window due to γ_i, and $q_{1,i}$ is the relative number of γ_1 coincident with γ_i. In most decay-scheme studies, the necessary $q_{1,i}$ values can either be measured directly in other coincidence experiments or deduced from the decay scheme.

Once the "q" values have been obtained for a series of gamma-gamma coincidence experiments, they are used in conjunction with the single-crystal intensities and the decay scheme to calculate the intensity of each gamma-ray transition. This procedure usually involves a series of successive approximations until internal consistency is achieved, especially if the decay scheme is complex.

Other quantitative aspects of coincidence counting which relate to the determination of disintegration rates will be found below in Section VIII.2.E.

VII. LOW-LEVEL COUNTING

1. General Remarks

Many chemical experiments lead to very small amounts of radioactive sample, either because of the low yield of the reaction under study, or because of the small amount of sample available. It may be found that if a conventional detector is used for counting such low-intensity samples, the sample counting rate is comparable to the background rate from cosmic rays and other environmental radiation sources.

When choosing between detector systems, the criterion for optimum counting precision in a given time is the "figure of merit" N_S^2/N_B, where N_S is the sample counting rate, and N_B is the background rate.[94] The system which gives the largest figure of merit is the most sensitive for the measurement of a particular nuclide. Therefore, the reduction in the background rate must be large in order to be effective, since the sample counting rate appears to the second power and the background only as the first. Increasing the sample counting rate by

improvement of geometry, reduction of absorption, or some other means is far more valuable. The other practical criterion for low-level counting is stability, because a single determination may extend over days or weeks.

Detectors used for low-level counting are similar to the ones already discussed but differ in their application. The choice of a particular detector, which must be considered separately from the various ways of reducing the background, will depend upon the specific activity of the material to be counted. When the specific activity is low, as in radiocarbon dating, there is no point in considering a method which will not permit introducing a large sample and counting with high efficiency. The beta-particle energy is also involved in the choice of a detector, since absorption effects in the sample and counter window are extremely acute for beta-particle energies below about 200 kev. On the other hand, absorption is a relatively minor consideration for high-energy beta particles.

The most difficult counting situation is encountered when the samples of interest combine a low specific activity with a low beta-particle energy. Typical samples of tritium (H^3) and C^{14} fall in this category. The usual techniques for low-level counting of these nuclides are gas counting and liquid scintillation counting.

The general problem of low-level counting has been reviewed by Arnold,[94] Kulp,[95] and DeVoe.[96] The report by DeVoe[96] is especially valuable because of the wealth of information it contains about the radioactive contamination of materials needed by workers attempting to detect minimal amounts of radioactivity.

2. Apparatus

A. Large-Volume Counters. A typical arrangement of a low-background large-volume counter is shown in Fig. 51(a). The detector is situated at the center of a steel shield; lead is usually avoided because of its associated radioactivity. The mercury shield around the detector is to stop any radiation produced in the walls of the tubes comprising the anticoincidence mantle.

The most important single feature is the anticoincidence mantle. This device, although shown in the figure as a ring of Geiger tubes, may also be a hollow cylinder of scintillator,

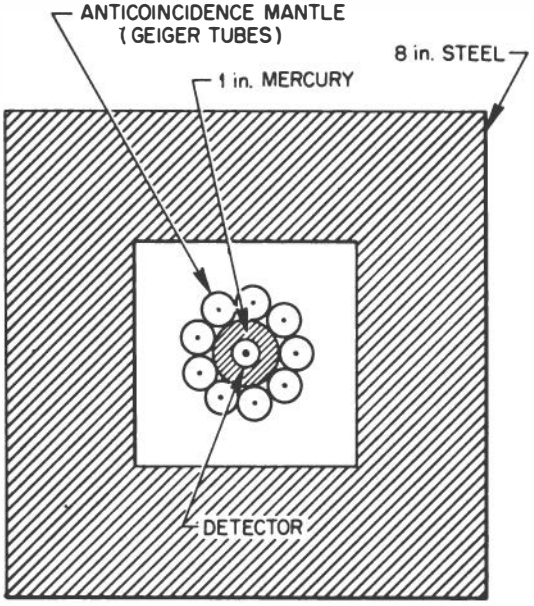

(a)

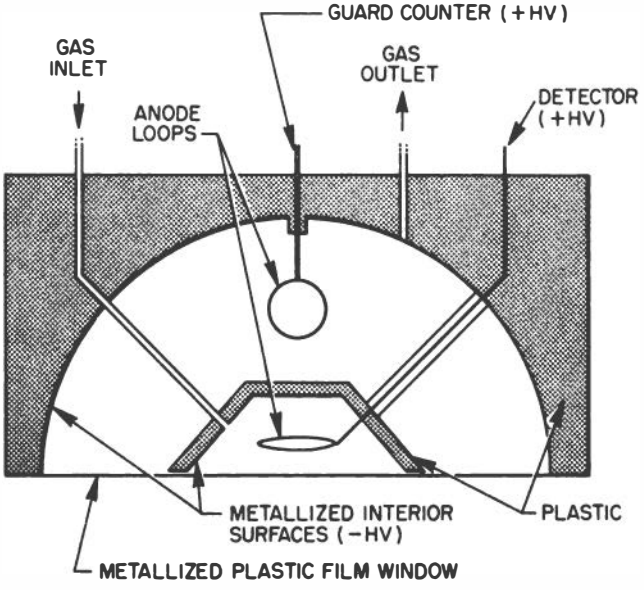

(b)

Fig. 51. Low-background counters. (a) Typical arrangement for obtaining very low backgrounds. (b) Low-background proportional counter covered by an anticoincidence, or guard counter.

coupled to one or more photomultiplier tubes. An anticoincidence circuit uses the signal from the mantle to exclude events in which the detector and the mantle simultaneously produce a count, since an event in both detectors would indicate the detection of a particle from outside the source region. The anticoincidence ring may effect a reduction in the background of a beta-ray counter of about 50. The overall reduction in background over a bare detector by the apparatus of Fig. 51(a) is often between 100 and 150.

It is difficult to reduce the background of a large NaI(Tl) gamma-ray detector by using an anticoincidence mantle. In the energy region of 0-3 Mev, the background of such a gamma-ray detector may be reduced by a factor of only 2 to 5 through the use of a liquid or a plastic scintillator anticoincidence mantle. For the high-energy range above 3 Mev, in which the background is chiefly due to mesons, the background is reduced[97] by a factor of 10^3 to 10^5.

B. Small-Volume Counters. When the counter can be made very small, the experimental arrangement is much simpler. For instance, because the sensitive volume of a liquid scintillation counter can be so small, the shielding is often accomplished by a mercury shield so thick that an anticoincidence mantle is not required.

An end-window beta proportional counter of small dimensions will have a low background simply because its sensitive volume is small. If this small counter is placed inside a larger detector [Fig. 51(b)] and the two are placed in anticoincidence, a reduction in the background of at least a factor of 10 may be obtained. This entire assembly may be inserted into a massive shield for a further background reduction. The "Omni/Guard" detector manufactured by Tracerlab, Inc., is designed in this way and has a background of < 0.5 c/m.

VIII. DETERMINATION OF THE DISINTEGRATION RATE

In this Part we will discuss the special techniques for determination of the disintegration rate, often called absolute counting to distinguish it from relative counting procedures. Absolute counting may be performed directly as in $4\pi\beta$ counting; more often, absolute counting involves equipment normally employed for relative counting which has been calibrated by use

of a standard source. For details of the techniques to be described, the reader may consult the excellent review by Steinberg,[98] and proceedings of several conferences on this subject.[99,100]

1. Absolute Alpha Counting

A. General Considerations. Alpha particles have a short range in matter, so a good alpha source must be very thin. By the same token, counter windows or other material through which the alpha particles must pass also should be thin; it is common to use windowless counters for such purposes.

Scattering in the sample itself is not a serious problem with alpha particles, since the particles scatter only slightly in thin sources. Scattering from the source mount is appreciable at small angles to the source plane but is negligible at angles normal to the source plane. The amount of backscattering increases with the atomic number of the scatterer and with decreasing energy of the particles.

A variety of geometries are used. The usual one for moderate precision is the internal sample counter (a proportional counter or ionization chamber) with 2π geometry. Here, the backscattered particles are also counted, so the effective geometry for sources on polished platinum plates is found to be in the range of 51 to 52%, depending on the energy. Work of the highest precision with sources on metal plates requires collimation to eliminate the backscattered particles; both low- and medium-geometry counters have been used very successfully. If the source to be standardized can be mounted on a thin, essentially weightless, film, then a 4π proportional counter may be used for accurate assay.[101,102]

Many alpha sources must be counted in the presence of intense beta activities; therefore, it is essential that the detector and electronic system have a short resolving time, lest beta-induced pulses pile up and be counted as though they were alpha pulses. Fast detectors suitable for precision alpha counting are scintillation counters, semiconductor detectors, and proportional counters.

B. Low-Geometry Counters. When very accurate assays are required, or when the source intensity is very high, a low-geometry alpha counter is used. The general technique has been

discussed by Curtis, et al.,[103] and Robinson.[36]

A design by Robinson is shown in Fig. 52. The chamber has a factor of about 1/2600 of 4π geometry. The chamber must be evacuated to a pressure of about 200 microns or less. Because the wall diameter is so near the collimator diameter, the eight baffles are required to prevent scattering particles off the walls and into the detector; without baffles, scattering amounts to about 1% of the total count. The high degree of collimation effectively eliminates backscattered particles from the source.

Many low-geometry chambers use a proportional counter as a detector, which requires a gas-tight window between it and the evacuated chamber. Some proportional counters also may require efficiency corrections because of the anode wire supports. The scintillation counter sketched in Fig. 52 is free of these problems.

If all important dimensions are known to 1 part in 10,000, then the accuracy is mainly limited by counting statistics. The plateaus can be held flat to 0.05% with proper attention to the electronic equipment, and the influence of sample size on the geometry is not great because of the large distance between source and detector. As an example of the accuracy of the method, assays of the same sample by workers at the AERE (Harwell, England), and LRL (Berkeley, California) agreed within 0.1%, using low-geometry chambers of different design.[104]

C. Precision, High-Geometry Counters. When the amount of activity to be assayed is small, it is necessary to use some sort of high-geometry configuration to obtain good counting statistics in a reasonable time. Although the 4π counter is a very attractive arrangement, the required source must be mounted on a nearly weightless backing. Most alpha sources are mounted on backing plates, for which the 4π method is not suitable. For relative counting it is quite convenient to use an internal sample counter with 2π geometry, for which the overall efficiency, or counting yield, may be calibrated with standards if desired.

When counting at high geometry, it is advisable to eliminate the backscattered alpha particles by reducing the geometry to about one π steradian, which leads to an acceptance angle of 120°. When this is done, the geometry factor becomes very sensitive to the size and position of the source.

This sensitivity to sample position is greatly improved by

masking the detector of a high-geometry counter with a stop of the proper shape. Figure 53 shows the design by Robinson.[100] The chamber has a calculated geometry of 0.19748. A 2 mm diameter source on platinum gave an essentially constant counting rate for displacements up to several mm from the center of the source holder. That this device is indeed a highly precise counter was established by a cross comparison with a low-geometry counter--the two agreed to within $\pm$ 0.03%.

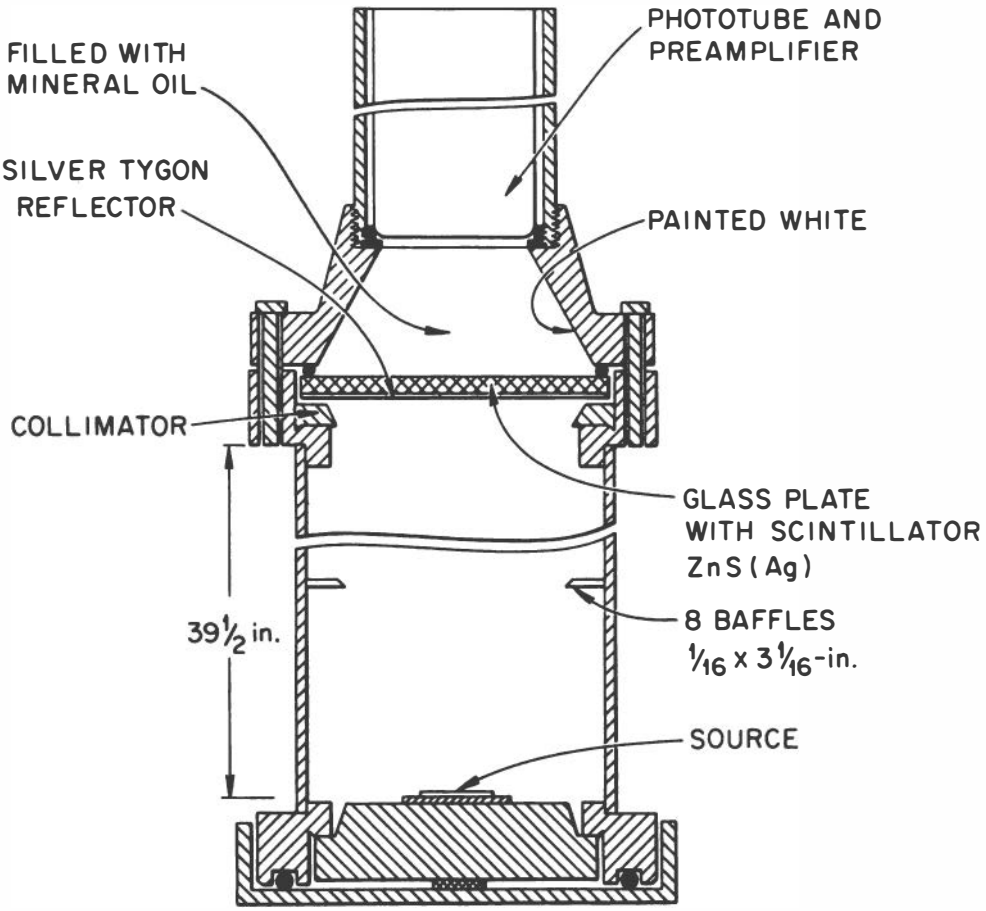

Fig. 52. Low-geometry alpha counter for high-precision absolute alpha counting (Robinson[36]).

2. Absolute Beta Counting

A. Introduction to Beta Counting Techniques. If an experimenter is so unfortunate as to be faced with the problem of determining the disintegration rate of a beta emitter, his

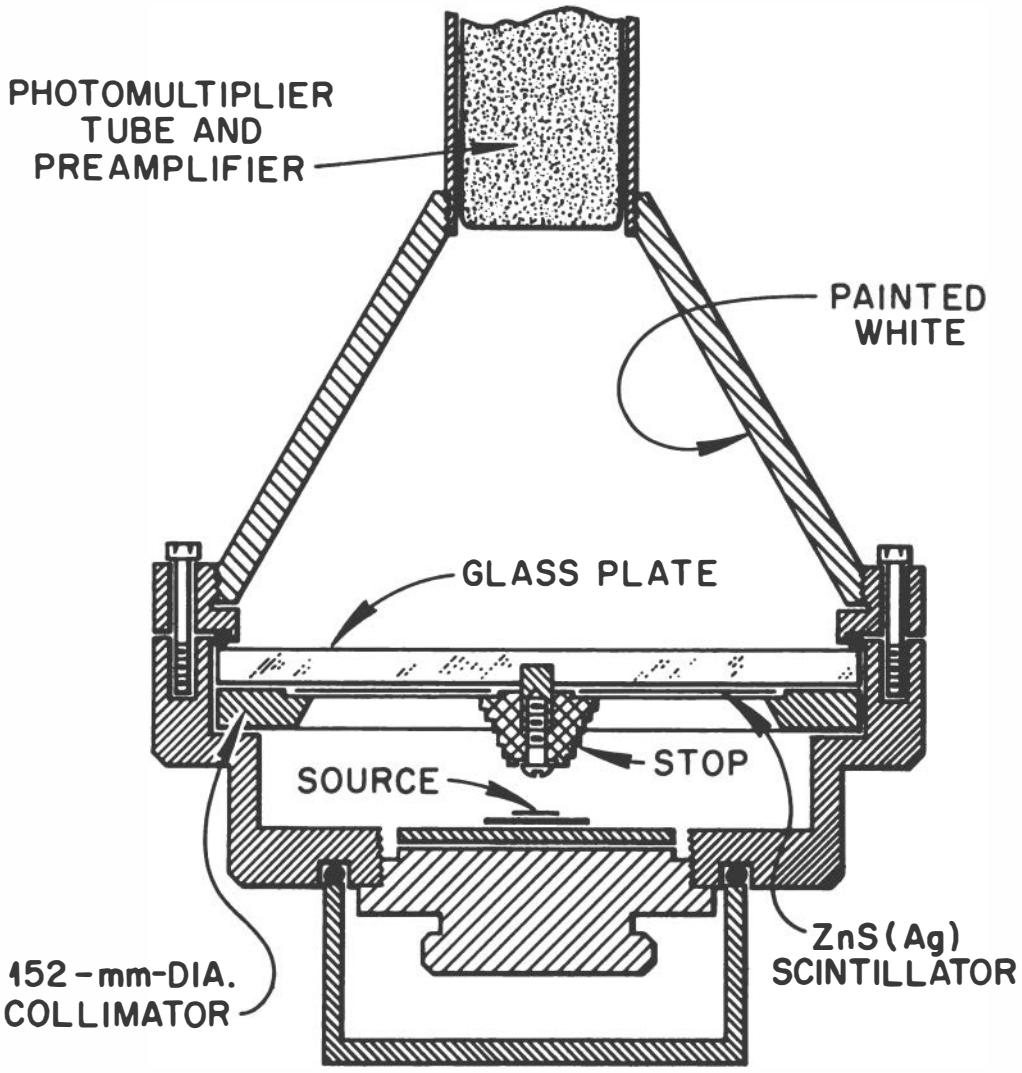

Fig. 53. Precision high-geometry alpha counter which uses a stop to reduce the effect of sample position on geometry (Robinson, in reference 100).

problem is much more complicated than the alpha assay problem already discussed. The complications arise from the effects of scattering and absorption of electrons in matter, combined with the distribution in energy of the beta particles. It is usual to combine all experimental quantities which affect the counting rate into a counting yield ϵ, which relates the observed counting rate N and the disintegration rate N_D:

$$\epsilon = \frac{N}{N_D} . \qquad (21)$$

Although ϵ is usually determined experimentally, it can, in principle, be separated into the following factors:[98] the geometry; the intrinsic efficiency of the detector; an absorption factor for the air between source and detector, in addition to the detector window; a correction for air scattering; a factor for the backscattering by the source support; a factor to correct for scattering by environment; and a correction for the self-absorption and self-scattering by the finite mass of the source. The review article by Steinberg[98] discusses the magnitudes and dependences of the various factors on the experimental situation.

It is usually possible to determine a beta disintegration rate with an end-window counter to better than 5%. The counting yield of an essentially weightless source on a thin backing can be standardized to this accuracy either by use of an absolute standard, or by use of experimentally determined values of geometry, absorption, and scattering effects.

Calibration standards must be used for the assay of thick beta sources to an accuracy of better than $\pm$ 10%. A carrier-free sample of the desired activity is prepared and its disintegration rate determined. Aliquots of the sample are then processed, taking care that the amounts of carrier, mounting procedures, and other details are the same as for the unknown. In this way, the counting yield is measured directly for the particular experiment.

B. End-Window Counters. By far the most common detector in use at present is the end-window counter. Much of the early information on beta counting was obtained with end-window Geiger tubes, although they have now been largely supplanted by end-window proportional counters (Section V.2.B.). The proportional counters are more stable and reliable, and because they usually are filled to one atmosphere pressure, their windows can be made very thin (0.2 to 1 mg/cm^2) for good sensitivity to low-energy beta particles. The mechanical dimensions of end-window Geiger and proportional counters are similar, as are the dimensions of their source holders; therefore, some of the published data for Geiger counters can still be used in modern counting applications.

C. 2π Counters. For counting either low-intensity samples, where a high geometry is needed, or low-energy beta particles, where it is desirable to eliminate the detector

window, a 2π counter is very convenient. An additional advantage of this arrangement is that anisotropic scattering effects are less important here than in the end-window case.

The general procedure for calibration of the counting yield is similar to that described above for end-window counters. A carrier-free sample on a nearly weightless backing does not eliminate scattering in a 2π geometry, because some structural material is almost certain to be nearby; for this reason, it is advisable to standardize the counting yield for sources mounted on a backing which gives saturation backscattering.

D. 4π Counting. The most generally used techniques for primary standardization is the 4π geometry beta counter, or $4\pi\beta$ counter. This instrument was described briefly in Section V.2.B. Coincident gamma rays or internal conversion electrons, when detected, are always counted simultaneously with the associated beta particle, and thus result only in a single count. Any discharges caused by scattering of the primary particle or by secondary radiation will also fall within the resolving time and will not affect the measured rate.

A well-designed $4\pi\beta$ proportional counter will have a geometrical efficiency in excess of 99.5% and a plateau whose slope is less than 0.1%; therefore, the accuracy with which the disintegration rate may be determined depends mainly on absorption in the source and in the mounting film. Absorption will in all likelihood remain the factor limiting the accuracy of $4\pi\beta$ counting. Self-absorption was studied for specific source materials by Pate and Yaffe,[105] and by Yaffe and Fishman,[100] who showed how their correction method could be applied to other 4π counter sources.

The source-film absorption correction has been determined in three ways: (1) the "sandwich" procedure of Hawkings, et al.,[106] in which the counting rate of a source on a known thickness of backing is measured, followed by a determination with an identical film covering the sample; (2) a calculated correction, proposed by Seliger and co-workers,[107] was based on measurements of 2π and 4π single-film and "sandwiched" counting rates; (3) a determination of the counting rate as a function of actual source film thickness was made by Smith,[108] and has been studied exhaustively by Pate and Yaffe.[109] Any of these methods is useful above a few hundred kev, but (3), the

absorption curve technique, appears to be the most accurate, even at energies below 100 kev.

Films to be used as source mounts should be rendered electrically conducting, preferably by vacuum evaporation of a metallic coating at least 2 $\mu g/cm^2$ thick. This coating will guard against distortion of the electric field by electrostatic charging of the source film or by a penetration of the field of one counter into the other.

A systematic study of the general technique of $4\pi\beta$ counting has been published by Pate and Yaffe.[102,105,109,110] Measurements at the National Bureau of Standards and the results of intercomparisons of sources by various laboratories were discussed by Seliger and co-workers.[107,111,112] The proceedings of a symposium on the metrology of nuclides[100] contains a series of useful papers on the latest techniques of $4\pi\beta$ counting.

Some work has also been performed using as 4π detectors liquid scintillation counters and counters with radioactive-gas filling. These techniques, which are as yet rather specialized and of limited application, are described in papers included in references 99 and 100.

E. Coincidence Counting.* When two radiations are emitted in sequence during the decay of a radionuclide, coincidence counting is a convenient and accurate method for determining the disintegration rate. Consider the simple case of a single beta group followed by a single gamma ray. The counting rate of the beta counter N_β is given by

$$N_\beta = N_D \epsilon_\beta \ , \qquad (22)$$

where N_D is the disintegration rate and ϵ_β the counting yield. Similarly, the gamma-ray counting rate N_γ is

$$N_\gamma = N_D \epsilon_\gamma \ . \qquad (23)$$

Here, ϵ_γ is the counting yield of the gamma detector. The coincidence rate N_c is

$$N_c = N_D \epsilon_\beta \epsilon_\gamma \ , \qquad (24)$$

*A recent report of the theory and practice of this technique was made by Campion.[113]

which reduces to

$$N_D = \frac{N_\beta N_\gamma}{N_c} . \qquad (25)$$

Note that the determination of the disintegration rate by this technique does not require that the counting yields be known. The counting rates in the beta, gamma, and coincidence channels must be corrected for background rates and dead-time losses. Because each detector must only be sensitive to a single type of radiation, the background correction in the beta channel must also include the contribution arising from the gamma sensitivity.

An additional correction to the coincidence rate is the random coincidence rate, $N_r = 2\tau N_\beta N_\gamma$; the rates in the beta and gamma channels should be total rates before background subtraction. As previously, 2τ is the coincidence resolving time. Another coincidence "background" arises from the detection of gamma-gamma cascades in the two detectors, if the decay scheme is complex.

Nuclides with several beta groups may be assayed by the beta-gamma coincidence technique, if the sensitivity of either the beta or gamma detector is the same for all branches of the decay scheme.[114] Because of its high, uniform efficiency, the $4\pi\beta$ counter makes a very useful beta detector for coincidence counting. When counting nuclides with complex decay schemes by the $4\pi\beta$-γ coincidence method, the corrections arising from the decay scheme usually turn out to be rather small.[113]

Since the beta-gamma coincidence technique is insensitive to counting losses from absorption in the source and its backing, it offers another way of calibrating the counting yield for thick sources in a $4\pi\beta$ counter.[113,115] With quantitative information about the decay scheme of a particular nuclide, it should be possible to standardize sources by $4\pi\beta$-γ coincidence counting to a few tenths of a per cent.[113]

3. Absolute Gamma Counting

Gamma-ray counting by the scintillation method was discussed above in Section II.3. Spectrometry at a defined solid angle will yield an accuracy of about $\pm$ 5%--more accurate data

require calibration with sources of known disintegration rates. Integral counters, such as well-type scintillation detectors, must be standardized.

The most precise instrument for secondary standardization of gamma emitters is the high-pressure ionization chamber (Section III.5.). A precision of about $\pm$ 0.05% can be obtained when intercomparing sources. The coincidence method of absolute counting is not limited to beta-gamma counting but may be extended to any coincident pair of radiations, such as beta-electron coincidences, X ray-gamma coincidences, and especially gamma-gamma coincidences. The National Bureau of Standards has used the gamma-gamma coincidence counting technique for assay[99,100] of Co^{60}. In this situation, where two cascade gamma rays are of equal intensities, disintegration rates can be obtained to as good an accuracy as by other methods.

IX. SOURCE MOUNTING

1. Introduction

By now it is probably obvious that the choice of a chemical separation procedure, the choice of a radiation detector, and the choice of source mount are not independent. Factors such as the nature of the radiation to be counted often will determine the type of source to be employed; the source, in turn, will usually place restrictions on the choice of chemical procedure and counting equipment. There is so much variety in these interrelated factors which must be considered that this section will not attempt to set down firm rules for choosing the best source-preparation method. Instead, some of the common ones will be discussed in a general way so that the experimenter will be given sufficient information about methods in use to make a choice for his own problem.

For a more extensive discussion it is suggested that the reader consult the summaries of the source-preparation problem by Overman and Clark[115] and Slätis.[116] These authors quote extensive references for further reading.

2. Desiccated Sources

A. Evaporation from Solution. It is often desirable to

prepare a source which is very thin. The most straightforward approach is evaporation of an aliquot of a carrier-free solution on a suitable backing. To produce a thin source this way is very difficult, because it is essential that the solution contain no chemical compounds which will contribute appreciable mass to the final deposit. A technique which avoids concentrating impurities in the final product is the use of a very small bed of ion-exchange resin to which the carrier-free activity is adsorbed; after washing, the activity is eluted in the smallest possible volume of reagent.[117]

An unavoidable feature of evaporation from solution is that solids will not form a uniform deposit. In some experiments, such as $4\pi\beta$ counting of low-energy beta particles, self-absorption of aggregates may be excessive, and another method of depositing the source may be required.

Metal Backing Plates. Alpha particles exhibit a short range in matter, and sources of these particles must be quite thin. As was seen in Section VIII.1., alpha backscattering is small and is easily determined, so a metal plate makes a convenient source backing.

If the volume of solution to be evaporated on a metal plate is very large, it may be helpful to confine the solution to the desired region by a border of Zapon lacquer. After drying, the lacquer and any volatile impurities can be removed by ignition in an induction heater or an open flame, provided that the sample proper is nonvolatile. Further information on the use of metal foils as source backings will be found in reviews by Dodson, et al.,[118] and by Hufford and Scott.[119]

A very useful spreading technique[118] for preparation of uniform foils of heavy elements calls for mixing the nitrate of the desired element, dissolved in an organic solvent, with a dilute solution of Zapon lacquer. This mixture is painted on a metal plate, and, after drying, the plate is heated to destroy the organic residue and to convert the nitrate to the oxide. After each ignition the deposit is rubbed with tissue to insure that successive layers will adhere. Quite uniform deposits with smooth vitreous surfaces can be prepared by application of many successive coats, each very thin. This procedure is generally useful for any case where the element deposited has a nonvolatile compound which can be dissolved in an organic solvent; the foil must have a melting point high enough to with-

stand ignition.

Another technique which makes use of an organic solution of a nitrate has been described by Carswell and Milstead.[120] In their method the solution is sprayed from a capillary tube by the influence of a strong electric field. The space from the capillary tip to the metal plate is adjusted so that only fine, dry particles are collected. Thin, uniform sources may be prepared, even on extremely thin gold-coated plastic films.[121]

Very Thin Backings. In many beta counting applications, it is necessary to mount carrier-free sources on as thin a backing as possible. The usual technique is to transfer an aliquot of the appropriate solution onto the thin film by means of a micro pipette. The liquid is carefully evaporated by gently heating with an infrared lamp; the process is accelerated by flowing a stream of air over the source during evaporation.

Methods for preparing thin films are to be reviewed in a monograph of this series by Yaffe.[122] The article on source and window technique by Slätis[116] remains a very useful reference on thin films and other aspects of the source problem.

Gamma-Ray Sources. Although any of the methods already described can be used to prepare gamma-ray sources, the relatively low absorption of gamma rays by matter makes possible a rather simple and rapid procedure for mounting an aliquot of solution for gamma-ray assay. This method uses a small disc of blotting paper or "filter accelerator" taped onto a card. An aliquot of the solution to be determined is merely allowed to soak into the paper. After the sample has been dried by using an infrared heat lamp, the source should be covered by cellophane or Mylar tape.

B. Use of Slurries. Frequently, it is convenient to transfer small amounts of precipitate to a source mount and evaporate the solvent. The precipitate may, for example, lie collected in the tip of a centrifuge tube at the last step of a chemical separation procedure. A suitable organic liquid (e.g., alcohol or acetone) is added, and the resulting slurry is drawn into a transfer pipette; when discharging the contents of the pipette into a planchet, care must be exercised to insure that the spreading of the precipitate is uniform. After drawing off excess liquid, the sample is dried on the planchet and then covered with a thin plastic film to prevent spillage.

There are occasions in which it may be convenient to perform the final centrifugation in a demountable centrifuge tube whose bottom is a source planchet. This method has the advantage that the final deposits obtained are more uniform than those formed by pipetting slurries.

C. Filtration of Precipitates. When large numbers of samples must be prepared, the most convenient method is filtration, using a filter paper disk as a combination source mount and filter. Rather large masses of precipitate can be accommodated, and with proper technique, the area and thickness can be controlled sufficiently to insure good reliability.

Several designs for filtration devices have been published[115] and a few are on the market. In all of these a disk of fine-grade filter paper (e.g., Whatman No. 42) lies on a flat support, which may be either a sintered glass filter disk or perforated stainless steel plate, attached to the end of a tube. A hollow cylinder of glass or stainless steel, into which the slurry is introduced, is clamped firmly over the top of the filter paper disk. Once the precipitate is caught on the filter paper it may be washed and dried before removing it from the apparatus. If there is a tendency for the cake of precipitate to break up, a dilute solution of organic binder such as collodion may be passed through the filter before the final drying.

When the weight of final precipitate is needed to determine a chemical yield, a tare weight should be determined by using several filter paper disks identical to those employed for the unknown. Naturally, the tare papers should be subjected to the same wash solutions, binder, and drying procedure as the unknown.

3. Sublimation

Some of the most uniform sources are prepared by sublimation in vacuum. This method is applicable when the radionuclide of interest can be prepared in a chemical compound whose vapor pressure is at least 0.1 mm at a temperature below that for rapid decomposition. Examples of this technique will be found in references 118, 119, and 123.

The apparatus consists of a demountable vacuum chamber, in which are situated either a crucible or a ribbon filament, with

the collector plate a fraction of an inch away. Usually it is desirable to evaporate the source solution onto a shallow trough or depression in the filament, so when the filament is heated the sublimed material is collimated onto the collecting plate. A crucible, heated with electrical resistance wire or by electron bombardment, has similar collimating properties.

For the preparation of thin sources, it is helpful to be able to swing the collector away during the initial heating of the sample. It is then possible to "cook off" various impurities (such as organic residues) at low temperature, without subliming them onto the source mount.

Most of the procedures for vacuum sublimation are time consuming and have yields of less than 50%. Pate and Yaffe[105] have designed a system for subliming from a crucible onto a thin film with nearly 100% yield. Their results suggest that it should be possible to prepare sources which are not only uniform and thin, but also contain a known aliquot of a stock solution. The possibilities of such a technique in the fields of $4\pi\beta$ and alpha-particle counting are very promising.

4. Electrodeposition

Perhaps the most convenient source mounting technique, except for simple evaporation of a solution, is electrodeposition. Although it is not, in principle, as generally applicable as vacuum evaporation, it has enjoyed widespread use, especially for samples of the heavy-element alpha-particle emitters. Very uniform films can be obtained by this method, ranging from trace amounts to a few mg/cm^2.

Because the method is so well suited to the preparation of alpha-particle sources, extensive literature has been published on the electrodeposition of the heavy elements. Procedures for polonium, thorium, uranium, neptunium, and plutonium have been reported in the published records of the Manhattan Project,[118, 119, 124] and an article by Ko[125] gives electrodeposition procedures for all the actinide elements through curium. Where no procedures are available for carrier-free electrodeposition of a particular element, information in the standard analytical and electrochemical texts may be used as a guide; however, as is well known, the carrier-free element may not behave in the same way as do weighable amounts. In such a

situation, it may be helpful to add a small amount of carrier to avoid these difficulties.

The apparatus for electrodepositing on radionuclides counting plates has been described in the literature; for example, in references 115, 118, 119, and 124. Several devices are available commercially.

5. Sources Containing Gases

Samples of certain nuclides, notably the rare gases, are most conveniently assayed as gases. The experimenter may elect to introduce the gas into an ionization chamber, proportional counter, or Geiger counter as a component of the detector gas; or, he may choose to contain the gas in some way and mount it externally to the counter.

The highly specialized and well-developed techniques for internal gas counting have been adequately described in the current literature, as the list of references given by Overman and Clark[115] attests. Application of the method to the use of nuclides such as C^{14} (as CO_2) has been treated by Tolbert and Siri.[15]

A gas simply may be pumped into a container having a thin window for the exit of the particles to be counted. In spite of its convenience, this technique is not often used for absolute counting because the counting geometry of such a diffuse source is not well defined. If gamma-ray counting is to be performed, a gas sample may be contained by adsorption on a bed of activated charcoal or on one of the clathrates. The trap requires such thick construction material that beta counting is to be preferred.

A method for preparing thin, permanent samples of rare gases on metals has been described by Momyer and Hyde.[126] In their method the rare gas is introduced, along with nitrogen or air as carrier gas, into a glass chamber containing two electrodes, which may be either two parallel platinum plates, or a helical anode surrounding a central wire collector (cathode) of platinum. A glow discharge is struck between the two electrodes at a pressure of 100-1000 microns, taking care to limit the current to only 2-3 ma. In 5 minutes it is possible to obtain yields of a few per cent. No detectable loss of gas occurs from these sources at room temperature, and they appear to be quite thin.

6. Liquid Sources

For the beta counting of liquid samples, the liquid scintillation method (Section II.2.) is ideal. The current literature may be consulted for the latest recipes for samples compatible with the most common solution scintillators. General information on the subject may be found in references 10, 15, and 115.

Gamma-ray emitters may be contained very conveniently in small, biological-type test tubes for counting in a well-type NaI(Tl) scintillation counter (Section II.3.C.). Larger aliquots of solution may be contained in centrifuge tubes of up to 50-ml capacity; these may be assayed in high-pressure, gamma-sensitive ionization chambers, such as were described in Section III.5.

REFERENCES

Many of the references below are to documents available from the Office of Technical Services (O.T.S.), Department of Commerce, Washington 25, D. C., and the Superintendent of Documents (Supt. Doc.), U. S. Government Printing Office, Washington 25, D. C. In each case the price of the document is given.

1. P. R. Bell, in K. Siegbahn, ed., Beta- and Gamma-Ray Spectroscopy, Chapter 5, North Holland Publishing Company, Amsterdam, 1955.

2. C. E. Crouthamel, ed., Applied Gamma-Ray Spectrometry, Pergamon Press, New York, 1960.

3. W. E. Mott and R. B. Sutton, in S. Flügge and E. Creutz, eds., Handbuch der Physik, Volume XLV, Springer, Berlin, 1958.

4. R. B. Murray, in A. H. Snell, ed., Nuclear Instrumentation and Methods, Wiley, New York, 1961.

5. G. D. O'Kelley, in L. C. L. Yuan and C. S. Wu, eds., Methods of Experimental Physics, Vol. 5A, "Nuclear Physics," Academic Press, New York, 1961, Chaps. 2.212 and 2.233.

6. F. N. Hayes, D. G. Ott, and V. N. Kerr, Nucleonics, 14, No. 1, 42 (1956).

7. J. B. Birks, I.R.E. Transactions on Nuclear Sci., NS-7, Nos. 2-3, 2 (1960).

8. W. L. Buck, I.R.E. Transactions on Nuclear Sci., NS-7, Nos. 2-3, 11 (1960).

9. H. Kallmann and M. Furst, in C. G. Bell and F. N. Hayes, eds., Liquid Scintillation Counting, Pergamon Press, New York, 1958, p. 3.

10. C. G. Bell and F. N. Hayes, eds., Liquid Scintillation Counting, Pergamon Press, New York, 1958.

11. D. G. Gardner and W. W. Meinke, Int. J. Appl. Radiation and Isotopes, 3, 232 (1958).

12. G. D. O'Kelley, N. H. Lazar, and E. Eichler, Phys. Rev., 101, 1059 (1956).

13. B. H. Ketelle, Phys. Rev., 80, 758 (1950).

14. R. L. Robinson and L. M. Langer, Phys. Rev., 109, 1255 (1958).

15. B. M. Tolbert and W. E. Siri, "Radioactivity," in A. Weissberger, ed., Physical Methods of Organic Chemistry (Technique of Organic Chemistry, Vol. I), 3rd ed., Interscience, New York, 1960, Part IV, p. 3335.

16. D. Steinberg, Nature, 182, 740 (1958).

17. R. D. Birkhoff, Health Physics Division Annual Progress Report for Period Ending July 31, 1959, Oak Ridge National Laboratory Report ORNL-2806, 1959, p. 153 (O.T.S. - $3.50).

18. G. E. Owen and H. Primakoff, Phys. Rev., 74, 1406 (1948); Rev. Sci. Instr., 21, 447 (1950).

19. M. S. Freedman, T. B. Novey, F. T. Porter, and F. Wagner, Jr., Rev. Sci. Instru., 27, 716 (1956).

20. R. L. Heath, Scintillation Spectrometry Gamma-Ray Spectrum Catalogue, Phillips Petroleum Company, Atomic Energy Division Report IDO-16408, 1957 (O.T.S. - $4.75).

21. W. E. Kuykendall and R. E. Wainerdi, Computer Techniques for Radioactivation Analysis, Texas Engineering Experiment Station Report TEES-2565-1, 1960 (O.T.S. - $2.50); Paper 198 presented at the International Conference on Use of Radioisotopes in the Physical Sciences and Industry (Copenhagen, Sept. 6-17, 1960).

22. L. E. Fite, D. Gibbons, R. E. Wainerdi, Computer-Coupled Automatic Activation Analysis, Texas Engineering Experiment Station Report TEES-2671-1, 1961 (O.T.S. - $2.25).

23. H. I. West, Jr., and B. Johnston, I.R.E. Transactions on Nuclear Sci., NS-7, Nos. 2-3, 111 (1960).

24. R. O. Chester, "Preliminary Studies of Computer Processing of Gamma Spectra," in Proceedings of the Total Absorption Gamma-Ray Spectrometry Symposium, U. S. Atomic Energy Commission Report TID-7594, 1960, p. 140 (O.T.S. - $3.50).

25. R. O. Chester and W. R. Burrus, "Unscrambling of Scintillation Spectra," in Neutron Physics Division Annual Progress Report for Period Ending September 1, 1960, Oak Ridge National Laboratory Report ORNL-3016, 1960, p. 249 (O.T.S. - $4.00).

26. R. L. Heath, "Data Processing Techniques for Routine Application of Gamma-Ray Scintillation Spectrometry," in Proceedings of the Total Absorption Gamma-Ray Spectrometry Symposium, U.S. Atomic Energy Commission Report TID-7594, 1960, p. 147 (O.T.S. - $3.50).

27. W. B. Strickfaden and R. M. Kloepper, IBM 704 Programs for Unfolding Complex Gamma-Ray Spectra, Los Alamos Scientific Laboratory Report LA-2461, 1961 (O.T.S. - $2.50).

28. W. R. Burrus, I.R.E. Transactions on Nuclear Sci., NS-7, Nos. 2-3, 102 (1960).

29. N. E. Scofield, A Technique for Unfolding Gamma-Ray Scintillation Spectrometry Pulse-Height Distributions, U.S. Naval Radiological Defense Laboratory Report USNRDL-TR-447, June, 1960.

30. N. H. Lazar, R. C. Davis, and P. R. Bell, I.R.E. Trans. on Nuclear Sci., NS-3, No. 4, 136 (1956); Nucleonics, 14, No. 4, 52 (1956).

31. E. A. Wolicki, R. Jastrow, and F. Brooks; U. S. Naval Research Laboratory Report NRL-4833, 1956 (O.T.S. - $1.00).

32. S. H. Vegors, L. M. Marsden, and R. L. Heath, Calculated Efficiencies of Cylindrical Radiation Detectors, Phillips Petroleum Company, Atomic Energy Div. Report IDO-16370, 1958 (O.T.S. - $2.50).

33. N. H. Lazar and E. D. Klema, Phys. Rev., 98, 710 (1955).

34. M. E. Rose, Phys. Rev., 91, 610 (1953).

35. D. O. Caldwell and J. R. Armstrong, Rev. Sci. Instr., 23, 508 (1952).

36. H. P. Robinson, "Alpha Standards," in G. G. Manov and W. C. Peacock, eds., Measurements and Standards of Radioactivity, Proceedings of an Informal Conference, Publication No. 573, National Academy of Sciences - National Research Council, Washington, 1958.

37. E. Fairstein, "Electrometers and Amplifiers," in A. H. Snell, ed., Nuclear Instrumentation and Methods, Wiley, New York, 1961.

38. H. W. Fulbright, "Ionization Chambers in Nuclear Physics," in S. Flügge and E. Creutz, eds., Handbuch der Physik - Encyclopedia of Physics, Vol. XLV, Springer, Berlin, 1958, p.1.

39. W. J. Price, Nuclear Radiation Detection, McGraw-Hill, New York, 1958.

40. B. Rossi and H. H. Staub, Ionization Chambers and Counters, McGraw-Hill, New York, 1949.

41. D. H. Wilkinson, Ionization Chambers and Counters, Cambridge University Press, Cambridge, 1950.

42. G. H. Dieke, in D. E. Gray, ed., American Institute of Physics Handbook, Section 7, McGraw-Hill, New York, 1957.

43. J. D. Craggs and H. S. W. Massey, "The Collisions of Electrons with Molecules," Sections 21, 22, in S. Flügge, ed., Handbuch der Physik - Encyclopedia of Physics, Vol. XXXVII, Springer, Berlin, 1959.

44. H. H. Staub, in E. Segre, ed., Experimental Nuclear Physics, Vol. I, Part I, Wiley, New York, 1953.

45. J. L. Putman, "Gamma-Ray Measurements and Standards," p. 69, in G. G. Manov and W. L. Peacock, eds., Measurements and Standards of Radioactivity, Proceedings of an Informal Conference, Publication No. 573, National Academy of Sciences - National Research Council, Washington, 1958.

46. R. J. Stephenson, High-Pressure Ionization Chamber, University of Chicago Metallurgical Laboratory Report MUC-RJS-2 (AECD-2463); F. R. Shonka and R. J. Stephenson, U. S. Atomic Energy Commission, Isotopes Division Circular IDA-7, 1949.

47. G. C. Hanna, "Alpha-Radioactivity," in E. Segre, ed., Experimental Nuclear Physics, Vol. III, Wiley, New York, 1959, p. 192 ff.

48. W. L. Brown, "Introduction to Semiconductor Particle Detectors," I.R.E. Transactions on Nuclear Sci., NS-8, No. 1, 2, (1960); "Properties of Space Charge Regions," in J. W. T. Dabbs and F. J. Walter, eds., Semiconductor Nuclear Particle Detectors, Publication No. 871, National Academy of Sciences - National Research Council, Washington, 1961.

49. A. K. Jonscher, Principles of Semiconductor Device Operation, G. Bell and Sons, London, 1960.

50. J. N. Shive, The Properties, Physics, and Design of Semiconductor Devices, D. Van Nostrand, Princeton, 1959.

51. H. K. Henisch, Rectifying Semiconductor Contacts, Clarendon Press, Oxford, 1957.

52. F. J. Walter, J. W. T. Dabbs, and L. D. Roberts, Rev. Sci. Instr., 31, 756 (1960).

53. J. Bardeen, "Flow of Electrons and Holes in Semiconductors," in E. V. Condon and H. Odishaw, eds., Handbook of Physics, Part 8, Chapter 4, McGraw-Hill, 1958.

54. J. L. Blankenship and C. J. Borkowski, I.R.E. Transactions on Nuclear Sci., NS-7, Nos. 2-3, 190 (1960); ibid., NS-8, No. 1, 17 (1961).

55. E. M. Pell, J. Appl. Phys., 31, 291 (1960).

56. J. H. Elliott, Thick Radiation Detectors Made by Ion Drift, University of California Radiation Laboratory Report UCRL-9538, 1961.

57. R. H. Kingston, ed., Semiconductor Surface Physics, University of Pennsylvania Press, Philadelphia, 1957; J. N. Zemel, ed., Semiconductor Surfaces, Proceedings of the Second Conference, Pergamon Press, New York, 1960 (also published as Vol. 14 of Phys. and Chem. Solids).

58. G. L. Miller and W. M. Gibson, Charge Collection in Semiconductor Particle Detectors, Brookhaven National Laboratory Report BNL-5391, 1961.

59. F. J. Biondi, ed., Transistor Technology, Vols. 2 and 3, Van Nostrand, Princeton, 1958.

60. P. F. Donovan, "Paint-on Particle Detectors," in J. W. T. Dabbs and F. J. Walter, eds., Semiconductor Nuclear Particle Detectors, Publication 871, National Academy of Sciences - National Research Council, Washington, 1961.

61. A. Chetham-Strode, J. R. Tarrant, and R. J. Silva, I.R.E. Transactions on Nuclear Sci., NS-8, No. 1., 59 (1961).

62. W. Hansen and F. S. Goulding, "Leakage, Noise, Guard Rings, and Resolution," in J. W. T. Dabbs and F. J. Walter, eds., Semiconductor Nuclear Particle Detectors, Publication No. 871, National Academy of Sciences - National Research Council, Washington, 1961, p. 204.

63. M. L. Halbert and J. L. Blankenship, Nuclear Instr. and Methods, 8, 106 (1960).

64. K. Way, et al., Nuclear Data Sheets, Nuclear Data Group, National Academy of Sciences - National Council (Printing and Publishing Office, National Academy of Sciences - National Research Council, 2101 Constitution Ave., Washington 25, D. C. - $17 annual subscription, back issues available).

65. D. R. Corson and R. R. Wilson, Rev. Sci. Instr., 19, 207 (1948); R. R. Wilson, D. R. Corson, and C. P. Baker, Particle and Quantum Detectors, Preliminary Report No. 7, National Research Council, Washington, D. C., January, 1950.

66. S. C. Curran, "The Proportional Counter as Detector and Spectrometer," in S. Flügge and E. Creutz, eds., Handbuch der Physik - Encyclopedia of Physics, Springer, Berlin, 1958.

67. S. C. Curran, "Proportional Counter Spectrometry," in K. Siegbahn, ed., Beta- and Gamma-Ray Spectroscopy, Chap. VI, North Holland Publishing Co., Amsterdam, 1955.

68. A. Gillespie, Signal, Noise, and Resolution in Nuclear Counter Amplifiers, Pergamon Press, New York, 1953.

69. A. A. Korff, "Geiger Counters," in S. Flügge and E. Creutz, eds., Handbuch der Physik - Encyclopedia of Physics, Springer, Berlin, 1958.

70. T. P. Kohman, in G. T. Seaborg, ed., The Transuranium Elements, National Nuclear Energy Series, Div. IV, Vol. XIV-B, Pt. II, McGraw-Hill, 1950.

71. R. L. Chase, Nuclear Pulse Spectrometry, McGraw-Hill, New York, 1961.

72. W. C. Elmore and M. Sands, Electronics, McGraw-Hill, New York, 1949.

73. H. W. Koch and R. W. Johnston, eds., Multichannel Pulse Height Analyzers, Publication 467, National Academy of Sciences - National Research Council, Washington, 1957.

74. H. W. Koch, op. cit., pp. 19-31.

75. E. Fairstein, Rev. Sci. Instr., 27, 475 (1956).

76. G. G. Kelley, I.R.E. National Conventional Record, Part 9, p. 63 (1957).

77. F. S. Goulding, R. W. Nicholson, J. B. Waugh, Nuclear Instr. Methods, 8, 272 (1960).

78. E. Fairstein, I.R.E. Trans. Nuclear Sci., NS-8, No. 1, 129 (1961).

79. T. L. Emmer, I.R.E. Transactions on Nuclear Sci., NS-8, No. 1, 140 (1961).

80. A. B. Van Rennes, Nucleonics, 10, No. 7, 20 (1952); 10, No. 8, 22 (1952); 10, No. 9, 32 (1952); 10, No. 10, 50 (1952).

81. Low Noise Amplifiers for Use with Solid-State Detectors, Office of Technical Information Extension, U. S. Atomic Energy Commission, Report TID-6119, August, 1960 (O.T.S. - $0.50).

82. J. Millman and H. Taub, Pulse and Digital Circuits, McGraw-Hill, New York, 1956, Chapter 11.

83. R. L. Chase, Rev. Sci. Instr., 31, 945 (1960).

84. F. S. Goulding and R. A. McNaught, Nuclear Instr. Methods, 8, 282 (1960).

85. S. DeBenedetti and R. W. Findley, "The Coincidence Method," in S. Flügge and E. Creutz, eds., Handbuch der Physik - Encyclopedia of Physics, Vol. XLV, Springer, Berlin, 1958, p. 222.

86. I. A. D. Lewis and F. H. Wells, Millimicrosecond Pulse Techniques, 2nd Ed., Pergamon Press, New York, 1959, p. 302.

87. H. Paul, Nuclear Instr. and Methods, 9, 131 (1960).

88. R. W. Peele and T. A. Love in Applied Nuclear Physics Progress Report for Period Ending September 1, 1957, Oak Ridge National Laboratory Report, ORNL-2389, 1958, pp. 249-259 (O.T.S. - $6.50).

89. E. Fairstein, in Instrumentation and Controls Division Annual Progress Report for Period Ending July 1, 1957, Oak Ridge National Laboratory Report ORNL-2480, 1957, pp. 1-3 (O.T.S. - $6.30, microfilm).

90. C. D. Goodman, G. D. O'Kelley, and D. A. Bromley, "A 20,000-Channel Pulse-Height Analyzer with a Two-Coordinate Address," in Proceedings of the Symposium on Nuclear Instruments, A.E.R.E., Harwell, Heywood and Co., Ltd., London, in press.

91. R. E. Bell, "Measurement by Delayed Coincidences," in K. Siegbahn, ed., Beta- and Gamma-Ray Spectroscopy, Chapter XVIII, North Holland Publishing Company, Amsterdam, 1955.

92. R. S. Weaver and R. E. Bell, Nuclear Instr. and Methods, 9, 149 (1960).

93. N. R. Johnson, E. Eichler, G. D. O'Kelley, J. W. Chase, and J. T. Wasson, Phys. Rev., 122, 1546 (1961).

94. J. R. Arnold, paper in W. C. Peacock, ed., Conference on Measurements and Standards of Radioactivity, Publication No. 573, National Academy of Sciences - National Research Council, Washington, 1958.

95. J. L. Kulp, paper in W. C. Peacock, ed., Conference on Measurements and Standards of Radioactivity, Publication No. 573, National Academy of Sciences - National Research Council, Washington, 1958.

96. J. R. DeVoe, Radioactive Contamination of Materials Used in Scientific Research, Publication 895, National Academy of Sciences - National Research Council, Washington, D. C., 1961.

97. R. W. Perkins, J. M. Nielsen, and R. W. Diebel, Rev. Sci. Instr., 31, 1344 (1960).

98. E. P. Steinberg, "Counting Methods for the Assay of Radioactive Samples," in A. H. Snell, ed., Nuclear Instrumentation and Methods, Wiley, New York, 1961, Chap. 5.

99. W. C. Peacock, ed., Conference on Measurements and Standards of Radioactivity, Publication No. 573, National Academy of Sciences - National Research Council, Washington, 1958.

100. Proceedings of the Symposium on Metrology of Nuclides, International Atomic Energy Agency, Vienna, Austria, Oct. 14-16, 1959, International Publications, New York, 1960.

101. W. S. Lyon and S. A. Reynolds, Nucleonics, 14, No. 12, 44 (1956).

102. B. D. Pate and L. Yaffe, Can. J. Chem., 33, 610 (1955).

103. M. L. Curtis, J. W. Heyd, R. G. Olt, and J. F. Eichelberger, Nucleonics, 13, (5), 38 (1955).

104. K. M. Glover and G. R. Hall, Nature, 173, 991 (1954).

105. B. D. Pate and L. Yaffe, Can. J. Chem., 34, 265 (1956).

106. R. C. Hawkings, W. F. Merritt, and J. H. Craven, Proceedings of Symposium on Maintenance of Standards, National Physical Laboratory, 1951; H. M. Stationer's Office, London, 1952.

107. H. H. Seliger and L. Cavallo, J. Research, Nat'l Bureau of Standards, 47, 41 (1951); W. B. Mann and H. H. Seliger, ibid., 50, 197 (1953).

108. D. B. Smith, 4-Pi Geiger Counters and Counting Technique, British Atomic Energy Research Establishment Report AERE-I-1210 (1953).

109. B. D. Pate and L. Yaffe, Can. J. Chem., 33, 929 (1955).

110. B. D. Pate and L. Yaffe, Can. J. Chem., 33, 1656 (1955).

111. H. H. Seliger and A. Schwebel, Nucleonics, 12, (7), 54 (1954).

112. W. B. Mann and H. H. Seliger, Preparation, Maintenance, and Application of Standards of Radioactivity, National Bureau of Standards Circular 594, 1958.

113. P. J. Campion, Intern. J. Appl. Radiation and Isotopes, 4, 232 (1959).

114. J. L. Putman, Brit. J. Radiol., 23, 46 (1950); in K. Siegbahn, ed., Beta- and Gamma-Ray Spectroscopy, Chap. XXVI, North Holland Publishing Company, Amsterdam, 1955.

115. R. T. Overman and H. M. Clark, Radioisotope Techniques, McGraw-Hill, New York, 1960.

116. H. Slätis, "Source and Window Technique," in K. Siegbahn, ed., Beta- and Gamma-Ray Spectroscopy, North Holland Publishing Co., Amsterdam, 1955.

117. P. G. Hansen and R. K. Sheline, Nuclear Instr., 2, 39 (1958); S. Bjornholm, O. B. Nielsen, R. K. Sheline, Nature, 178, 1110 (1956).

118. R. W. Dodson, A. C. Graves, L. Helmholz, D. L. Hufford, R. M. Potter, and J. G. Povelites, in A. C. Graves and D. K. Froman, eds., Miscellaneous Physical and Chemical Techniques of the Los Alamos Project, National Nuclear Energy Series, McGraw-Hill, New York, 1951, Chap. 1.

119. D. L. Hufford and B. F. Scott, in G. T. Seaborg, J. J. Katz, and W. M. Manning, eds., The Transuranium Elements, National Nuclear Energy Series, Div. IV, Vol. XIV-B, p. 1149, McGraw-Hill, New York, 1949.

120. D. J. Carswell and J. Milsted, J. Nuclear Energy, 4, 51 (1957).

121. J. S. Fraser and J. C. D. Milton, Physics Division Progress Report - January 1, 1958 to March 31, 1958, Atomic Energy of Canada Report AECL-587, 1958, p. 14 (Atomic Energy of Canada, Ltd. - $1.50).

122. L. Yaffe, Preparation of Thin Films, National Academy of Sciences - National Research Council, Nuclear Science Series Monograph, in press, 1961 (O.T.S.).

123. F. Asaro, F. L. Reynolds, and I. Perlman, Phys. Rev., 87, 277 (1952).

124. C. C. Casto, in C. J. Rodden, N. R. Furman, E. H. Huffman, L. L. Quill, T. D. Price, and J. I. Watters, eds.,

Analytical Chemistry of the Manhattan Project, National Nuclear Energy Series, Div. VIII-1, Chap. 23, McGraw-Hill, New York, 1950.

125. R. Ko, Nucleonics, 15, No. 1, 72 (1957).

126. F. F. Momyer, Jr., and E. K. Hyde, J. Inorg. Nuclear Chem., 1, 274 (1955).

USAEC Division of Technical Information Extension, Oak Ridge, Tennessee